RESERVOIR CHARACTERIZATION of the LOWER GREEN RIVER FORMATION, UINTA BASIN, UTAH

by
Craig D. Morgan, Thomas C. Chidsey Jr., Kevin P. McClure,
S. Robert Bereskin, and Milind D. Deo

OPEN-FILE REPORT 411 April 2003
UTAH GEOLOGICAL SURVEY
a division of
UTAH DEPARTMENT OF NATURAL RESOURCES

FOSSIL ENERGY

DOE/BC/15103-4
(OSTI ID: 805238)

RESERVOIR CHARACTERIZATION OF THE LOWER GREEN RIVER FORMATION, SOUTHWEST UINTA BASIN, UTAH

Final Report
October 1, 1998-September 30, 2002

By:
Craig D. Morgan, Utah Geological Survey
Thomas C. Chidsey, Jr., Utah Geological Survey
Kevin P. McClure, Utah Geological Survey
S. Robert Bereskin, Ph.D., Tesseract Inc.
Milind D. Deo, Ph.D., University of Utah

Date Published: December 2002

Work Performed Under Contract No. DE-AC26-98BC15103

Utah Geological Survey
Salt Lake City, Utah

National Energy Technology Laboratory
National Petroleum Technology Office
U.S. DEPARTMENT OF ENERGY
Tulsa, Oklahoma

DISCLAIMERS

Utah Geological Survey

This open-file report makes information available to the public which may not conform to Utah Geological Survey (UGS) policy, editorial, or technical standards. Therefore it may be premature for an individual or group to take actions based on its contents.

Utah Department of Natural Resources

Although this product represents the work of professional scientists, the Utah Department of Natural Resources, Utah Geological Survey, makes no warranty, expressed or implied, regarding its suitability for a particular use. The Utah Department of Natural Resources, Utah Geological Survey, shall not be liable under any circumstances for any direct, indirect, special, incidental, or consequential damages with respect to claims by users of this product.

United States Government

This report was prepared as an account of work sponsored by an agency of the United States Government. Neither the United States Government nor any agency thereof, nor any of their employees, makes any warranty, express or implied, or assumes any legal liability or responsibility for the accuracy, completeness, or usefulness of any information, apparatus, product, or process disclosed, or represents that its use would not infringe privately owned rights. Reference herein to any specific commercial product, process, or service by trade name, trademark, manufacturer, or otherwise, does not necessarily constitute or imply its endorsement, recommendation, or favoring by the United States Government or any agency thereof. The views and opinions of authors expressed herein do not necessarily state or reflect those of the United States Government or any agency thereof.

DOE/BC/15103-4
Distribution Category UC-122

Reservoir Characterization of the Lower Green River Formation, Southwest Uinta Basin, Utah

By
Craig D. Morgan, Utah Geological Survey
Thomas C. Chidsey, Jr., Utah Geological Survey
Kevin P. McClure, Utah Geological Survey
S. Robert Bereskin, Ph.D., Tesseract Inc.
Milind D. Deo, Ph.D., University of Utah

December 2002

Work Performed Under DE-AC26-98BC15103

Prepared for
U.S. Department of Energy
Assistant Secretary for Fossil Energy

Virginia Weyland, Project Manager
National Energy Technology Laboratory
National Petroleum Technology Office
One West Third Street, Suite 1400
Tulsa, OK 74103

Prepared by
Utah Geological Survey
1594 West North Temple, Suite 3110
P.O. Box 146100
Salt Lake City, UT 84114-6100
(801) 537-3300

TABLE OF CONTENTS

ILLUSTRATIONS

TABLES

PLATES

ABSTRACT

The oil-productive lower and middle members of the Green River Formation in the southwest Uinta Basin are divided into five distinct reservoirs. The reservoirs in stratigraphically ascending order are: (1) Uteland Butte, (2) Castle Peak, (3) lower Douglas Creek, (4) upper Douglas Creek, and (5) Garden Gulch. The changing depositional environments of Lake Uinta controlled the characteristics of each of the reservoirs. The Uteland Butte consists of carbonate and rare, thin shallow-lacustrine sandstone bars deposited during the initial rise of the lake. The Castle Peak reservoir was deposited during a time of numerous and rapid lake-level falls and rises, which developed a simple drainage pattern across the exposed shallow and gentle shelf with each cycle. The lower Douglas Creek reservoir records a time of active tectonism which created a steeper slope and a pronounced shelf break where thick cut-and-fill valleys developed during lake-level falls and rises. The upper Douglas Creek reservoir represents a return to a very gentle shallow shelf where channel deposits became stacked in a lowstand delta plain and amalgamated into some of the best reservoir rock in the southwest Uinta Basin. The Garden Gulch reservoir represents a time of major lake expansion with fewer, less pronounced, lake-level falls, resulting in isolated single-storied channel- and shallow-bar sandstone deposits.

The rocks exposed in Nine Mile Canyon are a good analog to the oil reservoirs in the southwest Uinta Basin. Examination of the exposures of the middle member of the Green River Formation in Nine Mile Canyon revealed a high degree of heterogeneity in reservoir-quality sandstone beds. The heterogeneity identified on outcrop indicates that a significant amount of the oil is being left behind in the Green River Formation reservoirs in the southwest Uinta Basin, at the current well spacing.

Numerical simulation models were constructed for three fields, which produce from the Uteland Butte, Castle Peak, and upper Douglas Creek reservoirs. Modeling indicates that primary recovery from each of the reservoirs is less than 5 percent of the oil in place.

INTRODUCTION

The Utah Geological Survey led a four-year study of the lower and middle members of the Eocene Green River Formation in the southwest Uinta Basin, Utah (figure 1). The Green River is a highly oil-productive formation consisting of lacustrine- and marginal-lacustrine rocks deposited in and around Eocene-aged Lake Uinta. The objectives of the study were to increase both primary and secondary hydrocarbon recovery through improved characterization (at the regional, unit, interwell, well, and microscopic scale) of fluvial-deltaic lacustrine reservoirs, thereby preventing premature abandonment of producing wells. The study will encourage exploration and establishment of additional water-flood units throughout the southwest region of the Uinta Basin, and other areas with production from fluvial-deltaic reservoirs.

A log-based correlation scheme and nomenclature that reflect, as near as possible, time-correlative depositional cycles of the lower and middle members of the Green River Formation were established. The cycles are at a scale that is easily recognizable on geophysical well logs and can be correlated throughout most of the southwest Uinta Basin. Logs from more than 1,300 wells were correlated, and data on cycle boundaries, total sandstone, and total feet of porosity, for each cycle, were entered into the well database and used for mapping.

Regional investigation of the surface exposures of the Green River Formation was conducted in Willow Creek, Nine Mile, and Desolation Canyons. Numerous stratigraphic sections in the Green River were measured and described. Photomontages of nearly 4 miles (6 km) of outcrop in Nine Mile Canyon where compiled and used for correlation of key marker beds. Spectral gamma-ray (GR) data were collected using an Exploranium® GR - 256 spectrometer with a GPX - 21 scintillation detector, over four stratigraphic sections; one in Willow Creek Canyon, and three in Nine Mile Canyon. Curves generated from the GR data were correlated with GR curves from wells in the area. Several carbonate marker beds are found in the middle member, which define large-scale (about 100-foot [30-m] thick) depositional cycles and are used to correlate the cycles for tens of miles along the outcrop and in the subsurface. Smaller scale depositional cycles have been identified on outcrop but are difficult to correlate regionally.

Five reservoirs were identified in the middle and lower members of the Green River Formation based on the regional chronostratigraphic correlations, investigation of well core, and examination of the surface exposures. The five reservoirs in stratigraphically ascending order are: (1) Uteland Butte, (2) Castle Peak, (3) lower Douglas Creek, (4) upper Douglas Creek, and (5) Garden Gulch. Each reservoir consists of one or more beds with similar paleodepositional history, petrology, and diagenesis that are unique to the reservoir.

A detailed study site was selected in Nine Mile Canyon, from Petes Canyon to Gate Canyon, both tributaries to Nine Mile. The exposure is about 2,000 feet (600 m) in the east-to-west direction and about 4,200 feet (1,280 m) in the north-to-south direction. The stratigraphic interval studied is slightly more than 100 feet (30 m) thick, bounded by carbonate beds. Eight sections were measured and described, and GR data gathered from five of the sections. To aid in the interpretation, the site was photographed from the canyon walls opposite the study site, and photomontages were compiled. Data from the study site serves as an important analog for the reservoir heterogeneity that can be expected in the interwell environment and at the scale of a typical Monument Butte area water-flood unit.

Geostatistial analyses were conducted and numerical simulation models were constructed for the Uteland Butte field (Uteland Butte reservoir), Brundage Canyon field (Castle Peak reservoir), and Monument Butte Northeast unit (upper Douglas Creek reservoir). The Uteland Butte and Brundage Canyon fields are in primary production while the Monument Butte Northeast is a secondary-recovery water-flood unit.

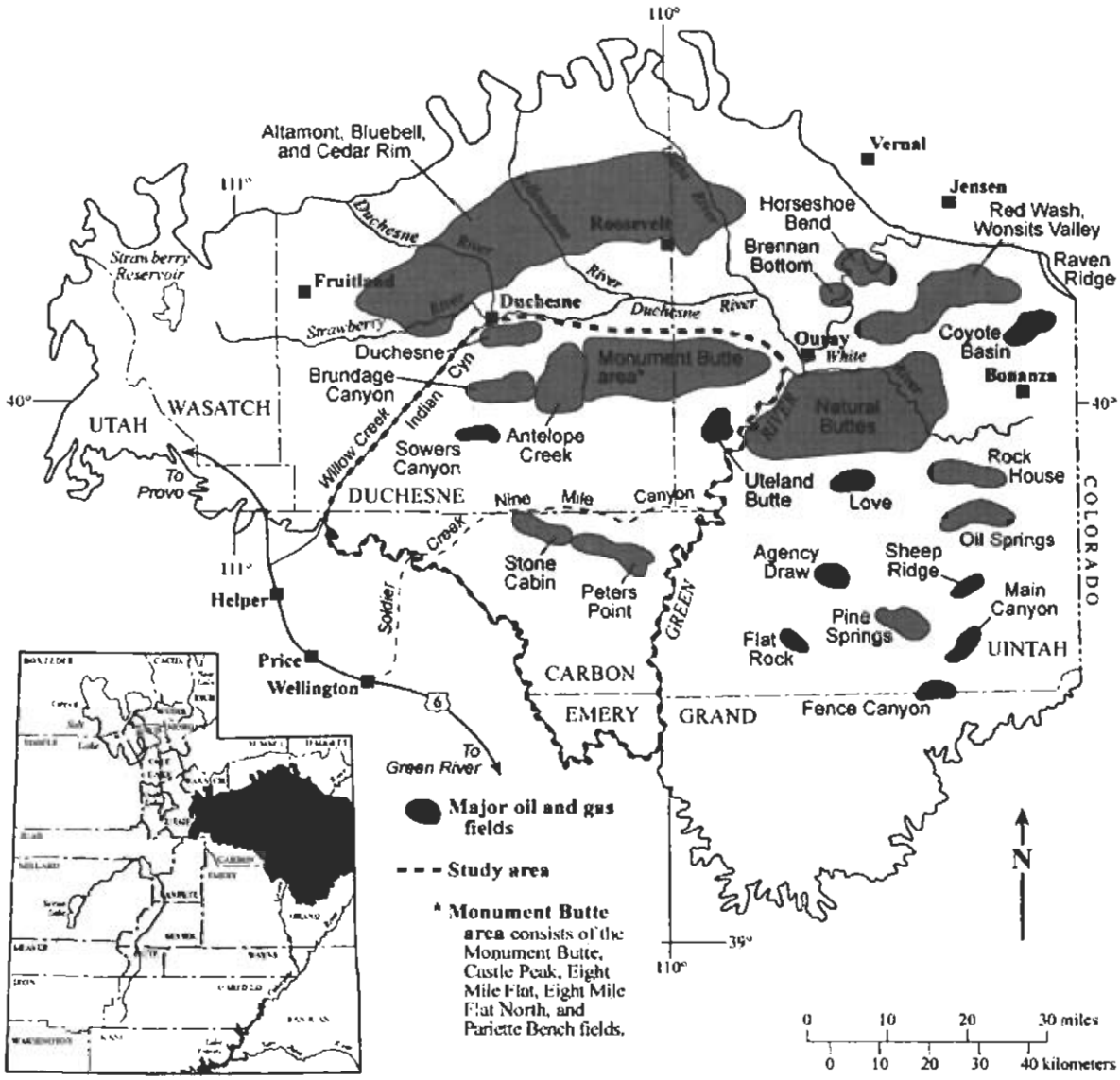

Figure 1. Location map of the Uinta Basin showing the southwest Uinta Basin study area.

Geophysical well log data were used to construct detailed the geostatistical models for the Monument Butte Northeast unit, that were upscaled to obtain reasonable number of grid blocks for reservoir simulation. Porosities, permeabilities, and water saturations required for reservoir simulation were generated from well log and core data. Comparison of the production results with the field data revealed that there was a phenomenogical deficiency in the model. This was addressed by incorporating hydraulic fractures into the models resulting in much better agreement between simulated production and actual field production data.

The Brundage Canyon and Uteland Butte fields were simulated in primary production. Only preliminary simulations were undertaken since a number of critical data elements could not be obtained from the operators. These studies revealed that the production performance of the Brundage Canyon field is much better than what can be predicted from simulations of a typical non-fractured, undersaturated reservoir, indicating that naturally occurring fractures are an important part of the Castle Peak reservoir. Uteland Butte field performance was that of a typical undersaturated reservoir.

GEOLOGIC SETTING

The Uinta Basin is a topographic and structural trough encompassing an area of more than 9,300 square miles (14,900 km^2) in northeast Utah (figure 1). The basin is sharply asymmetrical, with a steep north flank bounded by the east-west-trending Uinta Mountains, and a gently dipping south flank.

The Uinta Basin formed in Late Cretaceous Maastrichtian time, creating a large area of internal drainage, which was filled by ancestral Lake Uinta during the Paleocene and Eocene. Deposition in and around Lake Uinta consisted of open- to marginal-lacustrine sediments that make up the Green River Formation. Alluvial red-bed deposits that are laterally equivalent to, and intertongue with, the Green River make up the Colton (Wasatch) Formation.

More than 450 million barrels of oil (MMBO) (72 million m^3) have been produced from the Green River and Colton Formations in the Uinta Basin. The Cedar Rim, Altamont, Bluebell, and Red Wash fields produce oil from the northern shoreline deposits of Lake Uinta, while the fields in the greater Monument Butte area (Duchesne, Brundage, Sowers, Antelope Creek, and Uteland Butte fields, and the Monument Butte area [figure 1]) produce from southern deltaic shoreline deposits as preserved in the middle and lower members of the Green River. The southern shore of Lake Uinta was often very broad and flat, which allowed large transgressive and regressive shifts in the shoreline in response to climatic and tectonic-induced rise and fall of the lake. The cyclic nature of Green River deposition in the southwest Uinta Basin resulted in numerous stacked deltaic deposits. Distributary-mouth bars, distributary channels, and nearshore bars are the primary producing sandstone reservoirs in the area.

PREVIOUS STUDIES AND STRATIGRAPHIC NOMENCLATURE

The stratigraphic nomenclature used to describe the Green River Formation in the Uinta Basin, Utah, is as diverse as the rocks themselves. The nomenclature is based on facies, which are often bounded by subtle and interfingering relationships that are difficult to carry with confidence any great distance within the basin. Regional facies studies such as Fouch (1975) and Ryder and others (1976), have greatly increased our knowledge of Lake Uinta as represented by the deposits of the Green River Formation, but rapid facies change with poorly defined boundaries has often lead to confusing stratigraphic relationships, and questionable and confusing use of terminology.

In the eastern Uinta Basin, Bradley (1931) named and described the Douglas Creek, Garden Gulch, Parachute Creek, and Evacuation Creek Members of the Green River Formation. In the western Uinta Basin, Bradley (1931) defined the basal lacustrine phase, tongue of the Wasatch, second lacustrine phase, delta facies, oil shale facies, barren and saline facies (figure 2). Picard (1955) introduced the term black shale facies for the western Uinta Basin area for the rocks equivalent to the first lacustrine phase and Wasatch tongue of Bradley (1931). Abbott (1957) expanded the use of black shale facies to include the second lacustrine phase of Bradley (1931) and showed the delta facies to be equivalent to the Douglas Creek Member. Picard (1957a, 1957b) introduced the term green shale facies, which is equivalent to most of the delta facies. In the subsurface the black shale facies thickens from south to north at the expense of the green shale facies (Picard 1957a). Ryder and others (1976) defined the carbonate marker unit equivalent to the black shale facies below the carbonate marker bed.

Several workers have described the fluvial-deltaic and interfingering alluvial deposits associated with the southern shoreline of Lake Uinta in the southwest Uinta Basin (Cashion, 1967; Picard and High, 1970; Fouch, 1975; Ryder and others, 1976; Pitman and others, 1982). Remy (1992) described the exposures and depositional environments of the delta facies of the Green River in Nine Mile Canyon and some of its tributaries. Remy (1992) defines the Sunnyside delta interval in Nine Mile Canyon from the top of the carbonate marker bed to the C marker (Jacob, 1969), and from the C marker to the top of the S1 sandstone, just below the base of the Mahogany oil shale, as the transitional facies.

There are a few laterally extensive marker beds, which have been identified on the surface and in the subsurface (Jacob, 1969; Weiss and others 1990). These marker beds have been used for time-stratigraphic correlations that can cross facies boundaries. Several marker beds have been identified on the surface and correlated to well-log signatures in the subsurface. The top of the carbonate marker unit of Ryder and others (1976) is placed at the top of the carbonate marker bed, which has an easily recognizable well-log response throughout most of the southwestern Uinta Basin. Jacob (1969) defines several carbonate marker beds in Nine Mile Canyon such as the D marker which is about 500 feet (150 m) above the carbonate marker bed and contains a pisolite bed which makes it easy to identify throughout most of the western portion of Nine Mile Canyon, before it dips below the canyon floor. Jacob's (1969) C marker consists of three ostracod grainstones that he designated from base to top as C3, C2, and C1. The C1 marker is equivalent to the stromatolite marker of Remy (1989) and the C marker of Remy (1992). The C marker is about 700 feet (200 m) above the D marker.

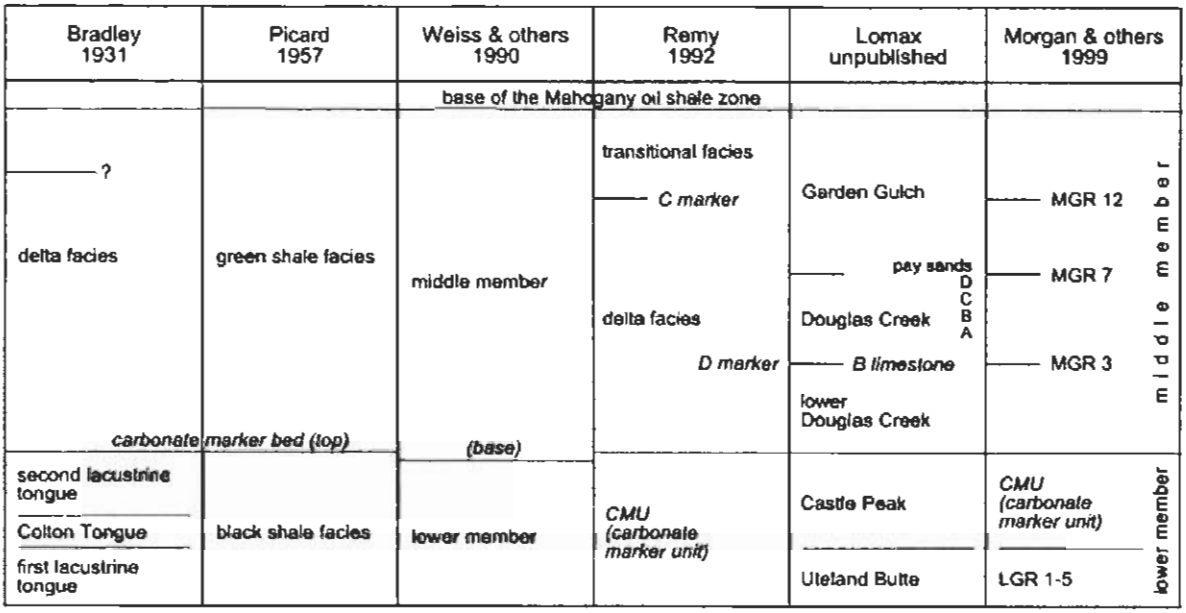

Figure 2. Generalized nomenclature for the Green River Formation (below the Mahogany oil shale zone) for the south-central to southwest Uinta Basin.

Weiss and others (1990) mapped a lower member, middle member, upper member, and saline member in the Nine Mile Canyon area. Weiss and others (1990) unlike previous workers, use the base of the carbonate marker bed instead of the top as a mapping horizon. To divide the lower member from the upper member we modified the lower member using the top of the carbonate marker bed as the top of the lower member - base of middle member. The modified lower member is equivalent to the black shale facies of Abbott (1957), the middle member from the top of the carbonate marker bed to the base of the Mahogany oil shale, is equivalent to all of the delta facies of Bradley (1931), Picard (1957), and the delta and transitional facies of Remy (1992). The upper member and saline member were not part of this study.

Recent workers have begun to use a sequence stratigraphic (chronostratigraphic instead of lithostratigraphic) approach to the Green River Formation. Crouch and others (2000) reported on their subsurface study of the Uteland Butte reservoir in Antelope Creek Field. Keighley and others (1999, 2001) studied the outcrops in Nine Mile Canyon while Borer and McPherson (1996), and Borer (1998), studied the outcrops at Raven Ridge and subsurface deposits at the neighboring Red Wash field. Our study uses chronostratigraphic correlations of surface outcrops and subsurface well logs to characterize the petroleum reservoirs in the lower and middle members of the Green River Formation in the southwest Uinta Basin.

STRATIGRAPHIC NOMENCLATURE AND CORRELATION MARKERS USED IN THIS REPORT

Members

Weiss and others (1990) divided the Green River Formation in the southwest Uinta Basin into informal members, in stratigraphically ascending order: (1) lower member, (2) middle member, (3) upper member, and (4) saline member. We studied only the lower and middle members. Weiss and others (1990) used the base of the carbonate marker bed to define the top of the lower member-base of middle member of the Green River Formation but previous workers used the top of the carbonate marker bed to define the top of the carbonate marker unit (Ryder and others, 1976; and Remy, 1992). The lower member includes the Uteland Butte reservoir also known as Bradley's (1931) first lacustrine phase, or the basal carbonate (Little, 1988) and the Castle Peak reservoir or carbonate marker unit (Ryder and others, 1976). We have adopted the lower and middle member terminology, but use the top of the carbonate marker bed as the top of the lower member - base of middle member (figure 3). The carbonate marker bed is easily identifiable on well logs throughout the region. The middle member is defined as from the top of the carbonate marker bed to the base of the Mahogany oil shale. The middle member contains the lower and upper Douglas Creek reservoirs and Garden Gulch reservoir. The middle member also consists of the Douglas Creek Member and part of the Garden Gulch Member (Bradley, 1931) and Remy's (1992) delta and transitional facies.

Log Cycles

The +2,000-foot-thick (600-m), Tertiary-aged lacustrine deposits of the middle and lower members of the Green River Formation contain the primary oil-producing reservoirs in the southwest Uinta Basin, Utah. We established a log-based correlation scheme and nomenclature that reflect, as near as possible, time-correlative depositional cycles of the middle and lower members of the Green River Formation (Morgan and others, 1999). The log-cycles are at a scale that is easily recognizable on geophysical well logs, typically range from 50 to 100 feet (15-30 m) thick, and can be correlated throughout most of the southwest Uinta Basin (figure 4).

The log cycles are numbered from the base of the member upward and were defined by gamma-ray and resistivity log patterns. Log patterns that may represent coarsening-upward sequences overlain by a flooding event or a rise-to-fall sequence were identified in key wells. The correlations were then made on regional east-to-west and north-to-south well-log cross sections (figure 5 and plates 1 through 4). Correlations that were difficult to make or appeared to have a limited extent were dropped. The correlations resulted in five cycles in the lower member of the Green River Formation (LGR) plus the carbonate marker unit, which was not divided because the log-cycle pattern was too small for reliable regional correlation. In the middle member (MGR), 18 cycles were identified although MGR 1 and MGR 2 proved to be unreliable correlations and were not picked in most well-log correlations.

The top of the uppermost cycle, MGR 18, correlates to the middle marker of Ryder and others (1976). This is the top of the stratigraphic sequence that we studied. There is about 500 to 600 feet (150-180 m) of middle Green River section from the top of the middle marker to the base of the Mahogany oil shale.

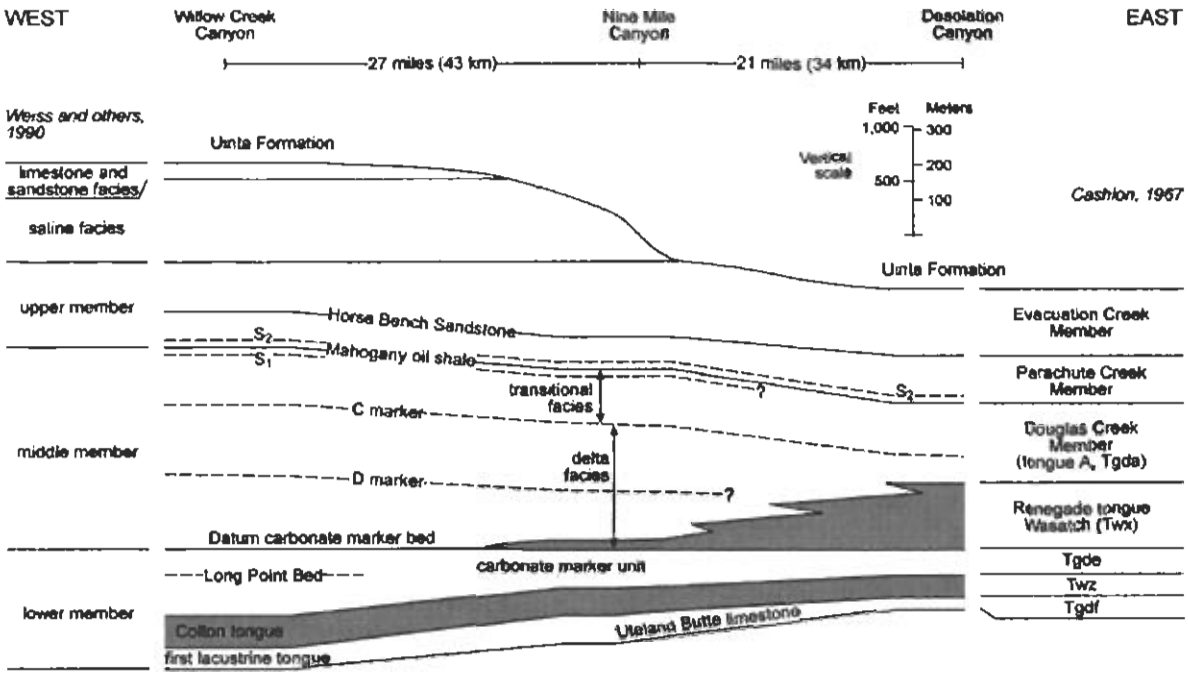

Figure 3. West to east stratigraphic cross section showing the stratigraphic nomenclature used in this report and some of the common stratigraphic names used by other workers.

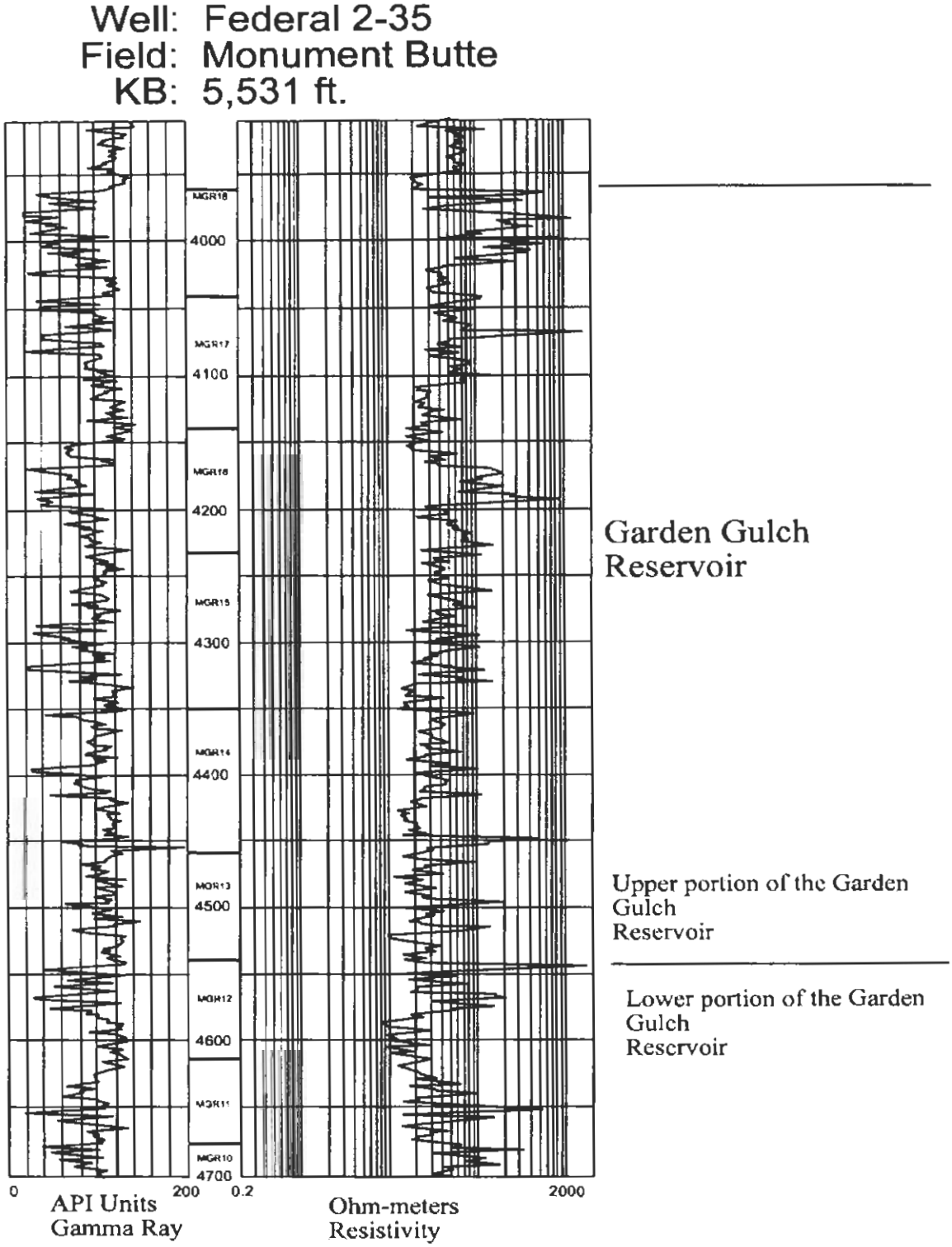

Figure 4. Type log showing the log cycles and oil reservoirs in the middle member (MGR) and lower member (LGR) of the Green River Formation. CMU is the carbonate marker unit of the lower member. Well location is NE1/4SE1/4 section 35, T. 8 S., R. 16 E., of the Salt Lake Base Line Salt Lake Base and Merdian.

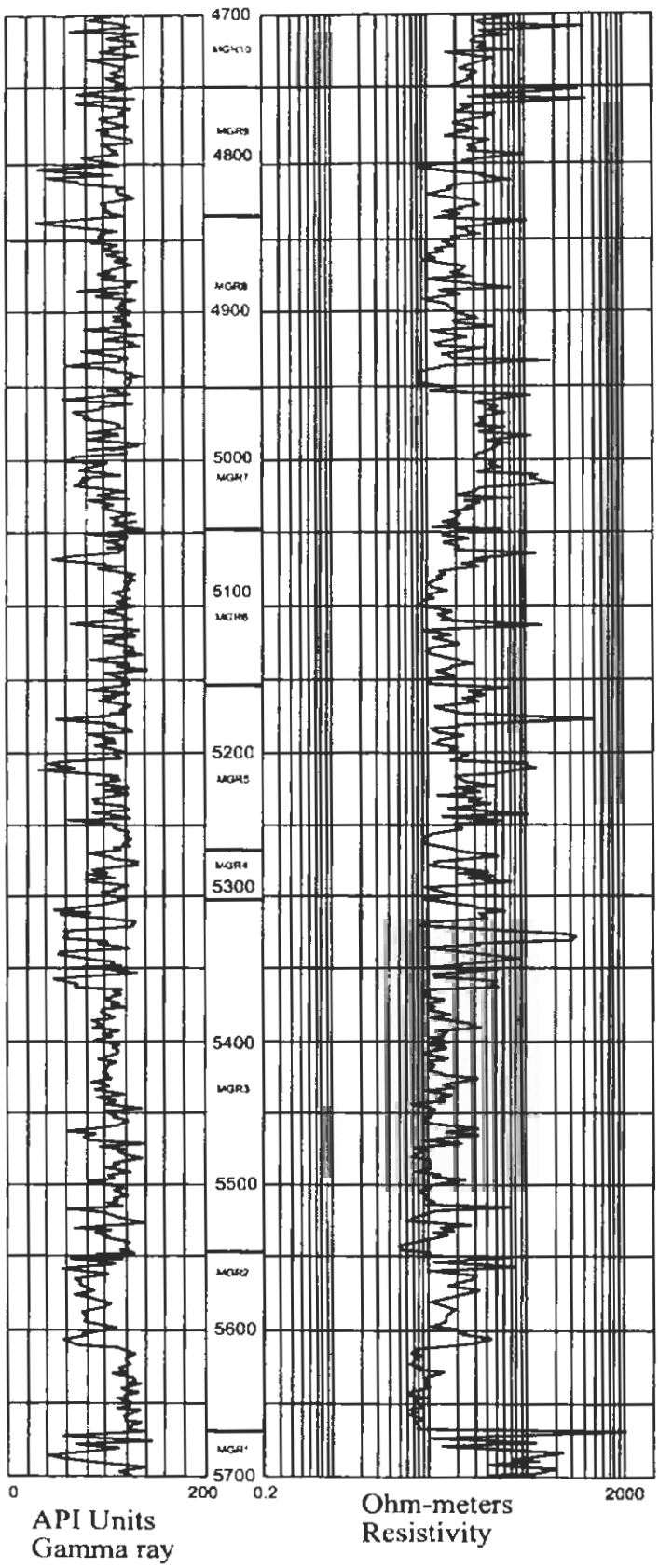

Lower portion of the Garden Gulch Reservoir

Upper Douglas Creek Reservoir

Lower Douglas Creek Reservoir

Figure 4 continued.

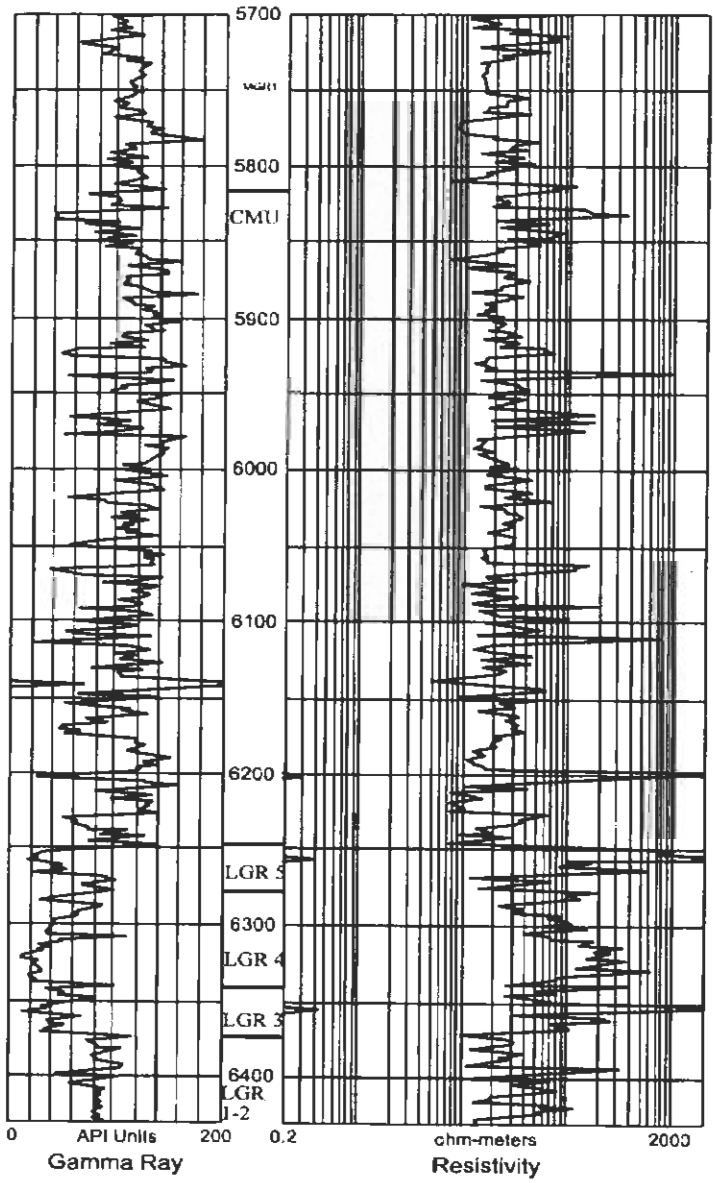

Total Depth 6,440 ft.

Figure 4 end.

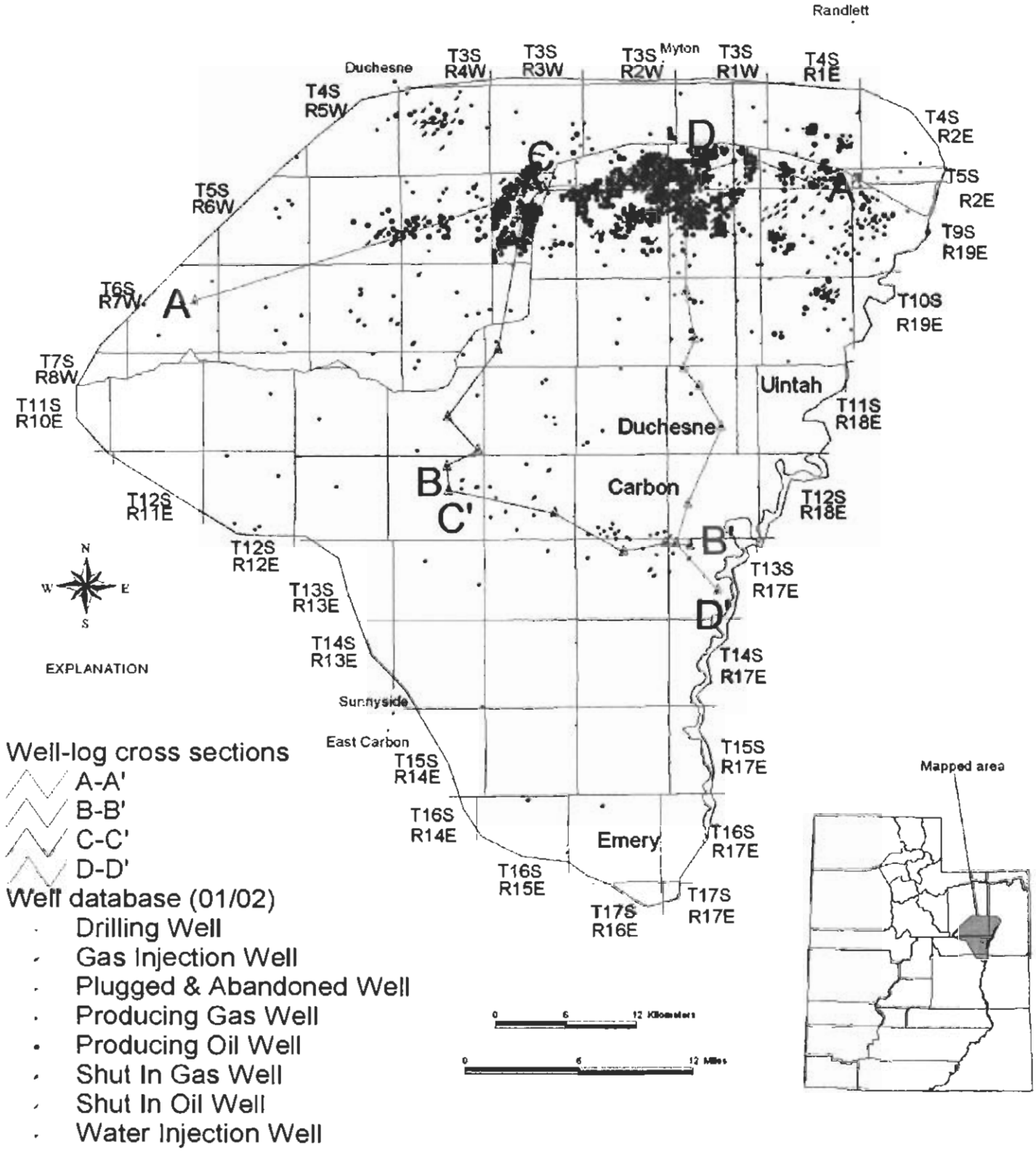

Figure 5. Map showing the location of regional well-log cross sections A – A' (plate 1), B – B' (plate 2), C – C' (plate 3), and D – D' (plate 4).

Log cycles LGR1 through LGR 5, are the Uteland Butte reservoir, also known as the basal Green River carbonate, or the first lacustrine tongue of Bradley (1931). The five divisions are based on the work of Little (1988) and can be correlated from surface outcrop to subsurface well logs. The carbonate marker unit or Castle Peak reservoir was not divided into log cycles because the patterns were too thin for regional correlations. Hackney and Crouch (2000) working in the Antelope Creek field (T. 5 S., R. 3 W., Uinta Base Line [UBL]) identified 17 different cycles in the Castle Peak reservoir. Some cycles in the MGR do not have the typical cyclic log pattern but are packages underlain and overlain by cyclic sequences. These packages could represent a period of stable lake level or a period of high cyclicity resulting in a series of sequences at a scale smaller than what we are studying. Regardless, these packages can be correlated and mapped regionally.

OUTCROP STUDIES

Exposures of the lower and middle members were studied to gain a better understanding of the regional paleodepositional history and stratal architecture of the stratigraphic sequence. The regional outcrop study when combined with the subsurface study, defined the trapping mechanism for the various reservoirs and is a useful tool for future exploration. A more limited exposure referred to as the Nutter's Ranch study site was investigated in more detail. The Nutter's Ranch study site consists of a stratigraphic sequence about 100 feet (30 m) thick with an extent of about 1 square mile (2.6 km^2). The Nutter's Ranch study site is a good analog for some of the reservoir beds in the greater Monument Butte area and provides insights into the potential reservoir heterogeneity that can exist in the interwell environment.

Exposures of the lower and middle member of the Green River Formation were studied in Willow Creek, Nine Mile, and Desolation Canyons and many of their tributaries. Eight stratigraphic sections (Appendix A) were measured and described totaling 8,813 feet (2,686.2 m). Gamma-ray data was gathered over four sections totaling 5,500 feet (1,680 m). Seven stratigraphic sections by Remy (1992) were field checked and graphically redrawn to match the style and scale of the UGS measured sections (Appendix B). Key marker beds were correlated between the stratigraphic sections relying in part on the correlations of Remy (1992) and Keighley and others (2002) (figure 6 and plates 5, 6, and 7). A 3.75 mile (6.0 km) portion of the north wall of Nine Mile Canyon was photographed, montages were constructed and used for correlation (Appendix C). The gamma-ray curves were used to help correlate between stratigraphic sections and to correlate from surface sections to subsurface well logs (figure 7 and plates 8 and 9).

Stratigraphic Correlation and Sequence Stratigraphy

During the latest Cretaceous through middle Eocene the Uinta Basin was an intermountain basin where Ancient Lake Uinta and associated fluvial deposition resulted in more than 3,000 feet (900 m) of siliciclastic and carbonate sediments. The sediments make up the Colton Formation and the Flagstaff Member, lower, middle, upper and saline members of the Green River Formation. The region was subtropical to semi-arid with strong seasonality and storm tracts generally from west to east, parallel to the long axis of Lake Uinta. Jacob (1969) interpreted the delta facies in the southwest Uinta Basin as being deposited on a shallow shelf, generally in water depths no more than a few tens of feet.

The Colton Formation and the lower and middle members of the Green River Formation are exposed in Willow Creek Canyon. The exposures in Willow Creek Canyon include Bradley's (1931) first and second lacustrine phase and overlying delta facies, which are correlative to Picard's (1957a and 1957b) black shale and green shale facies. The Mahogany oil shale is exposed near the top of Willow Creek Canyon.

The lower member of the Green River Formation is exposed in the western portion of Nine Mile Canyon. Most of the exposures in Nine Mile Canyon are the delta and transitional facies in the middle member. The Mahogany oil shale is at or near the top of the most of the cliffs in Nine Mile Canyon. The Colton Formation, and the lower and middle members of the Green River, are exposed in Desolation Canyon and many of its tributaries.

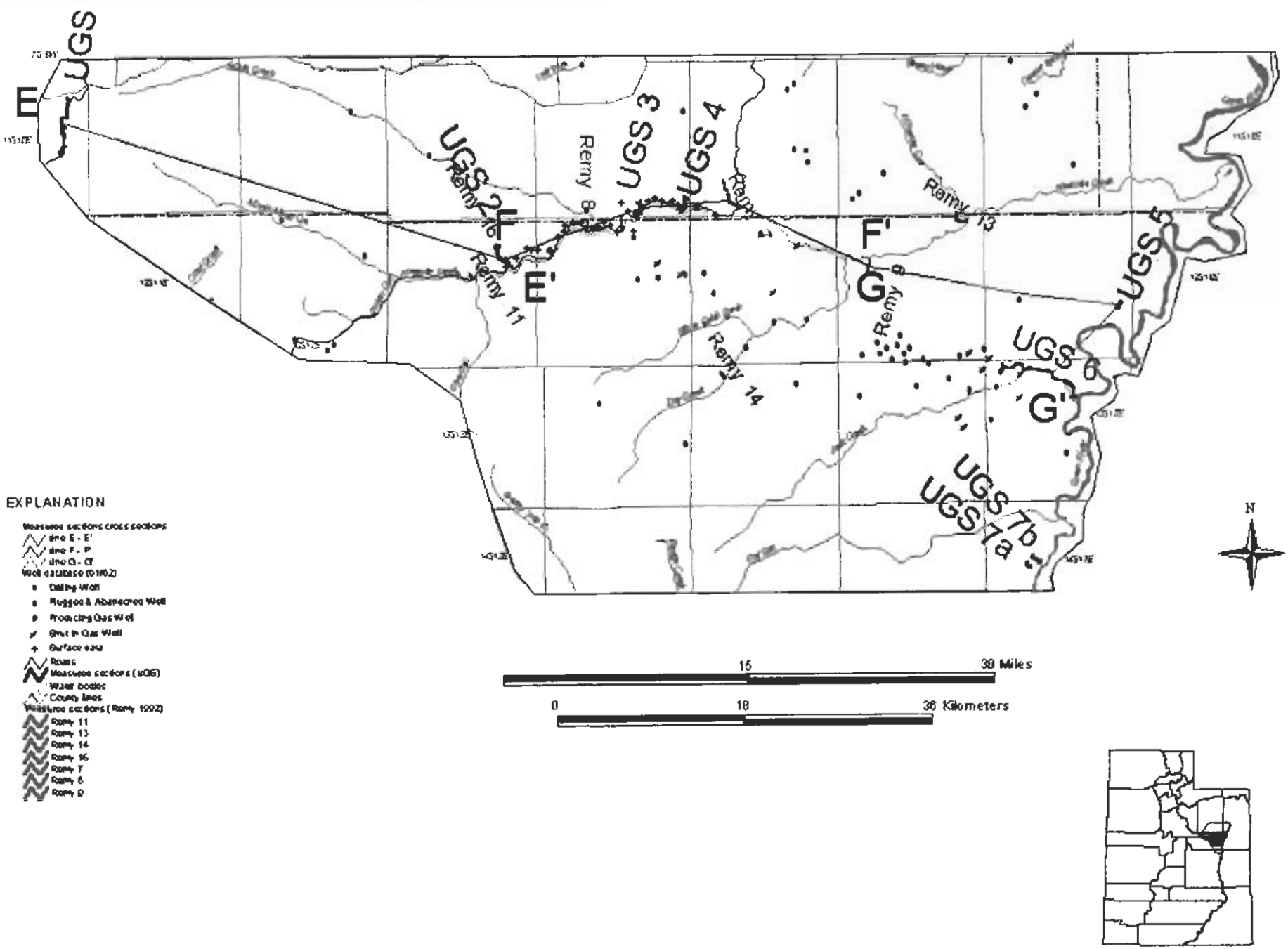

Figure 6. Map showing the location of the surface stratigraphic cross sections E – E' (plate 5), F – F' (plate 6), and G – G' (plate 7).

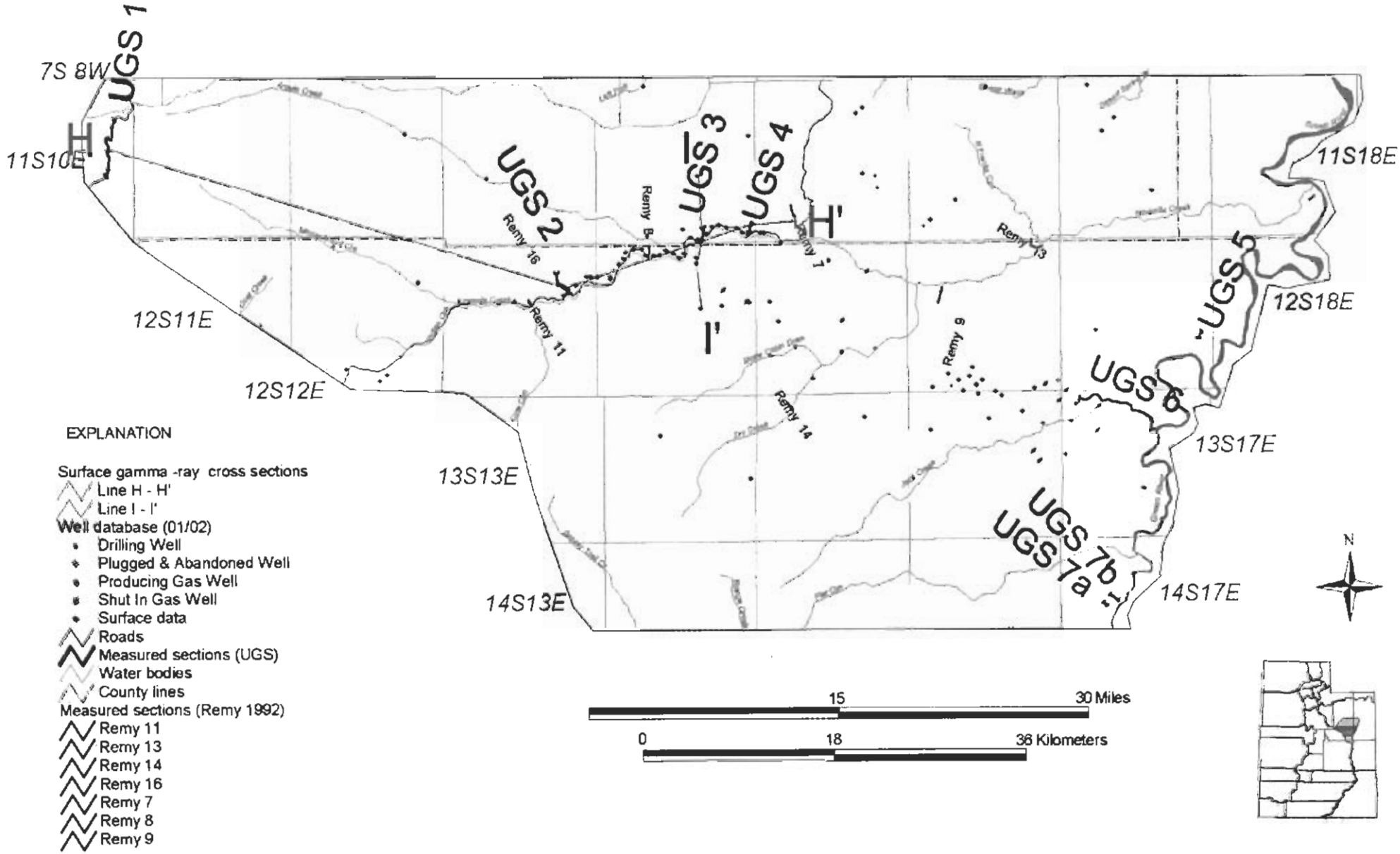

Figure 7. Map showing the location of the surface gamma-ray log cross sections H - H' (plate 8) and I - I' (plate 9).

Ryder and others (1976), and Fouch (1975), divided the Green River Formation into three major facies: (1) open lacustrine, (2) marginal lacustrine, and (3) alluvial. The three facies have been used to describe the paleodepositional history of the Colton and Green River Formations throughout the existence of Lake Uinta (Fouch, 1975; Ryder and others, 1976; Franczyk and others, 1992; and Remy, 1992). Chronostratigraphic interpretation of the paleodepositional environments of Lake Uinta have been based on key carbonate marker beds such as Jacob's (1969) C and D markers, and Ryder and others (1976) middle marker and carbonate marker beds. The Green River Formation, especially the middle member, is dominated by large scale (100 feet [30 m]) and smaller scale (30 feet [10 m]) depositional cycles caused by lake level fluctuations. Ryder and others (1976), Fouch and Pitman (1991, 1992), and Fouch and others (1992, 1994), and many others have described the cyclic nature of the Green River.

Borer (1998) and Borer and McPherson (1996), have presented high-resolution sequence stratigraphic interpretations for the Green River Formation at Raven Ridge and nearby Red Wash oil field. Keighley and others (2002, 2001, 1999) studied the sequence stratigraphy of the delta facies from the D marker to the C2 marker in Nine Mile Canyon.

Keighley and others (2002) identified 11 markers in Nine Mile Canyon, which they used to divide the sequence into depositional units or cycles 20 to 90 feet (6 - 30 m) thick. The markers are named in ascending stratigraphic order, M1, equivalent to the D marker, through M11, equivalent to the C2 marker. All of the markers are carbonate beds except M2, which is a thin (1 inch [3 cm]) oil shale. The markers are laterally extensive and can be traced for more than 10 miles (16 km). A marker bed will sometimes be locally absent when it is truncated by overlying fluvial sandstone. Keighley and others (2002) described the sequence as alternating 60-foot (20-m) thick floodplain-dominated intervals and 30-foot (10-m) thick lacustrine-dominated intervals.

Keighley and others (2002) defined two types of sequence boundaries in Nine Mile Canyon that represent significant basinward shifts in facies. Type A sequence boundaries are defined as offshore lacustrine facies that pass abruptly upward into floodplain-dominated intervals and/or where the lacustrine - floodplain transition is across a surface that is a mappable unconformity over the study area. Type B sequence boundaries are defined as lacustrine-dominated intervals that lack any distinct offshore facies and any unconformable contact with overlying floodplain-dominated strata. Type A sequences are more pronounced base-level falls while Type B sequences are higher frequency, lower magnitude lake-level falls.

We used Keighley and others (2002) correlation markers (M1 - M11) and sequence boundaries in Nine Mile Canyon. We designated the C1 marker of Jacob (1969) as M12 and identified additional sequence boundaries in the lower member of the Green River Formation, below the interval studied by Keighley and others (2002) (plates 5, 6, and 7).

Nutter's Ranch Study Site

To better understand the potential reservoir heterogeneity in the Green River Formation we selected a location for detailed study referred to as the Nutter's Ranch study site (figure 8), that contains a well-exposed, large-scale depositional cycle. The Nutter's Ranch study site lies within section 32, T. 11 S., R. 15 E. (Salt Lake Base Line [SLBL]), in Duchesne County. Wells in the Monument Butte area are drilled on 40 acre (16.2 ha) spacing resulting in about 1,320 feet (402 m) between wells. The typical water-flood unit in the Monument Butte area is a square mile (one section) or larger, with wells in the center of every 40 acre (16.2 ha) lot, or 16 wells per section. The wells are initially completed as oil wells, but after they have all been drilled, every other well is converted to a water injection well, resulting in eight producing and eight

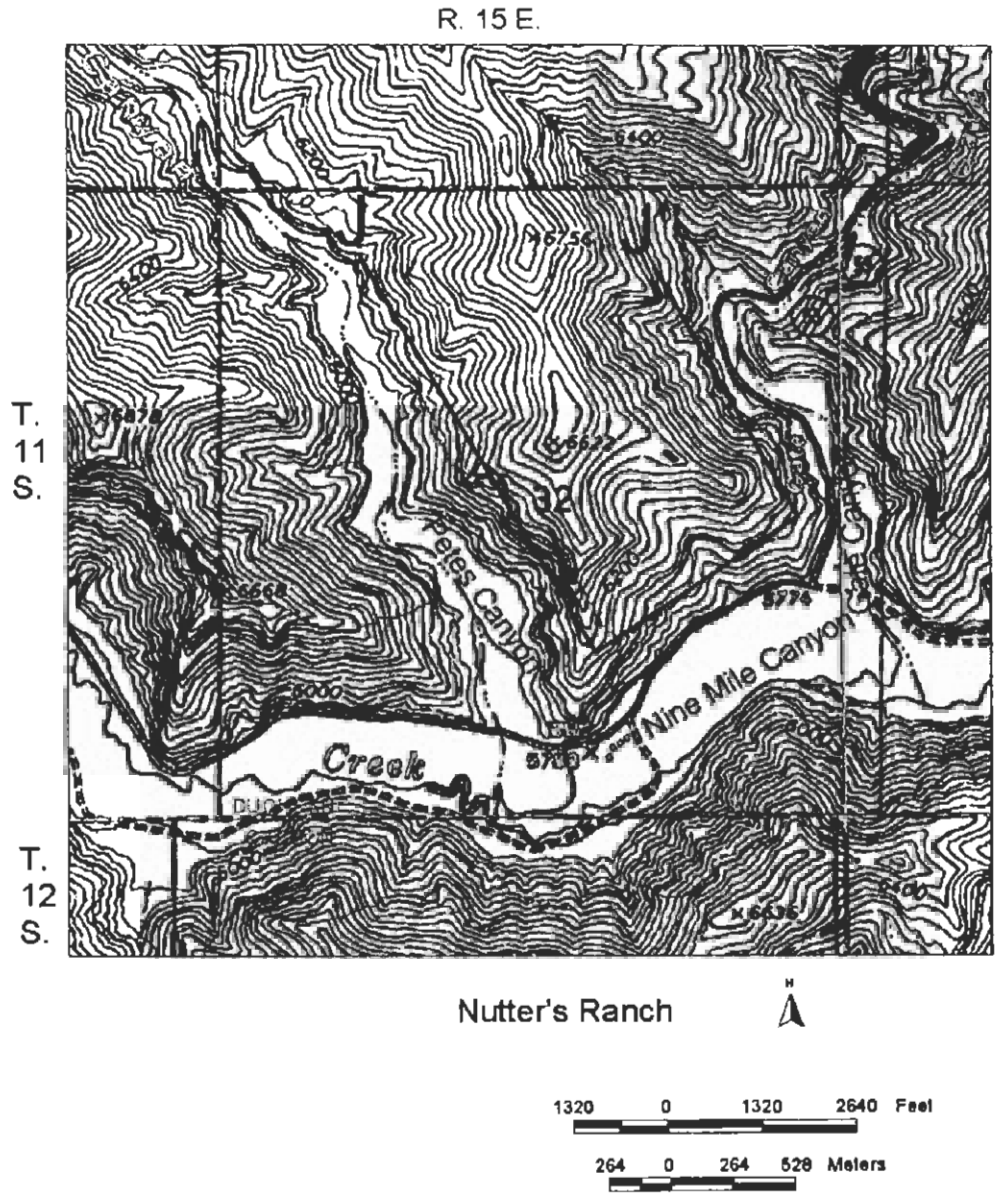

Figure 8. Map of Nutter's Ranch study site in Nine Mile Canyon, between Petes and Gate Canyons, showing the location of stratigraphic cross section J – J' (plate 10).

injection wells per section. Detailed examination of the outcrop helped us identify the potential heterogeneity that can exist between wells in two dimensions as well as over a square mile, as an analogy to a typical water-flood unit in the Monument Butte area.

The Nutter's Ranch study site includes portions of Petes Canyon and Gate Canyon, and the portion of Nine Mile Canyon between Petes and Gate Canyons. The exposure is about 2,000 feet (600 m) in the east-to-west direction in Nine Mile Canyon, and in the north-to-south direction in Gate Canyon, and about 4,200 feet (1,280 m) in the north-to-south direction in Petes Canyon. The stratigraphic interval studied is slightly more than 100 feet (30 m) thick, and is bounded by carbonate beds M8 at the base and M9 at the top (figure 9). Eight sections were measured and described, and GR data were gathered from five of the sections (plate 10). To aid in the stratigraphic interpretation, the site was photographed from the canyon walls opposite the study site, and photomontages were compiled (Appendix D). The photomontages were used to map out individual beds and their relationships. Data from the study site provide an example of the reservoir heterogeneity that could be encountered in a typical Monument Butte area water-flood unit and in the interwell environment.

The lithologies and depositional interpretations described in the Nutter's Ranch study site are shown in table 1.

Two-Dimensional Reservoir Model of the Nutter's Ranch Study Site

Two imaginary wells along the Nine Mile Canyon portion of the Nutter's Ranch study site are shown 1,320 feet (402 m) apart to illustrate the type of reservoir heterogeneity that could exist between two wells drilled on 40 acre (16.2 ha) spacing units. Both of the imaginary wells encounter a carbonate bed above (M9) and below (M8), and two reservoir-quality sandstone beds. Well logs would show excellent correlation of the carbonate and sandstone beds (figure 10). As a result, good lateral continuity of the sandstone beds would be expected. However, in this example, the upper sandstone in the two wells comprises two separate deposits (Ss-e and Ss-f) that would probably have very poor fluid flow between them (figure 11). Ss-e is an amalgamated channel deposit that has good reservoir potential but Ss-f is a crevasse splay deposit that has complex internal heterogeneity in the proximal channel facies and high clay content in the distal bar facies. The lower sandstone (Ss-c) is the same bed in both of the wells, but has been locally cut out by the overlying channel sandstone (Ss-d). In some places Ss-e has incised down to Ss-c, creating a potential for fluid-flow communication between the two sandstone beds. Ss-d nearly cuts out Ss-c and is a potential reservoir that is not penetrated by either of the imaginary wells. Ss-a is laterally continuous but thin and has poor porosity and permeability due to abundant clay. Ss-b is a very narrow bed that would rarely be penetrated by a well with 40 acre (16.2 ha) spacing and would probably not have sufficient storage capacity to be an economical oil reservoir.

Three-Dimensional Reservoir Model of the Nutter's Ranch Study Site

Thickness of the three potential reservoir sandstone beds (Ss-c, Ss-d, and Ss-e) were determined by direct measurement (plate 10) and by extrapolating between the measured sections using the photomontages (Appendix D). The sandstone thickness values and associated Universal Transverse Mercator (UTM) coordinates were entered into the Nutter's Ranch Arcview database. The section (section 32, T. 11 S., R. 15 E., SLBL) which contains the study site, was divided into 40 acre (16.2 ha) lots and the UTM coordinates for the center of each lot was determined and entered into the database as an oil well location with a well number (figure 12). Every other well was designated as a water injection well, the typical pattern for a water flood in the Monument Butte area. The imaginary wells in the two-dimensional model were

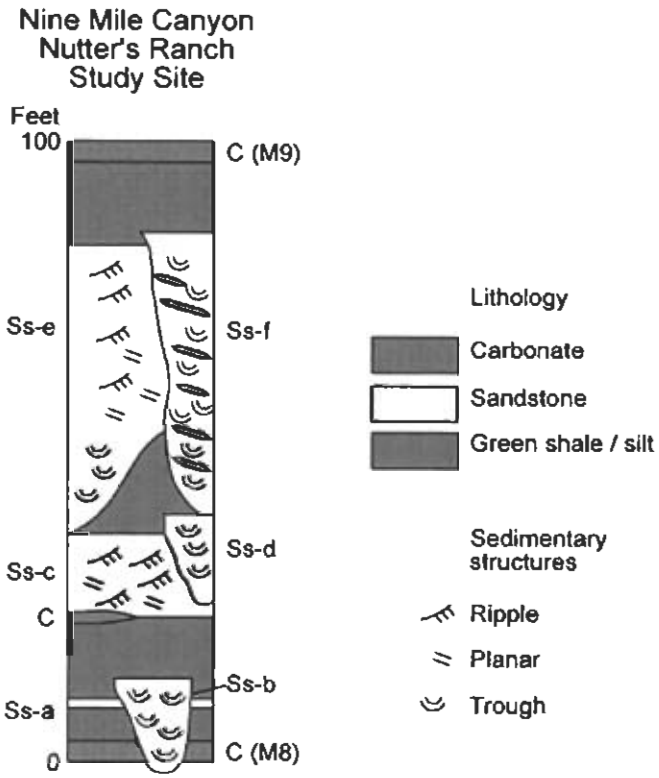

Figure 9. Composite vertical stratigraphic section of a 100-foot depositional cycle in the Nutter's Ranch study site in Nine Mile Canyon. Abbreviations (Ss-a, Ss-b, for example) refer to bed definitions in table 1.

Table 1. Lithology, description, and depositional interpretations from the Nutter's Ranch study site.

Lithology (bed designations)	Description	Depositional environment
Carbonate (C)	Oolitic/ostracodal grainstone and micrite, typically contains fossil hash. The beds weather orange.	Lagoonal, beach to shallow nearshore.
Sandstone (Ss-a)	Fine grain, rippled, tabular, thin (<3 feet), laterally continuous except where it is cut by channel sandstone body.	Flood-plain sheet flow.
Sandstone (Ss-b)	Fine grain, deeply incised channel-form bed, trough cross-beds, rip-up clasts and ooids common in lower portion, upper portion some ripples and soft-sediment deformation.	Nonsinuous streams on the upper delta plain.
Sandstone (Ss-c)	Fine grain, channel-form bed, laterally extensive amalgamated channels, planar base due to restrictive carbonate bed preventing downward cutting, promoting lateral migration. Fining upwards with upward decrease in scale of sedimentary structures from trough and low angle cross-beds to planar and rippled. Szantat (1990) Type I sandstone body.	High sinuosity, anatomizing channel deposit in the lower delta plain.
Sandstone (Sd-d)	Fine grain, channel-form bed, laterally limited, incised, individual channel deposit, concave upward lower bounding surface, fining upwards with upward decrease in scale of sedimentary features from lateral accretion beds, trough and low angle cross-bedding to planar and rippled.	Meandering distributary channel.
Sandstone (Ss-e)	Fine grain, channel-form bed, laterally extensive amalgamated channel deposits, concave upward lower bounding surface, fining upwards with upward decrease in scale of sedimentary features from lateral accretion beds, trough and low angle cross-bedding to planar and rippled. Szantat (1990) Type II sandstone body.	High sinuosity, anatomizing channel deposit in the lower delta plain.
Sandstone (Ss-f)	Fine grain, incised channel-form bed, laterally limited, typically inclined trough sets with shale drapes.	Proximal crevasse splay.
Sandstone (Ss-f)	Fine grain, coarsening upward with generally flat top, rippled, thin 1 to 3 feet thick, laterally extensive.	Distal crevasse splay.
Shale and siltstone	Green to gray-green shale and siltstone, typically thinly covered, highly weathered. Some thick covered slopes interpreted to be underlain by shale and siltstone.	Upper and lower delta plain, flood plain to mudflat, to swamp, possibly abandoned channel and overbank deposit.

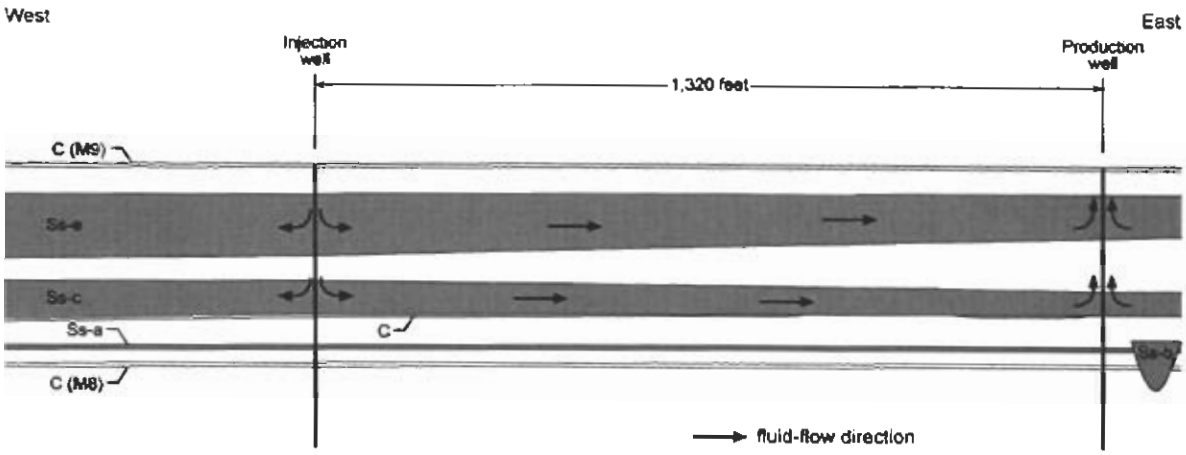

Figure 10. Hypothetical two-dimensional correlation and potential fluid-flow pattern between two imaginary wells "drilled" at the Nutter's Ranch study site. The correlations are based only on the data the "wells" penetrated and assume a continuous reservoir (Ss-e and Ss-c) between the two wells (see table 1 for lithologic unit descriptions).

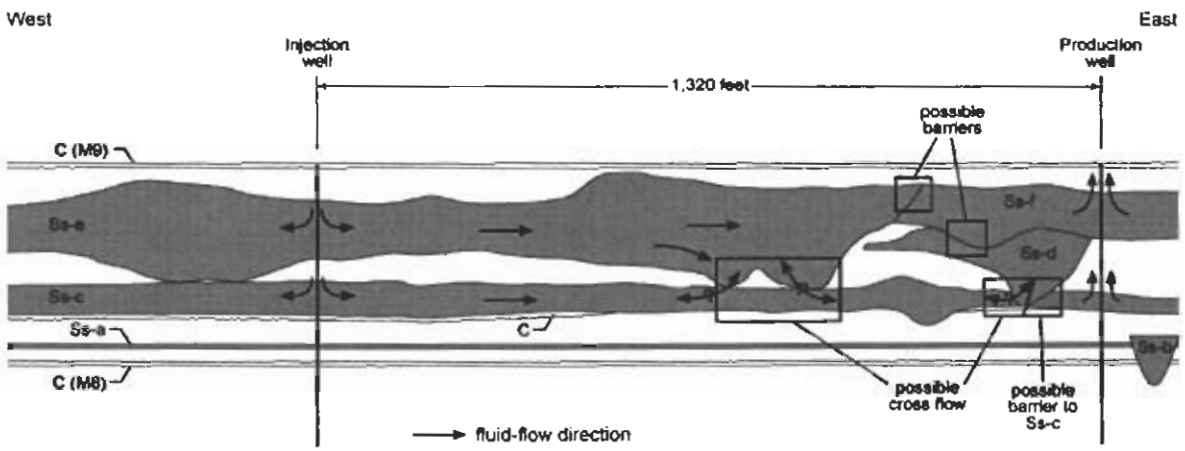

Figure 11. Actual two-dimensional correlation and potential fluid-flow pattern between the same two imaginary wells "drilled" at the Nutter's Ranch study site as in figure 10. The waterflood effectiveness and the "total oil produced" is much less than in the hypothetical model due to the reservoir heterogeneity. If a barrier exists between Ss-f and Ss-e, and a barrier exists between Ss-d and Ss-c, then oil in Ss-e and most of the oil in Ss-c will not be produced. Oil in Ss-d will also probably not be produced. The production "well" will only produce oil from Ss-f and a very limited amount of oil from Ss-c (see table 1 for lithologic unit descriptions).

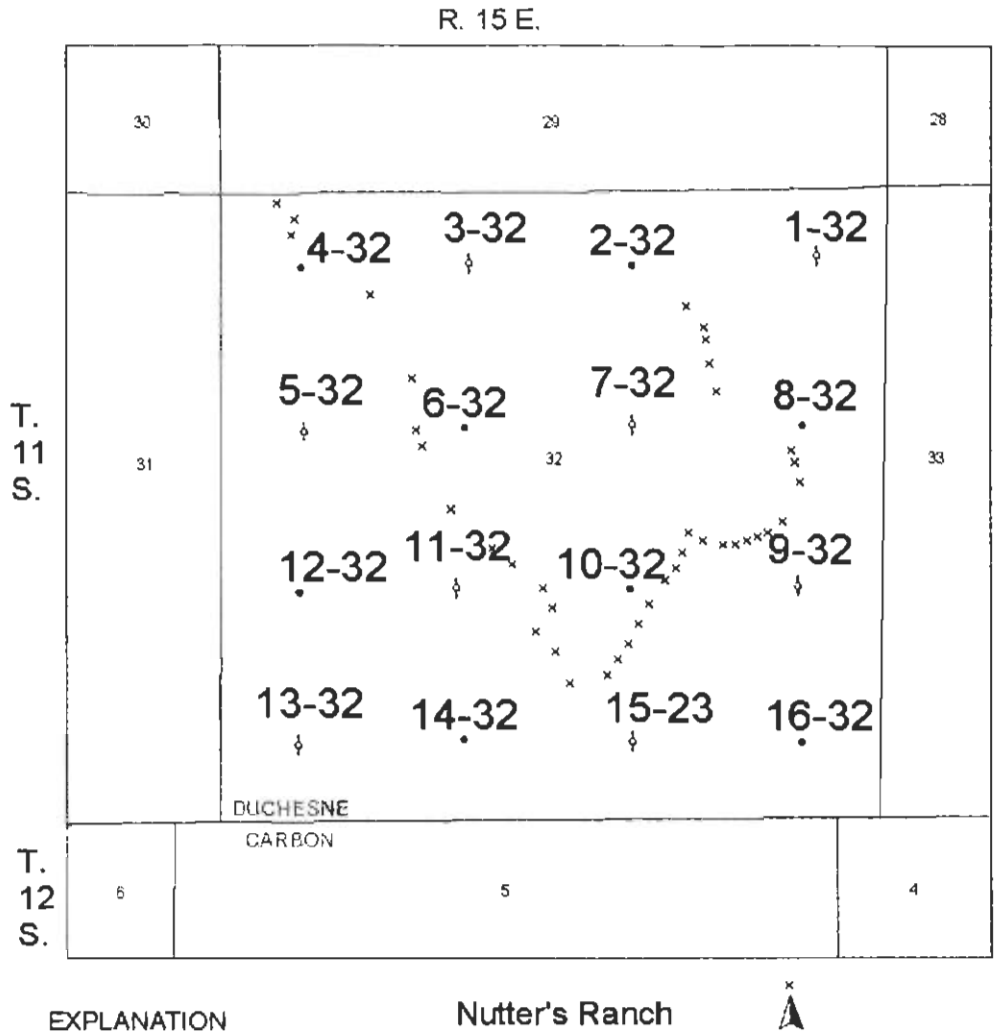

Figure 12. Map of Nutter's Ranch study site with imaginary well locations in the center of 40 acre lots.

located directly along the outcrop. The imaginary wells for the three-dimensional model are the centers of 40 acre (16.2 ha) lots and are not the same as the two-dimensional model imaginary well locations.

A draft of sandstone thickness maps based on the outcrop values, were constructed using Arcview Spatial Analyst® and by hand contouring. Sandstone thickness for each of the three beds were assigned to the imaginary wells based on the draft thickness maps and entered into the database. Final sandstone thickness maps for the three beds were generated using Arcview Spatial Analyst.

Ss-c (figure 13) is the most laterally extensive of the three potential reservoir beds. The bed is laterally extensive because it overlies a muddy limestone that it could not cut through, causing the channel to spread out. The alternating pattern of producer well and injector well would have some success in this bed. However, the thickest portion of this bed in the northwest quarter of the section is not penetrated and would be produced by wells on the flanks of the sandstone trend. Ss-d, which was shown in the two-dimensional model to nearly cut out Ss-c, isolates a portion of Ss-c in the center of the eastern most portion of the section.

Ss-d is narrow and has a very limited extent in the study area (figure 14) and would contain a very limited volume of oil. The 8-32 production well and 9-32 injection well penetrate the Ss-d but not along the axis of the sandstone bed. As a result, only a small portion of the limited oil volume of Ss-d would be produced.

Ss-e is moderately laterally extensive in the study site but is generally thicker, where present, than Ss-c (figure 15). The alternating pattern of production well and injection well appears to be moderately effective in Ss-e. Some of the thickest sandstone is between injection well 7-32 and production well 8-32. Production well 8-32 penetrated only 4 feet (1.2 m) of Ss-e, as a result, it would probably be a very poor producer and most of the oil contained in the thick sandstone between the two wells would remain in the ground.

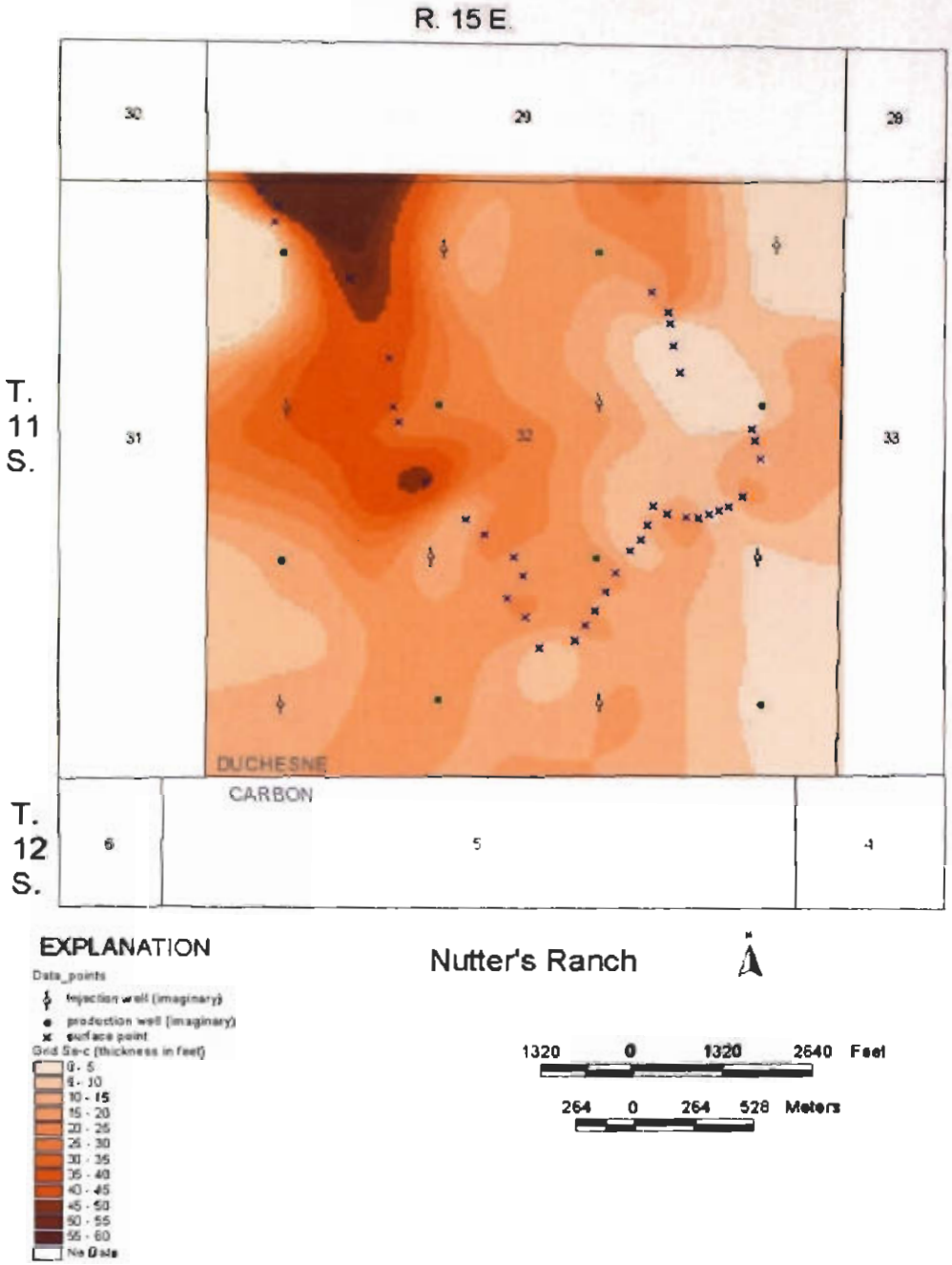

Figure 13. Map of Ss-c bed in the Nutter's Ranch study site. Grid interval is 5 feet.

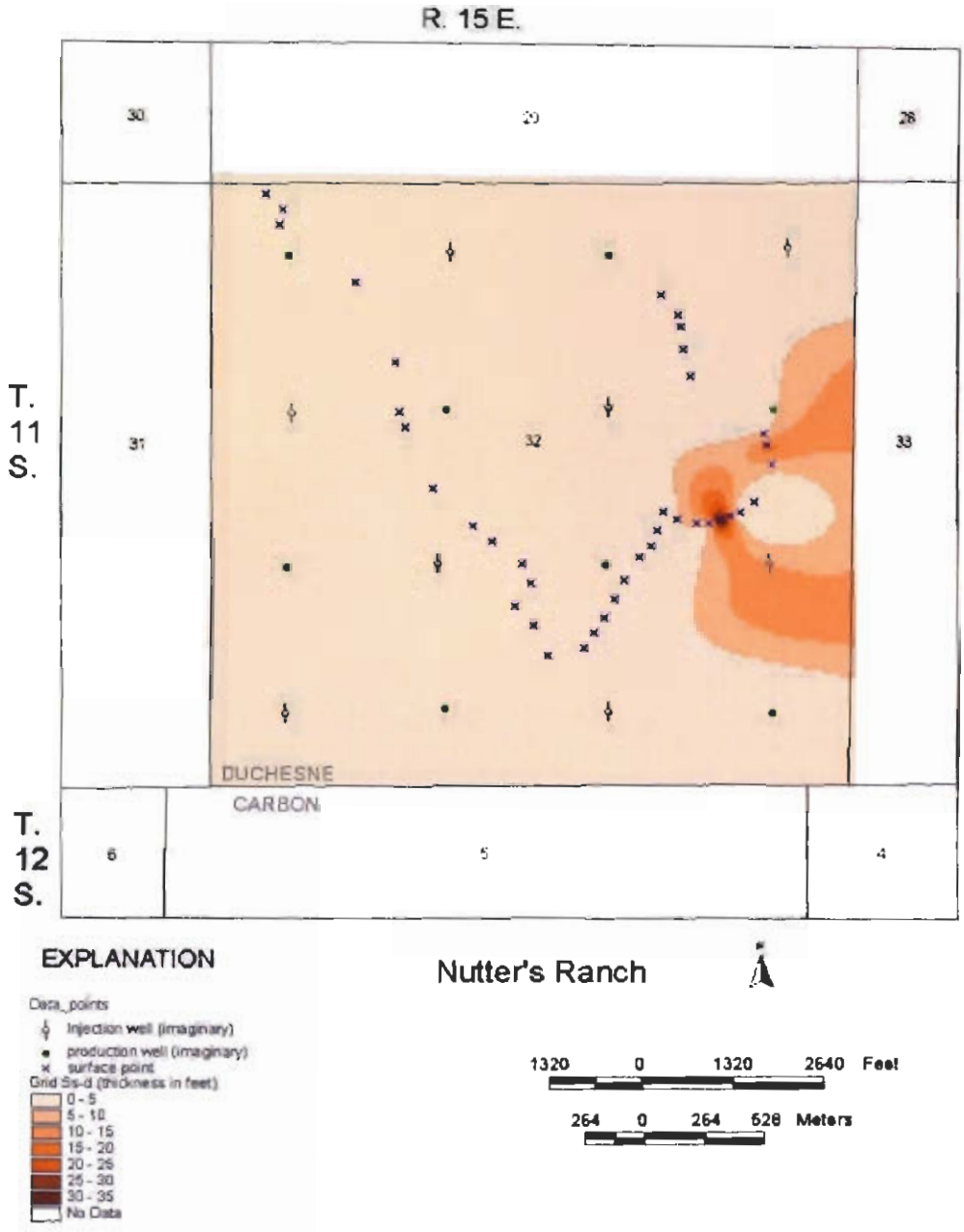

Figure 14. Map of Ss-d bed in the Nutter's Ranch study site. Grid interval is 5 feet.

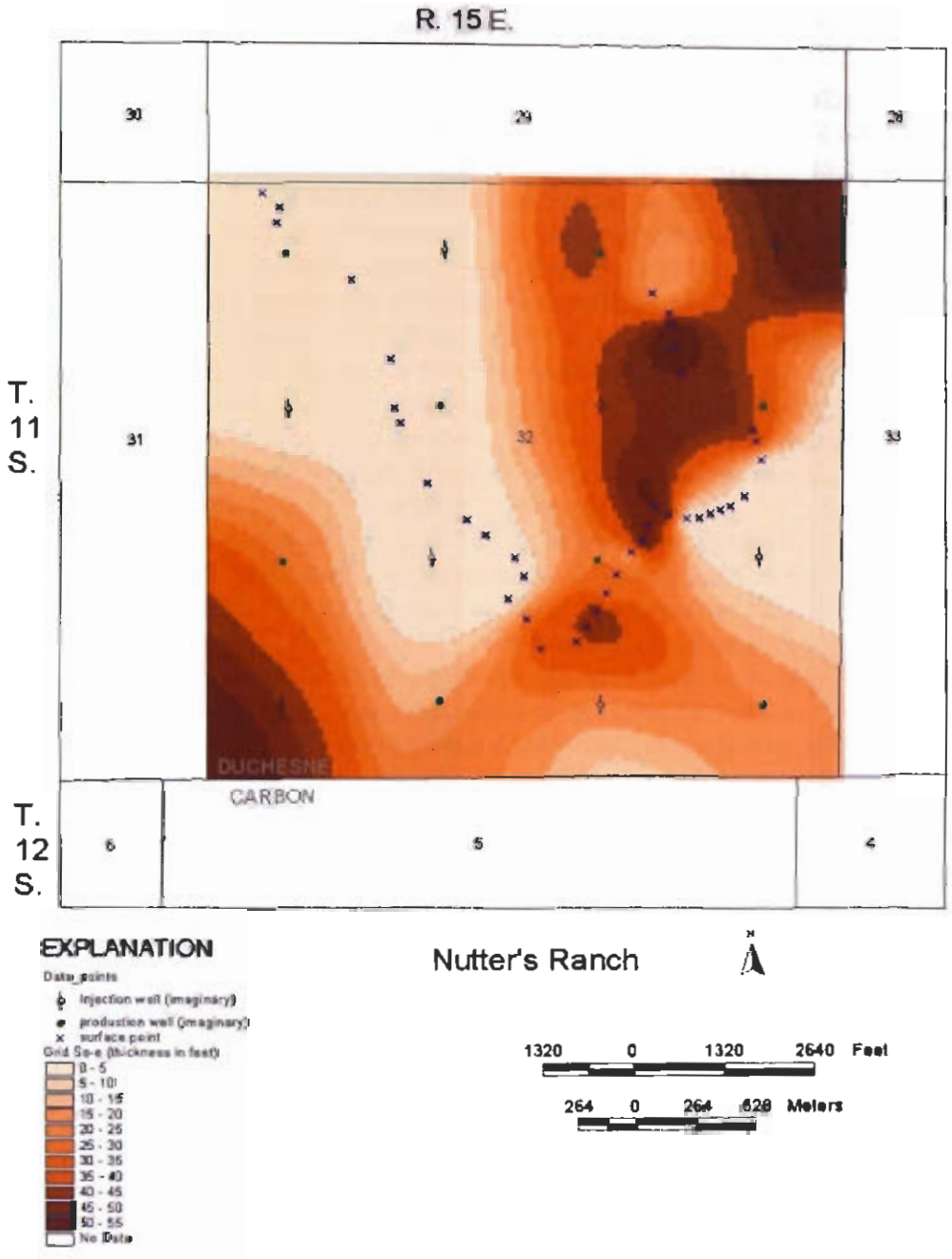

Figure 15. Map of Ss-e bed in the Nutter's Ranch study site. Grid interval is 5 feet.

HYDROCARBON RESERVOIRS IN THE LOWER AND MIDDLE MEMBERS OF THE GREEN RIVER FORMATION

Uteland Butte Reservoir

The Uteland Butte reservoir is the first major transgression of the lake after deposition of the alluvial Colton Formation. The Uteland Butte includes LGR 1 through LGR 5 log cycles (figure 4) and ranges in thickness from less than 60 feet (20 m) to more than 200 feet (60 m) in the southwest Uinta Basin. The Uteland Butte is equivalent to the first lacustrine phase of Bradley (1931), black shale facies of Picard (1955), lower black shale facies of Abbott (1957), basal limestone facies of Little (1988) and Colburn and others (1985), the Uteland Butte limestone of Osmond (1992), and the basal limestone member of Crouch and others (2000).

The Uteland Butte consists of limestone, dolostone, calcareous mudstone and siltstone, and rare sandstone. Most of the limestone beds are ostracodal grain-supported or mud-supported grainstone, packstone, or wackestone. Grainstone is more common near the shallow shoreline of the lake where as deeper distal deposits are commonly argillaceous limestone. A cryptocrystalline, dolomitized compacted wackestone with ostracods has been found near the top of the Uteland Butte in some core. The dolomite often has more than 20 percent porosity but is so finely crystalline that the permeability is low (single millidarcy or less).

Crouch and others (2000) working in Antelope Creek field (T. 5 S., R. 3 W., UBL) described the deposition of the Uteland Butte reservoir as a period of shoreline retrogradation and lake-level deepening. The lithology is described as micritic limestone, dolomicrite, and calcareous mudrocks. Little (1988), working in the Minnie Maud to Willow Creek Canyon area, described the deposition as shallow-water mud flats to offshore lacustrine. The lithology is dolomitized ostracodal and pellet grainstone and packstone, pelecypod-gastropod sandy grainstone interbedded with silty claystone or carbonate mudstone. Little (1988) describes 3- to 6-foot (1-2 m) thick beach- or bar-sandstone beds in the Minnie Maud area but absent in Willow Creek Canyon. Overall, siliciclastic rocks are rare in the Uteland Butte reservoir.

The Uteland Butte reservoir was deposited during a rapid and extensive lake-level rise. The Uteland Butte is distinctive in the abundance of carbonate and lack of sandstone which could have been caused by one or both of the following situations: (1) the rapid lake-level rise caused siliciclastic sediments to be deposited in the proximal alluvial channels, or (2) the main inflow into the lake was far from the southwest Uinta Basin area, perhaps flowing into the southern arm of the lake south and west of the San Rafael uplift.

The Uteland Butte reservoir is oil productive throughout most of the southwest Uinta Basin. The Uteland Butte is a secondary objective and usually perforated along with beds in the Castle Peak, lower Douglas Creek, and upper Douglas Creek reservoirs. The Uteland Butte is the primary producing reservoir in the Uteland Butte field (T. 10 S., R. 18 E., SLBL). Log cycles LGR 1 and LGR 2 are transitional with the underlying alluvial Colton Formation and are often not fully penetrated by wells in the southwest Uinta Basin. The interval LGR 3 through LGR 5 was mapped because it is typically fully penetrated and has a very distinctive log character that is easily recognized throughout the southwest Uinta Basin. The isopach of LGR 3 through LGR 5 (plate 11) is divided into three areas: (1) the proximal area which varies considerably in thickness due to interfingering of lacustrine and alluvial Colton deposits, (2) a northeast to southwest thin where shallow lacustrine beach- and bar-sandstone beds were deposited, and (3) the thick distal area.

The isopach thin extends from the Uteland Butte field in the northeast to the Minnie Maud area in the southwest. Sandstone is the most productive bed in the Uteland Butte field. Little (1988) described beach- and bar-sandstone deposits in the Minnie Maud area that are absent in Willow Creek Canyon to the west-northwest. The isopach thin defines the shallow lacustrine shelf where the sandstone beds were deposited and is the best area to explore for new oil deposits in the Uteland Butte reservoir.

The Uteland Butte reservoir is perforated in numerous wells in the distal area where the reservoir is almost entirely carbonate, having no sandstone. Crouch and others (2000) report that the carbonate in the Antelope Creek field has 0.4 to 0.01 md permeability resulting in very low oil recovery. As a result it is a secondary objective and not the primary target of drilling.

The cryptocrystalline dolomitic wackestone has not been extensively explored. This bed is potentially widely distributed throughout the southwest Uinta Basin. The dolomitized wackestone would be a low-volume oil producer similar to the carbonates in the Antelope Creek field because of the low permeability. As a result, many explorationists may have overlooked this objective. If areas of better developed permeability (sweet spots) can be found, the high porosity of the bed should yield significant oil potential.

Castle Peak Reservoir

The Castle Peak reservoir is defined as the stratigraphic interval from the top of the Uteland Butte (LGR 5) to the top of the carbonate marker bed of Ryder and others (1975) (figure 4). The Castle Peak is equivalent to the Wasatch (Colton) tongue and second lacustrine phase of Bradley (1931), the Colton tongue and carbonate marker unit of Ryder and others (1975), and is included in Picard's (1955) black shale facies. The alluvial Colton tongue is exposed in Willow Creek and Nine Mile Canyons but extends only a few miles north. Above the Colton tongue the Castle Peak consists of interbedded black shale, limestone, limy mudstone, with some sandstone and siltstone. The sandstone beds, which are productive in some areas, are generally fine to medium grained, and were deposited as isolated channels.

The Castle Peak sandstone is typically medium-grained (0.36 to 0.44 mm), poorly to moderately sorted, angular to very well rounded, mostly lithic arkose or feldspathic litharenite. Most of the other sandstone beds in the lower and middle members of the Green River Formation are very fine to fine grained.

Framework elements of the Castle Peak sandstone include monocrystalline and polycrystalline quartz, potassium feldspar (orthoclase and microcline), plagioclase, chert, sheared metaquartz, recrystallized metaquartz, hydrothermal quartz, intrusive rock fragments, dolomite, siltstone and mudstone clasts, carbonate ooids, isolated mica booklets (biotite, chlorite, and muscovite), some red-brown hematite staining, and assorted heavy minerals including zircon, epidote, tourmaline, sphene, and rare amphibole.

The Castle Peak sandstone are typically highly compacted with extensive quartz and feldspar cementation. Porosity and permeability in the sandstone is typically a result of dissolution of feldspars and some of the rock fragments. Trumbo (1993) reports an average porosity of 11 percent and 0.1 md permeability for the Castle Peak sandstone in Brundage Canyon and Sowers Canyon fields (T. 5 S., R. 4 W. to 5 W., UBL). Fractures in the sandstone most commonly develop at the base of the bed where the carbonate content is usually highest resulting in increased brittleness.

Hackney and Crouch (2000) working in the Antelope Creek field (T. 5 S., R. 3 W., UBL) defined 17 cycles of relative lake level rise and fall. They described the cycles as consisting of "progradational and retrogradational sandstone beds bounded above and below by transgressive

limestone that onlap shoreward." In the Nine Mile Canyon area south of Antelope Creek field, the Castle Peak consists of a tongue of the Colton Formation overlain by multiple channel sandstone and floodplain deposits with a few interbedded limestone beds.

The Castle Peak stratigraphic interval thins from south to north (plate 12). An isopach map of the sandstone in the Castle Peak show a thick in the southern (highstand) and northern (lowstand) portions of the study area with an intervening thin (plate 13). The highstand deposits consist of alluvial sandstone (Colton tongue) and marginal lacustrine sandstone deposited during highstand lake levels. The lowstand consists of isolated marginal lacustrine channel sandstone encased in carbonate deposited during lake level fall and rise. The intervening zone of sediment bypass provides a regional updip trap for hydrocarbons in the Castle Peak. The sandstone beds in the Castle Peak are typically single, isolated channel deposits with limited lateral extent; channel stacking is rare. In the greater Monument Butte area, a drill hole will typically encounter a single channel (or none) in each depositional cycle. The lack of channel stacking is attributed to the short duration of the lake level rise and fall cycles. As a result, the drainage for each cycle never advanced beyond the initial stage. Schumn and Ethridge (1994) show that the initial drainage pattern on an exposed shelf is typically a series of parallel unconnected channels.

Lower Douglas Creek Reservoir

The lower Douglas Creek reservoir is defined as the stratigraphic interval from the top of the lower member of the Green River Formation (carbonate marker bed) to the base of the upper Douglas Creek (top of log-cycle MGR 3) (figure 4). The lower Douglas Creek is part of the middle member and ranges in thickness from 270 to 700 feet (80 to 200 m) in the southwest Uinta Basin (plate 14). The proximal lower Douglas Creek includes the alluvial deposits of the Renegade Tongue (Cashion, 1967) of the Colton Formation. The distal lower Douglas Creek is considered part of the black shale facies of Picard (1955) consisting of marginal-lacustrine and open-lacustrine deposits of interbedded sandstone and shale with some thin carbonate beds.

Throughout the region many of the sandstone beds in the lower Douglas Creek were deposited by channels and shallow bars, which locally contain oil. The primary reservoir in the lower Douglas Creek is turbidite and shallow lacustrine sandstone beds deposited in narrow cut-and-fill valleys along the shelf break during several lake level fall-and-rise cycles. Lutz and others (1994) described the lower Douglas Creek as moderate- to low-density turbidite channel deposits, debris flow and gravity flow deposits. Thickness of the sandstone in the cut-and-fill valleys can vary from more than 100 feet (30 m) in a well to zero in a neighboring well 1,320 feet (402.3 m) away. In areas where cut-and-fill did not occur less-productive marginal-lacustrine sandstone was deposited, as a result, a sandstone isopach does not accurately define the cut-and-fill reservoir area (plate 15). The 50-foot sandstone contour in the northern portion of the mapped area does crudely define a division of gradual thicks and thins from a more rapid change in thickness north of the contour. This may represent the approximate boundary of the shelf edge or it may just be a result of decreasing data points from north to south. The lower Douglas Creek is the only stratigraphic interval in the lower or middle members where there is evidence of a sharp shelf break in the southwest area. The shelf break may have developed in response to increased tectonic subsidence of the basin.

Two rock types comprise the majority of the sandstone beds in the lower Douglas Creek reservoir. Rock-type 1 is a very poorly sorted combination of silt and very fine grained sand that commonly contains detrital clay coating around many of the grains as well as large clasts of highly compacted dolomitic and illitic mudstone. Rock-type 1 typically has poor porosity and permeability due to tight grain packing, sporadic detrital clay coating, and pseudomatrix

formation of mudstone clasts. Rock-type 2 is a laminated assemblage of very fine to fine grained sandstone that has the appearance of a chaotic breccia of haphazardly distributed carbonate mudstone clasts in a poorly sorted silt to very fine grained matrix with abundant soft-sediment deformation features. Rock-type 2 typically has low porosity and permeability due to tight grain packing, illite coating the grains, and a general lack of secondary intergranular pores. Fractures in the lower Douglas Creek sandstone are rare due to the clay content reducing the overall brittleness of the beds.

Upper Douglas Creek Reservoir

The upper Douglas Creek reservoir is defined as the stratigraphic interval from the top of the lower Douglas Creek (MGR 3) to the top of the Douglas Creek Member of the Green River Formation (MGR 7) of Bradley (1931) (figure 4). The upper Douglas Creek is part of the middle member and ranges in thickness from 250 feet (75 m) to less than 500 feet (150 m) in the southwest Uinta Basin (plate 16). The upper Douglas Creek is the primary reservoir in the greater Monument Butte area of the southwest Uinta Basin. The reservoir consists of amalgamated channel and distributary-mouth bar sandstone deposited on the distal lower delta plain of Lake Uinta. The upper Douglas Creek reservoir is a lowstand deposit with an area of sediment bypass forming the updip trap. A similar highstand deposit is mapped in the proximal position where the rocks are exposed in the Nine Mile and Desolation Canyons.

Two rock types comprise most of the sandstone beds in the upper Douglas Creek reservoir. Rock-type 1 is the most abundant and is typically very fine to fine grained (median 0.11 to 0.17 mm), moderately well sorted to well sorted, subangular to subround. The framework assemblage is similar in composition and abundance to the medium-grained sandstone in the Castle Peak sandstone except the very fine to fine grained sandstone has more biotite, chlorite, and muscovite, and the mudstone fragments are dolomitic, ankeritic, and carbonate allochems including ankeritic/dolomitic ooids, ankeritic/dolomitic rip-ups, ostracods, or interclasts.

Some of the sandstone show early cementation with iron-poor calcite, which greatly reduced the effects of compaction. Later dissolution of the iron-poor calcite resulted in some beds with permeabilities in the tens of md and porosity more than 20 percent. Some of the sandstone had a later stage of cementation with dolomite, ankerite, siderite, and iron-rich calcite, which greatly reduced the rock pore space. Partial dissolution of the late-stage cementation has resulted in 10 percent or more porosity with permeability rarely exceeding 20 md in some sandstone beds.

Rock-type 2 is a sandstone consisting of very fine grained sand and coarse silt with increased clay content. Rock-type 2 is a ripple drift lamination facies found at the upper portion of a fining upward sandstone sequence. The rock-type 2 sandstone is more poorly sorted, angular to subangular, has more of the grains are coated with illite, and contains more mica, especially muscovite, than the rock-type 1 sandstone. Examination of rock-type 2 sandstone shows that severe compaction occurred soon after deposition, which developed abundant microstylolites. Rarely is early iron-poor calcite cement found in rock-type 2. Dissolution of feldspars is minor, resulting in low porosity (less than 10 percent) and low permeability (0.1 md or less).

Garden Gulch Reservoir

The Garden Gulch reservoir is defined as the stratigraphic interval from the top of the Douglas Creek to the top of MGR 18 (figure 4). The Garden Gulch ranges from 550 feet (167.6 m) to more than 1,200 feet (365.8 m) thick in the southwest Uinta Basin. The Garden Gulch was divided into a lower portion (MGR 12 to MGR 7), which is equivalent to upper portion of the delta facies in Nine Mile Canyon (Remy, 1992) and an upper portion (MGR 18 to MGR 12), which is equivalent to most of the transitional facies (Remy, 1992). The thickness map of the lower portion of the Garden Gulch (plate 17) shows slight evidence of the delta shape. The thickness map of the upper portion of the Garden Gulch (plate 18) shows a strong west-to-east to slightly southwest-to-northeast trend, indicating a normal shoreline without the influence of a well-developed delta.

The Garden Gulch consists of interbedded sandstone, shale, and limestone. The Garden Gulch was deposited during a time of overall lake-level rise, transitional from the underlying delta facies in the Douglas Creek Member to the overlying deep-lake oil shale deposits of the upper member, resulting in less total sandstone and generally individual, isolated channel and bar deposits. The sandstone in the Garden Gulch reservoir is similar in composition to the upper Douglas Creek sandstone. There are fewer fining upward sequences and therefore less type-2 ripple drift laminated facies.

PALEODEPOSITIONAL HISTORY OF THE HYDROCARBON RESERVOIRS IN THE LOWER AND MIDDLE MEMBERS OF THE GREEN RIVER FORMATION

The deposits of the lower and middle members of the Green River Formation record a transitional lake history from passive carbonate shoreline to active delta building to major lake expansion and deepening.

The Uteland Butte interval was deposited over the alluvial sediments of the Colton Formation during a major lake expansion. Shoreline, and shallow open-lacustrine deposition was dominated by carbonate with very minor amounts of siliciclastic (figure 16). The lack of siliciclastic deposition is attributed to two causes: (1) the rise in base level where by most siliciclastic to deposition occurred in the fluvial channels before reaching the lake, and (2) the southwest Uinta Basin was not the site of the main in flow into the lake.

The Castle Peak interval was deposited during a period of numerous rapid lake level fall-and-rise cycles. A general parallel drainage pattern developed across the lower portion of the exposed, low-angle shelf during lake-level fall with an updip area of sediment bypass (figure 17). A rapid rise in the lake level resulted in isolated channels encased in lacustrine carbonate above and below, in the distal northern portion of the southwest Uinta Basin.

The top of the lower member-base of middle member marks a significant change in the structure of the southwest Uinta Basin. The top of the lower member is the carbonate marker bed, which was deposited during a lake highstand. The carbonate marker bed ranges from shallow lacustrine laminated algal limestone and grainstone in the proximal reaches (Nine Mile Canyon) to muddy limestone in the more distal open lacustrine reaches of the lake (Willow Creek Canyon and Antelope Creek-Monument Butte area). The lower member is overlain by lower Douglas Creek, which consists of alluvial deposits of the Renegade Tongue (Cashion, 1967) in Desolation and Nine Mile Canyons, and the green shale facies (Picard, 1957, 1955) in Willow Creek Canyon, a significant basinward shift of facies. But in the Antelope Creek-Monument Butte area, the lower Douglas Creek is composed of the black shale facies, an open-lacustrine deposit. The lake may have been reduced in size as evidenced by the basinward shift of the shoreline, but may have also deepened in the distal reaches, as evidenced by the deposition of black shale. Tectonic movement in the basin is needed to cause a regression of the shoreline with accompanying deepening of the lake. The lower Douglas Creek reservoir in the Antelope Creek-Monument Butte area consists of black shale with thick (100+ feet [m]) sandstone beds deposited in very narrow cut-and-fill valleys (figure 18) formed during lake-level falls, indicating a slope with a steep shelf break, which did not exist during deposition of the lower member.

The upper Douglas Creek of the middle member of the Green River Formation, represents deposition in an active lowstand delta built on a gentle slope, resulting in significant shifts in the shoreline during rise-and-fall cycles of the lake. The shallow shelf was the site of several depositional cycles that resulted in amalgamation and stacking of distributary channels and distributary mouth bars in both lowstand (greater Monument Butte area) and highstand (Nine Mile Canyon area) deltas (figures 19 and 20). The lowstand delta deposits are dominantly dolomitic black shale and marginal- to shallow-lacustrine distributary-channel and mouth-bar sandstone. The highstand delta deposits contain more marginal-lacustrine green shale, grainstone and micrite, and distributary- and fluvial-channel sandstone. A zone of sediment bypass separates the highstand and lowstand areas.

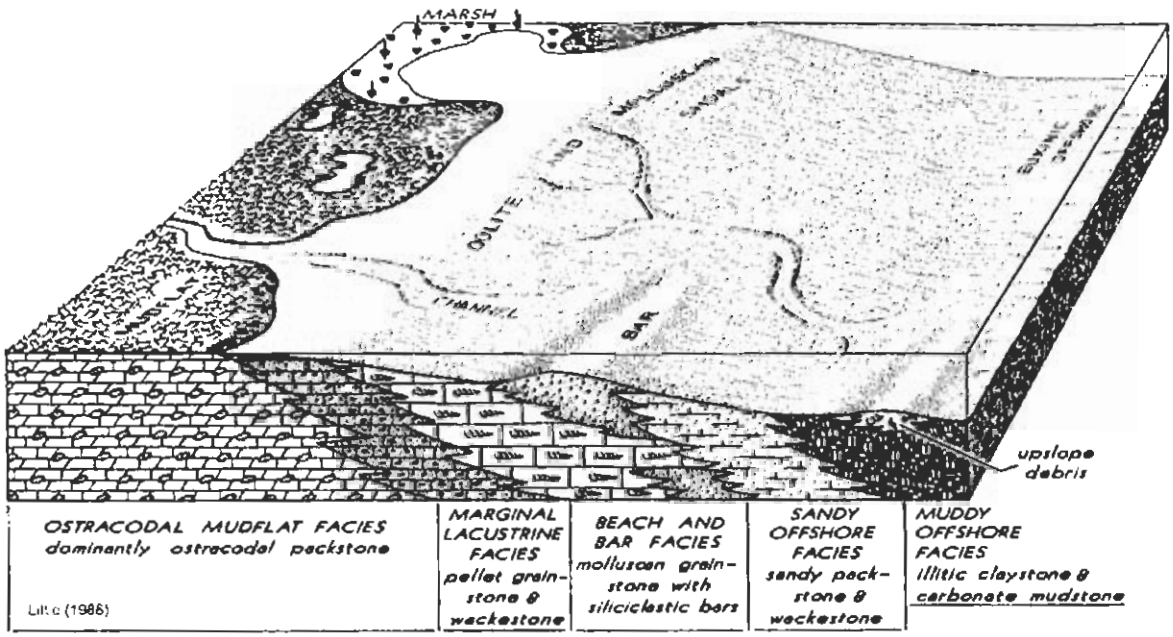

Figure 16. Conceptual three-dimensional diagram depicting the major facies of the Uteland Butte interval of the lower member of the Green River Formation (modified from Little, 1988).

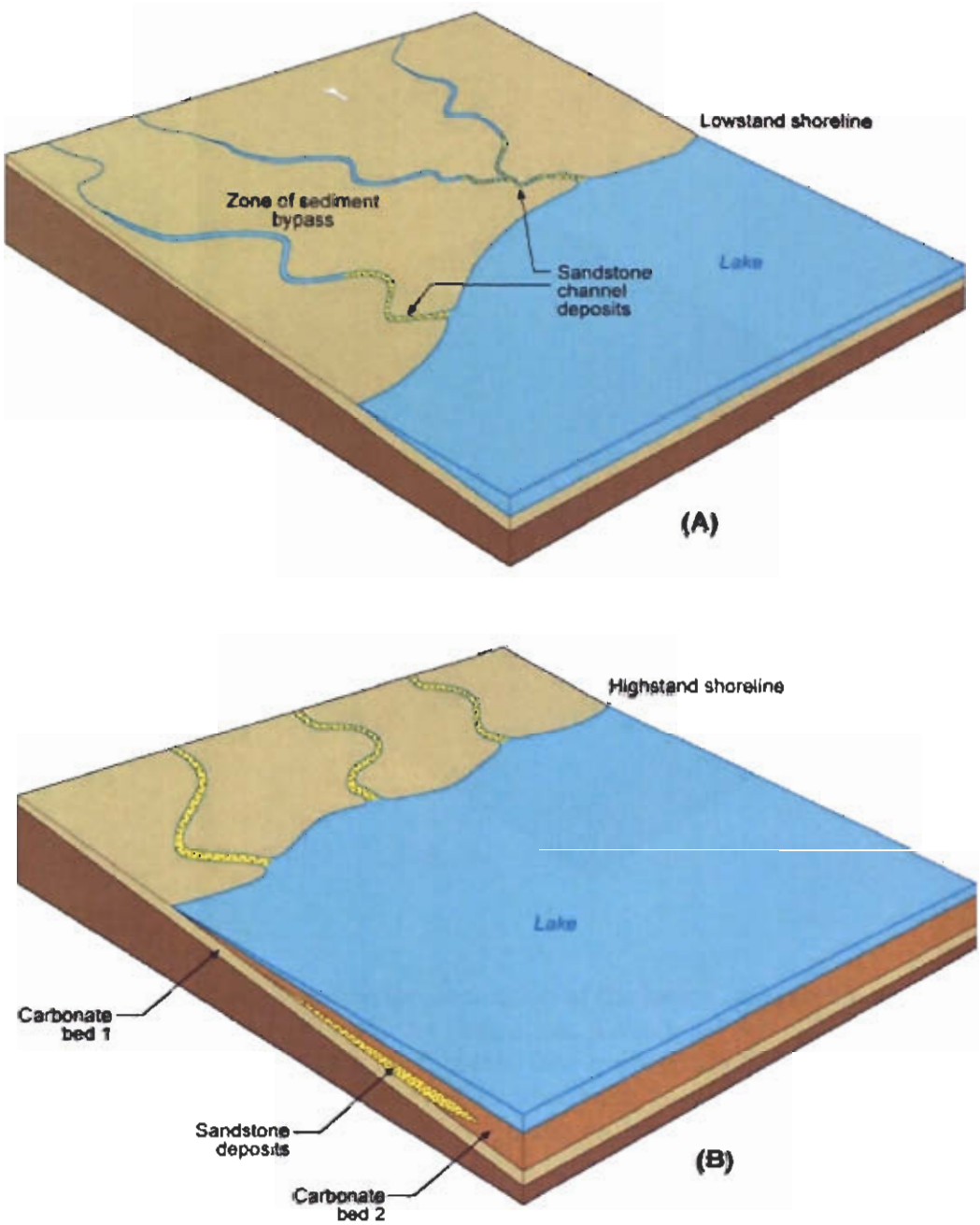

Figure 17. Diagrams depicting the deposition of the Castle Peak interval of the lower member of the Green River Formation. (A) Lake-level fall results in a lowstand shoreline and initial parallel drainage across a gently sloping shelf. (B) Lake-level rise results in a highstand shoreline. Sandstone is deposited in the lower reaches of the lowstand channels during initial lake-level rise, resulting in sandstone encased in carbonate.

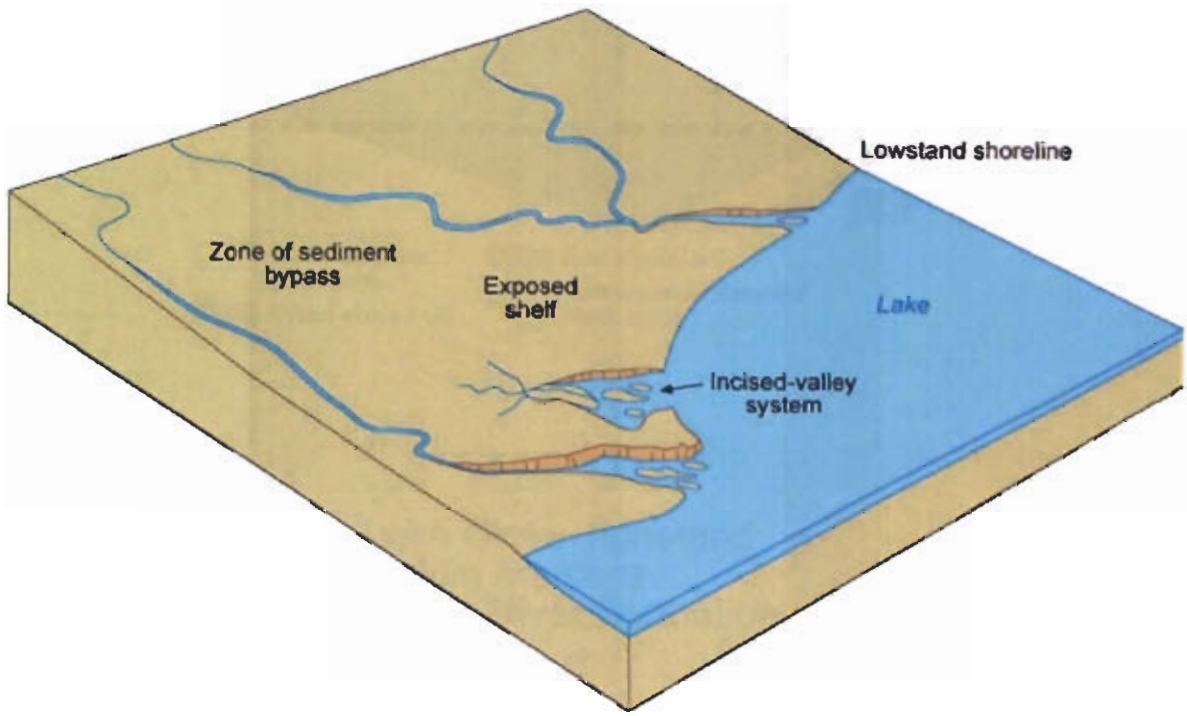

Figure 18. Diagram depicting the deposition of the lower Douglas Creek reservoir of the middle member of the Green River Formation. Lake-level fall results in deeply incised valleys cut along the exposed shelf break. The exposed shelf and lowstand shoreline are dominantly composed of open lacustrine black, silty, dolomitic shale. Lake-level rise results in the incised valleys filling with siliclastic shallow-lacustrine, gravity-flow and turbidity deposits.

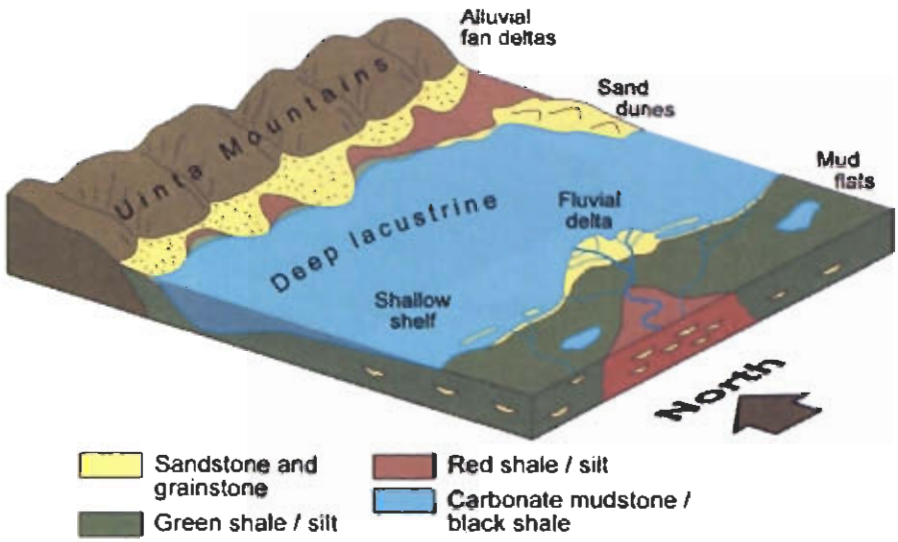

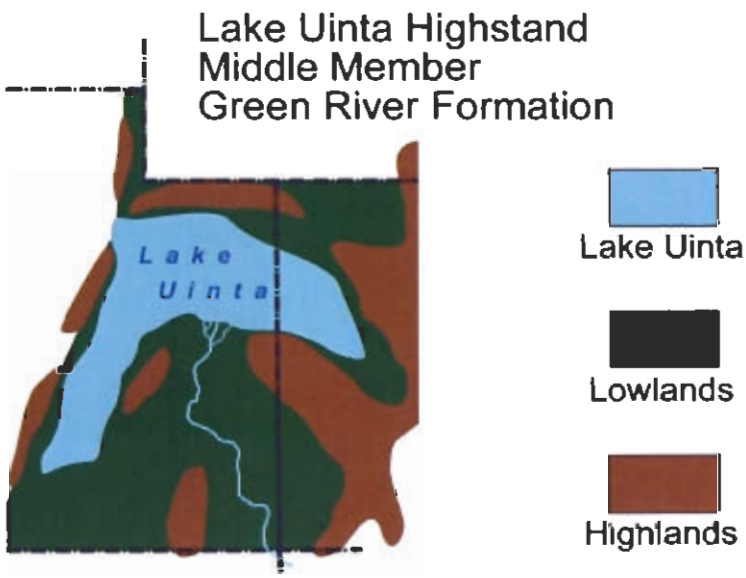

Figure 19. (A) Block diagram depicting a highstand delta deposited during the upper Douglas Creek interval of the middle member of the Green River Formation. (B) Paleogeography of Lake Uinta during highstand deposition of the upper Douglas Creek reservoir (modified from McDonald, 1972).

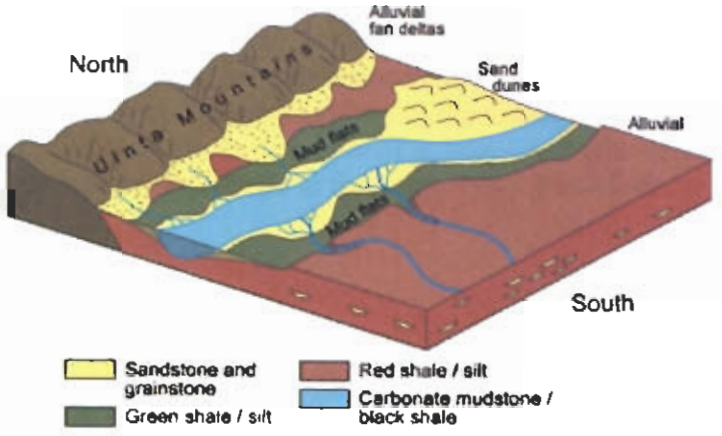

A

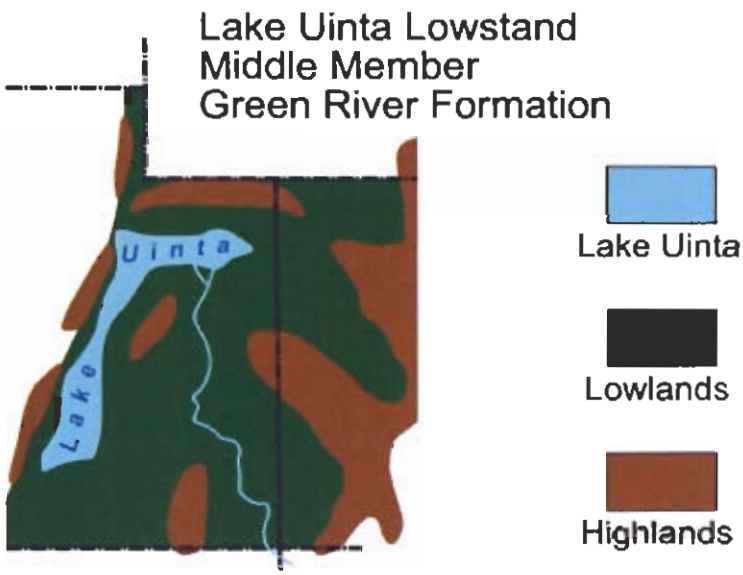

B

Figure 20. (A) Block diagram depicting a lowstand delta deposited during the upper Douglas Creek interval of the middle member of the Green River Formation. (B) Paleogrography of Lake Uinta during lowstand deposition of the upper Douglas Creek (modified from McDonald, 1972).

The Garden Gulch interval of the middle member of the Green River Formation, represents deposition during a period of significant expansion of the lake. The end of the Garden Gulch and middle member, is marked by the Mahogany oil shale in the upper member, which was deposited during the maximum expansion and maximum depth of the lake. Distributary-channel and shallow-lacustrine bars in the Garden Gulch were deposited during lake-level falls. But with the lake generally expanding, lake-level falls resulted in fewer, more isolated, individual channel deposits in the southwest Uinta Basin.

OIL FIELD EXAMPLES

Geological characterization, consisting of correlating and mapping all perforated beds, was carried out on portions of three oil fields: (1) Uteland Butte, (2) Brundage Canyon, and (3) Monument Butte Northeast (figure 21). The fields are examples of three different reservoir types found in the southwest Uinta Basin (figure 4). The Uteland Butte field produces oil from the Uteland Butte reservoir (units LGR 1 through LGR 5), also known as the basal Green River carbonate of the lower member. The Brundage Canyon field produces oil from sandstone beds in the Castle Peak reservoir, also known as the carbonate marker unit in the lower member. The Monument Butte Northeast water-flood unit produces from the upper Douglas Creek reservoir, units MGR 4 through MGR 7 (B, C, and D sands in operator terminology). Additionally, most wells are perforated in other beds throughout the lower and middle members of the Green River Formation.

Uteland Butte Field

The Uteland Butte oil field covers parts of sections 2, 3, 10, and 11, T. 10 S., R. 18 E., SLBL, Uintah County, Utah. The wells are perforated in the Uteland Butte reservoir (units LGR 5 through LGR 1), also known as the basal Green River carbonate in the lower member of the Green River Formation (figure 4). The reservoir is dominantly carbonate, varying from limestone to limy dolomite to dolomite, with rare thin sandstone beds in an area of regional north dip and no structural closure (figure 22). The field is in primary production. The wells are low volume, typically producing less than 100,000 barrels (16,000 m^3) of oil per well (figure 23). The field has a normal decline in monthly oil production (figure 24). Most of the gas production from the Uteland Butte field is from deeper Colton and Mesaverde beds. The monthly gas production is erratic due to seasonal demand for the natural gas.

Bed thickness defined with the gamma-ray curve, and porosity determined by the density and neutron logs, show only minor variation over the field area and do not define the reservoir and trap. Subtle permeability changes related to the gradual lithology variations probably provide the stratigraphic trap in the Uteland Butte field. The Uteland Butte reservoir is a secondary objective in most other fields in the southwest Uinta Basin because of the low volume of oil production.

Most of the perforated beds in the Uteland Butte field are carbonate except bed 1c, which is a sandstone. Bed 1c is perforated in all of the wells (plates 19 and 20) and is responsible for most of the production. Bed 1c ranges from 8 to 22 feet (2.4 to 6.7 m) thick in the Uteland Butte field (figure 25).

Brundage Canyon Field

The Brundage Canyon oil field covers most of T. 5 S., R. 4 W., and the eastern portion of T. 5 S., R. 5 W., UBL, Duchesne County, Utah. Our study focused on all of section 25 and part of section 24, T. 5 S., R. 5 W., UBL, and parts of sections 19 and 30, T. 5 S., R. 4 W., UBL (figure 26). There are 10 beds perforated in one or more wells in the portion of the Brundage Canyon field studied (plates 21 and 22).

The objective in Brundage Canyon field is sandstone beds in the Castle Peak reservoir, also known as the carbonate marker unit of the lower member of the Green River Formation. The field is in primary production. Sandstone distribution and porosity are important reservoir

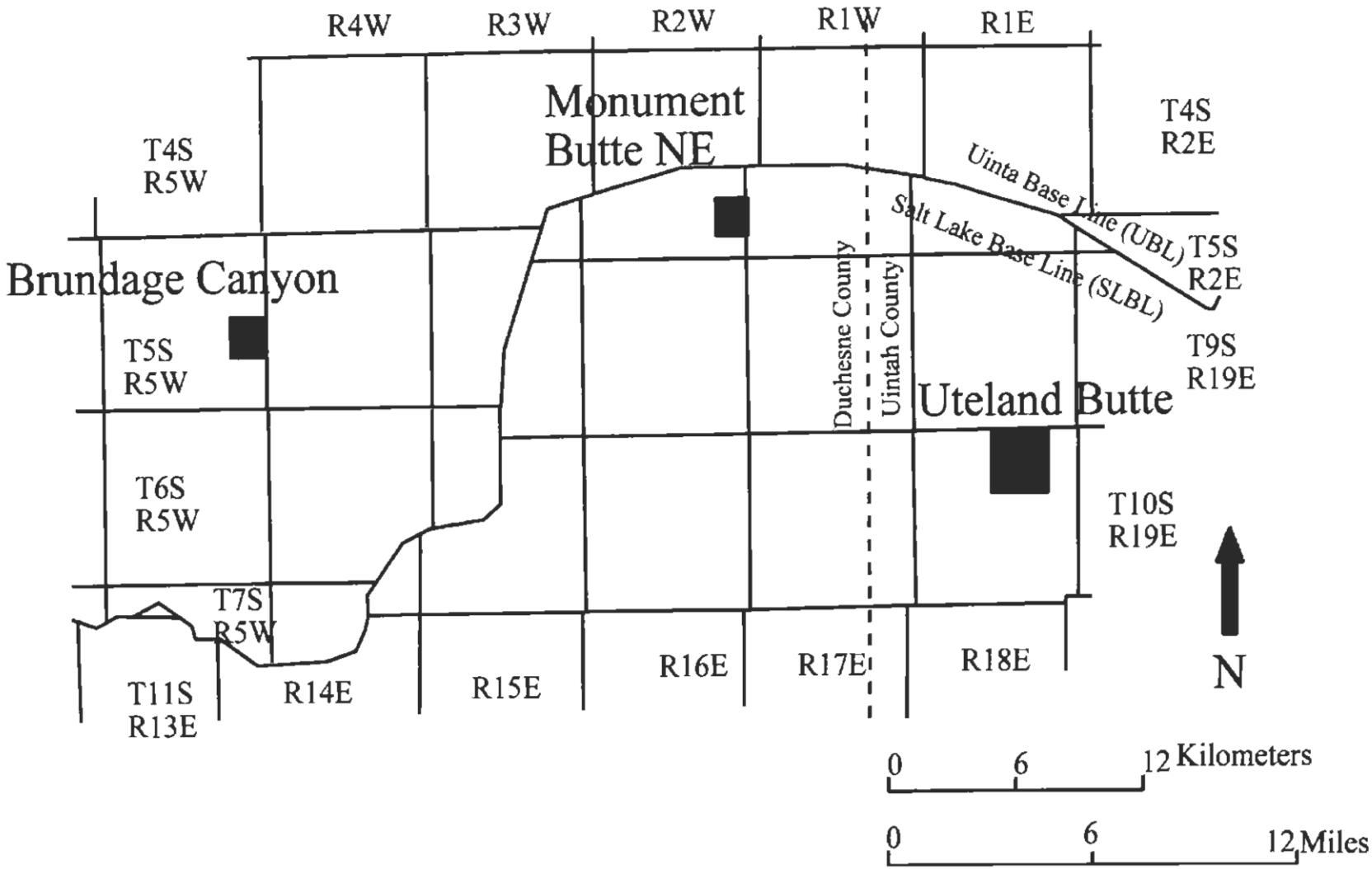

Figure 21. Map showing the location of the Uteland Butte and Brundage Canyon fields, and Monument Butte Northeast unit, that were studied in detail for this report.

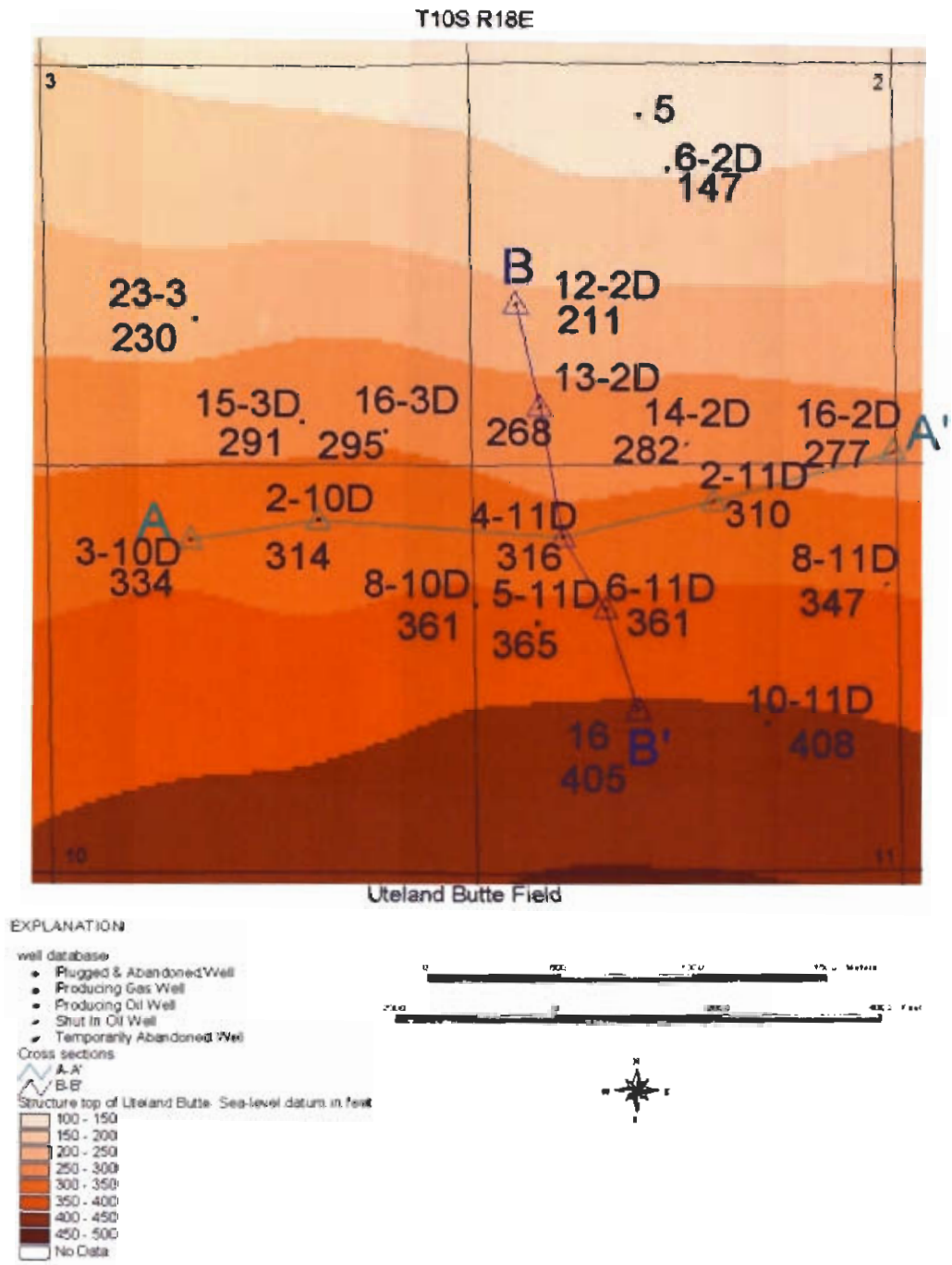

Figure 22. Map of Uteland Butte field showing wells, well numbers, cross section locations, and gridded structure of the top of the Uteland Butte reservoir. Grid interval is 50 feet, sea-level datum. Cross section A – A' is plate 19 and cross section B – B' is plate 20.

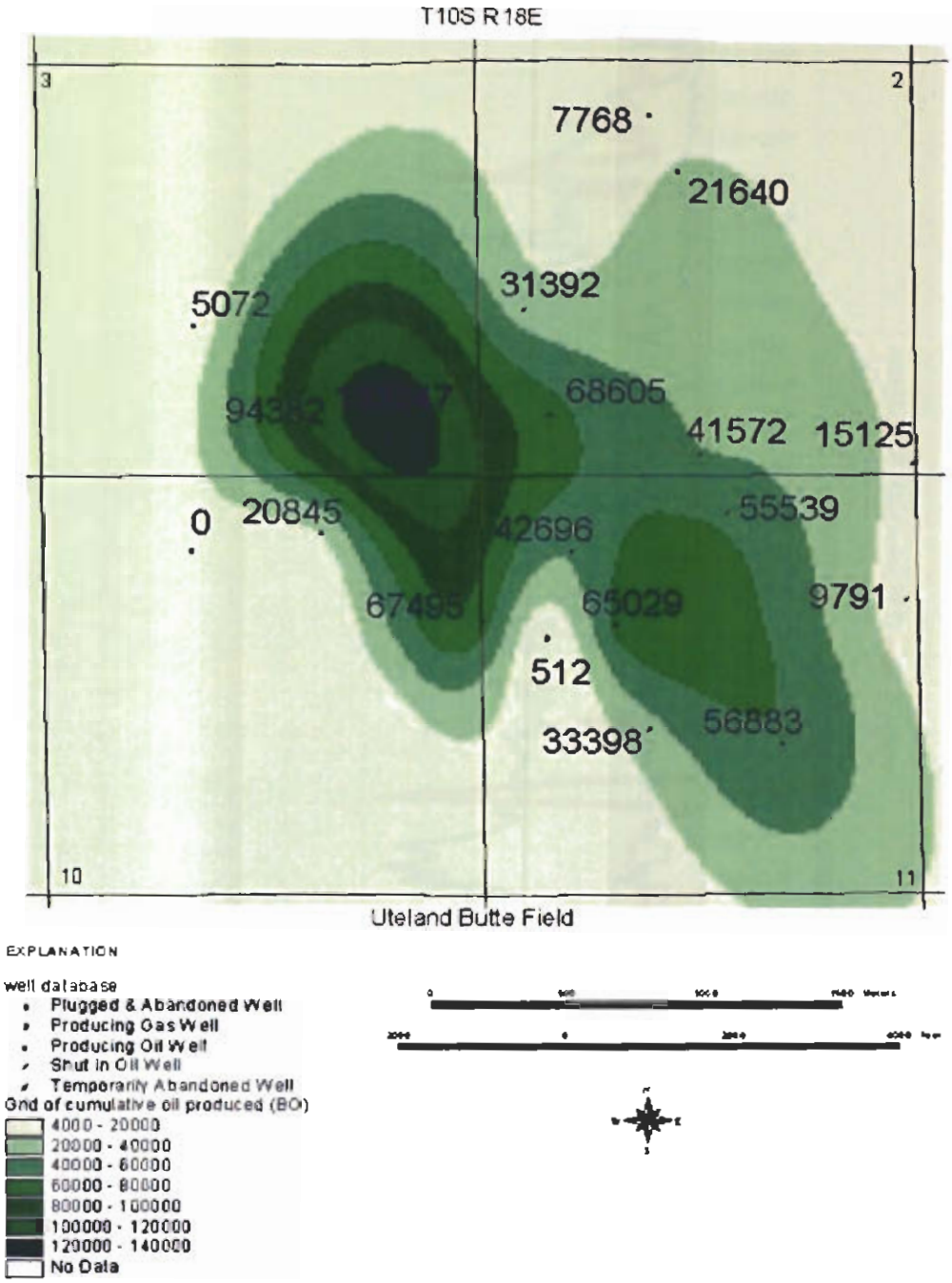

Figure 23. Gridded distribution of cumulative oil produced from each well in the Uteland Butte field, grid interval is 20,000 barrels of oil. Data source: Utah Division of Oil, Gas and Mining (February 28, 2001).

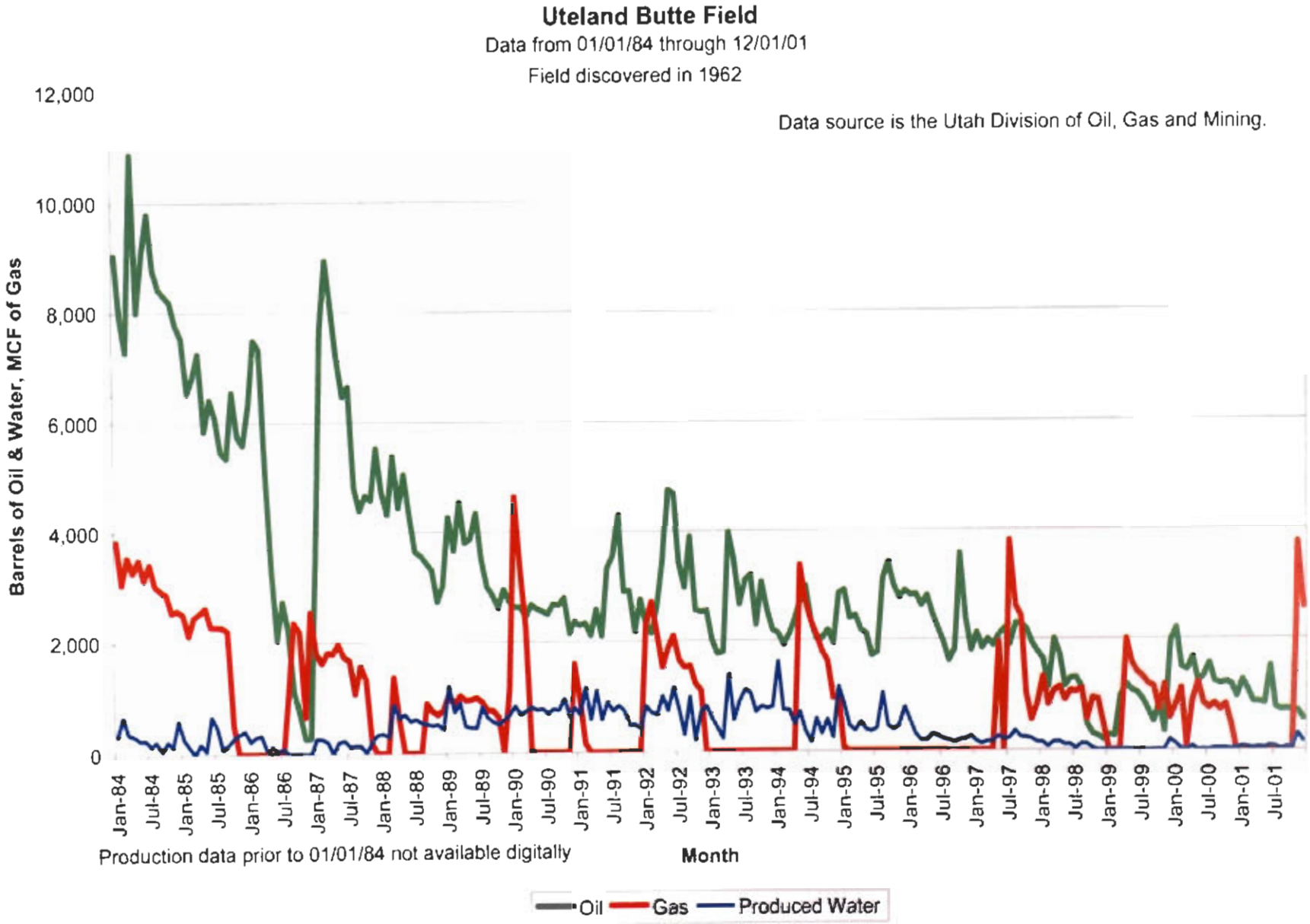

Figure 24. Monthly production of oil, gas, and water from the Uteland Butte field.

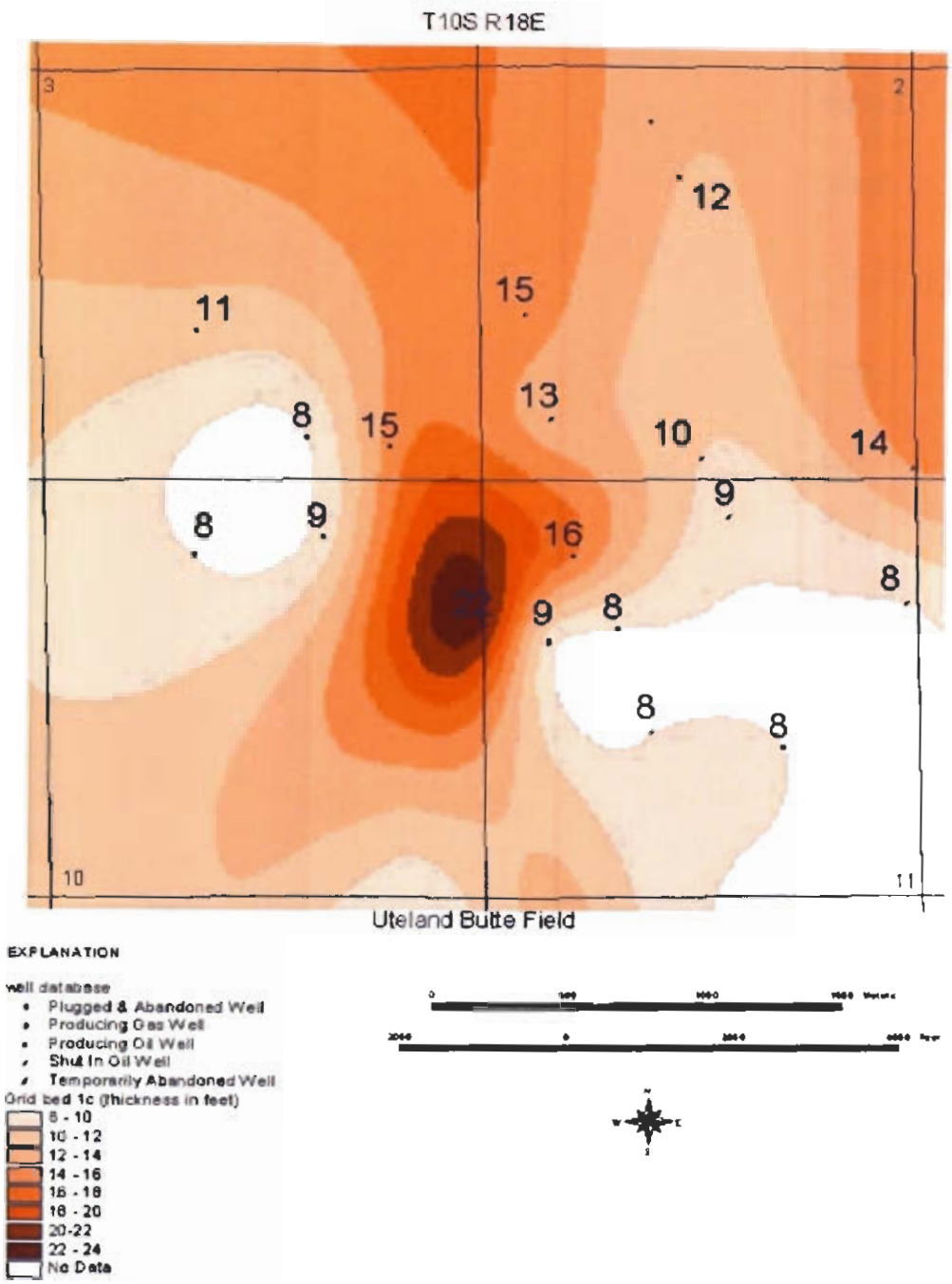

Figure 25. Gridded thickness map of the Uteland Butte 1c bed in the Uteland Butte field. Grid interval is 2 feet.

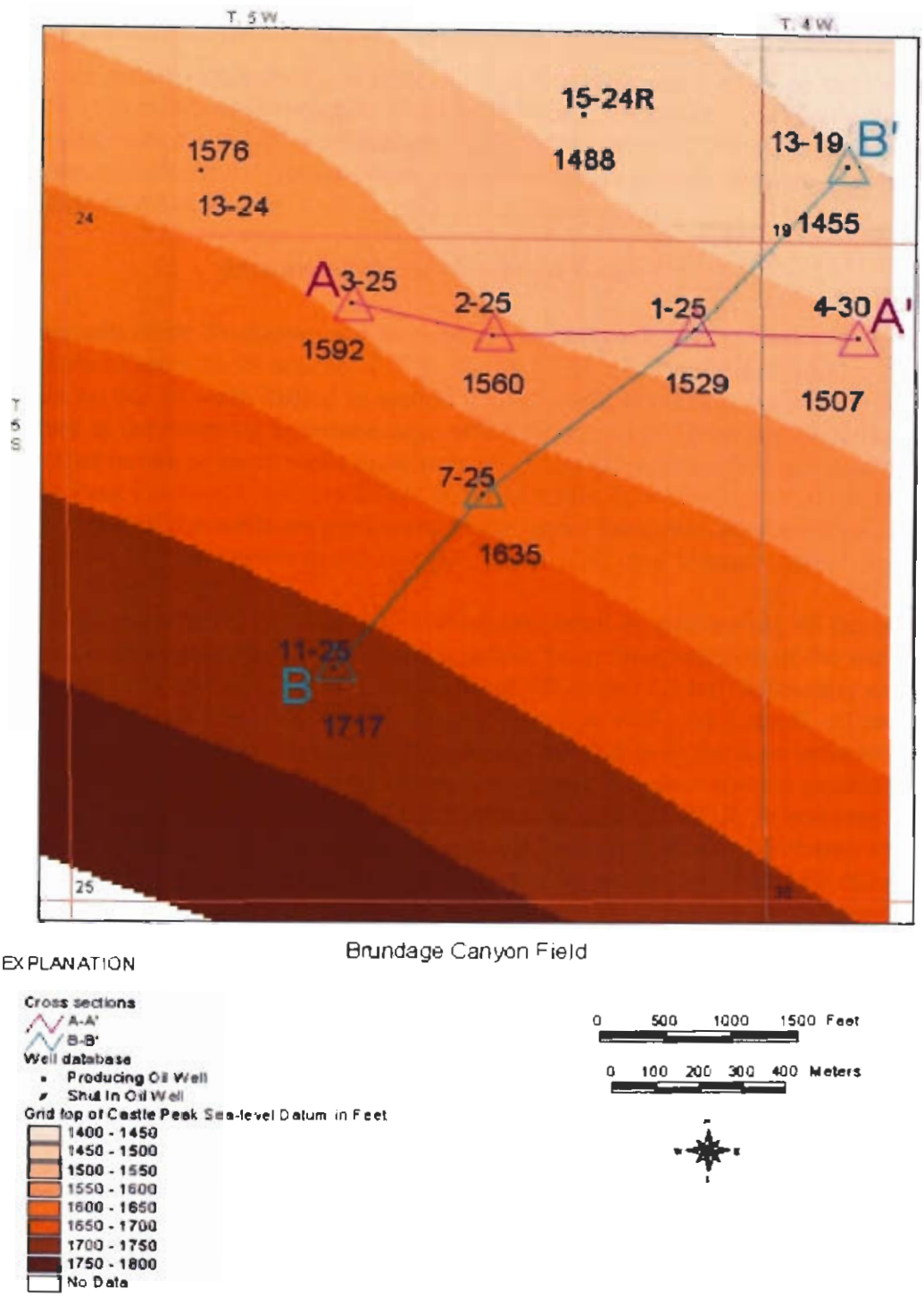

Figure 26. Map of the Brundage Canyon field showing wells, well numbers, cross section locations, and gridded structure of the top of the Castle Peak reservoir. Grid interval is 50 feet, sea-level datum. Cross section A – A' is plate 21 and cross section B - B' is plate 22.

parameters but reservoir quality is very dependent on natural fractures in the sandstone beds. As a result, individual well performance can vary widely (figure 27). Monthly production for the Brundage Canyon field has slowly increased over the years due to additional wells being drilled and produced (figure 28). Water production and the gas-to-oil (GOR) ratio has remained relatively constant.

Non-fracture density-log porosity is typically 2 to 4 percent and 8 to 12 percent when density and neutron porosities are averaged. The Castle Peak c (figure 29) and Castle Peak f (figure 30) sandstone beds are the thickest and generally most porous of the perforated beds in the Brundage Canyon study area. The sandstone thickness trends of both beds are oblique to the trend of the cumulative oil produced.

Monument Butte Northeast Unit

The Monument Butte Northeast unit (secondary recovery water-flood unit) covers all of section 25, and parts of sections 24 and 26, T. 8 S., R. 16 E., SLBL, Duchesne County, Utah. The study focused on the 16 wells drilled in section 25, but wells bordering the section were correlated and used in the mapping to reduce edge effect (figure 31). There are 27 beds, which have been perforated in one or more wells in section 25. Secondary objectives are sandstone beds in the Castle Peak (plates 23 and 24), lower Douglas Creek (plates 25 and 26), and Garden Gulch reservoirs. Most of the wells are perforated in the upper Douglas Creek reservoir (units MGR 4 through MGR 7), also known as the Douglas Creek B, C, and D sands, which are the primary objective (plates 27 and 28).

Wells in Monument Butte Northeast unit were completed by perforating all the beds that had a favorable show of hydrocarbon while drilling and/or from interpretation of the well logs. When section 25 was fully drilled (16 wells, one well per 40 acres [1.6 ha]) secondary recovery was begun. Every other well was converted to a water-injection well. As a result, oil production per well does not accurately reflect the contribution each well makes to the total production from the unit. However, the distribution of the oil production (figure 32) does show a pattern very similar to the MGR 7b sandstone trend (figure 33), indicating that the MGR 7b bed may be responsible for the majority of the oil production from the Monument Butte Northeast unit. The monthly production of oil, gas, and water, show a reduction in gas production and a reduction in the oil-production decline, after water injection began (figure 34). The monthly oil production has not increased but the decline is very slow.

Some of the best developed beds in the upper Douglas Creek reservoir are the MGR 7b (figure 33), MGR 6b (figure 35), and MGR 5b (figure 36). Each of these beds have lenticular thickness trends that are not optimally exploited by the current injection-production well pattern, but no single pattern would be optimal for all perforated beds. Many of the secondary objective beds are not being fully exploited during the secondary recovery phase of production because some are only perforated in injection wells while others are only perforated in producing wells. Sandstone thickness of the lower Douglas Creek reservoir trends west to east through the Monument Butte Northeast unit (figure 37). The trend is intersected by two injection wells in the western half of the trend and two production wells in the eastern half of the trend.

The producer-injector pattern does not always fully exploit the primary objectives. Many of the beds could be more effectively exploited with a pattern based on the sandstone trend. This could be accomplished by infill drilling along the sandstone trends or drilling short horizontal laterals from existing wells.

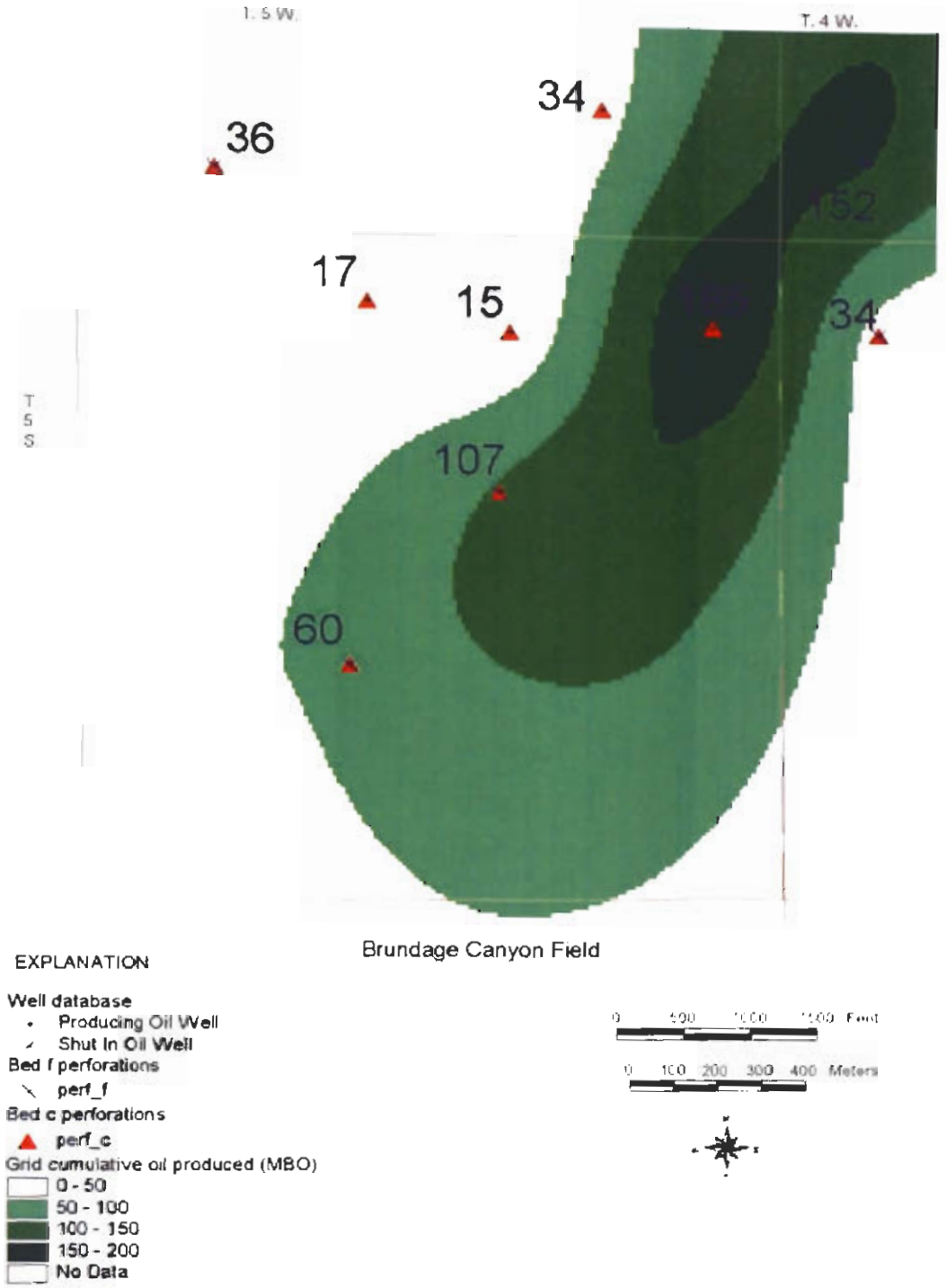

Figure 27. Gridded distribution of cumulative oil produced from each well in the Brundage Canyon field, grid interval is 50,000 barrels of oil. Data source: Utah Division of Oil, Gas and Mining (May 31, 2000).

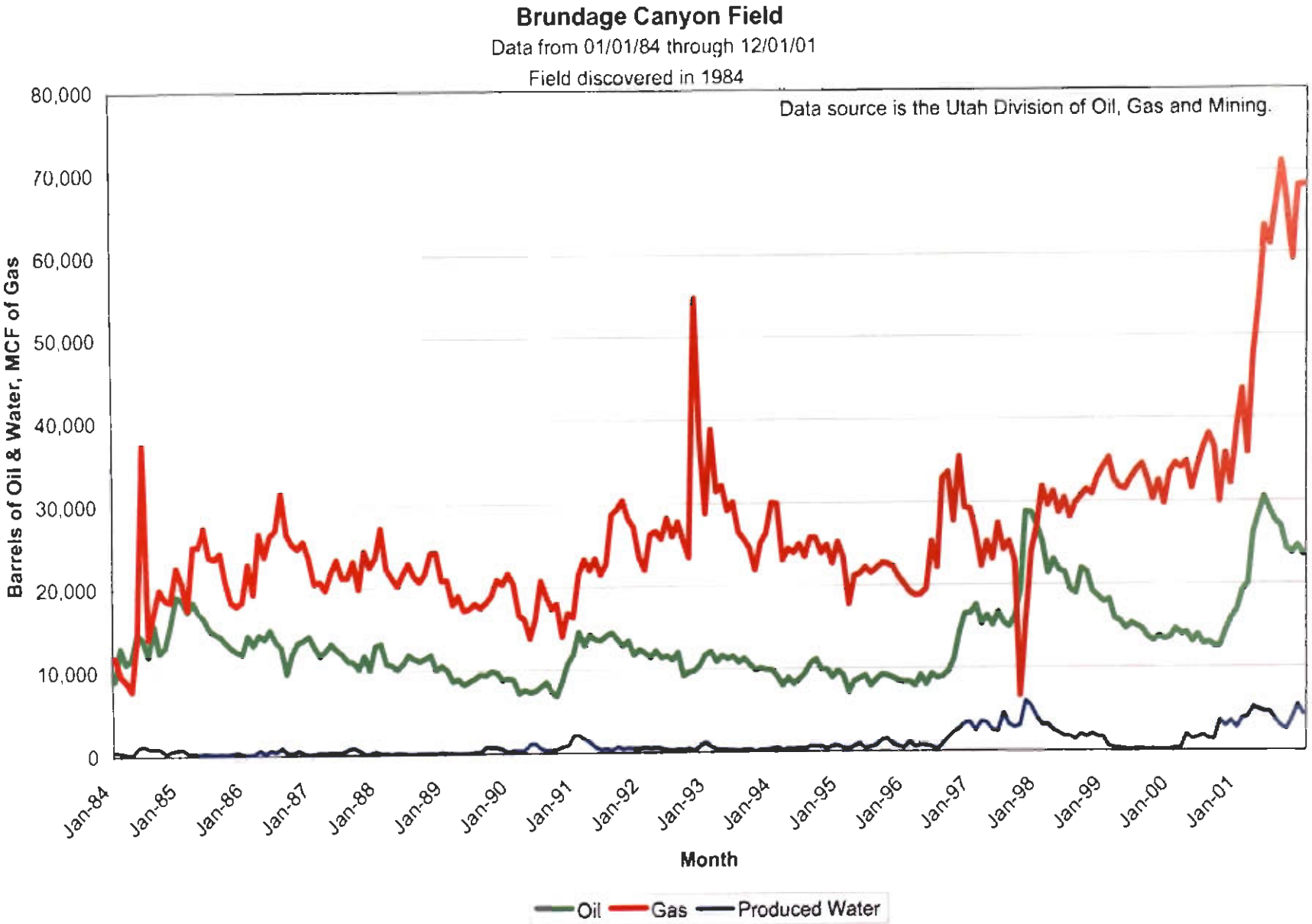

Figure 28. Monthly production of oil, gas, and water from the Brundage Canyon field.

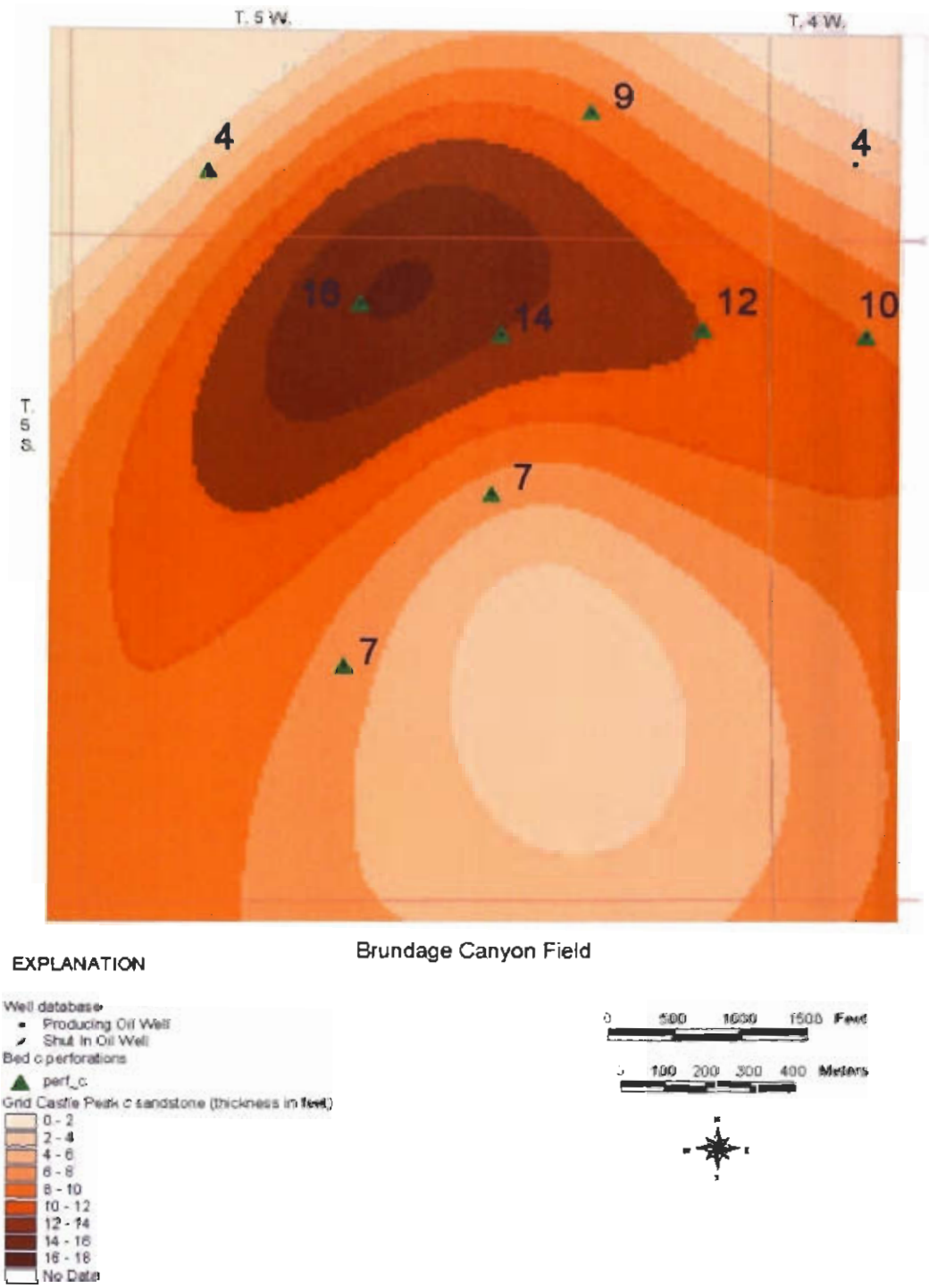

Figure 29. Gridded thickness map of the Castle Peak c sandstone in the Brundage Canyon field. Grid interval is 2 feet.

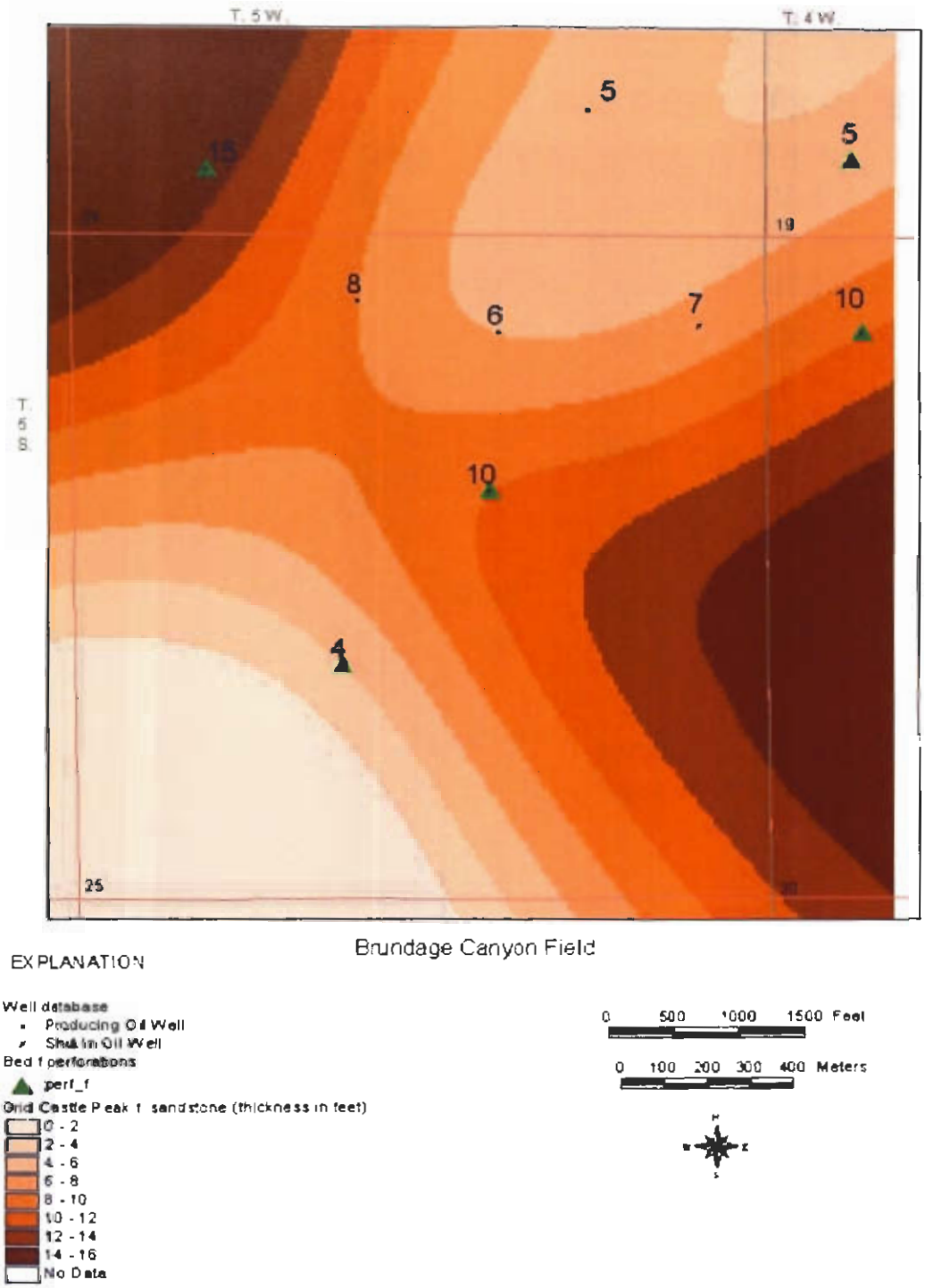

Figure 30. Gridded thickness map of the Castle Peak f sandstone in the Brundage Canyon field. Grid interval is 2 feet.

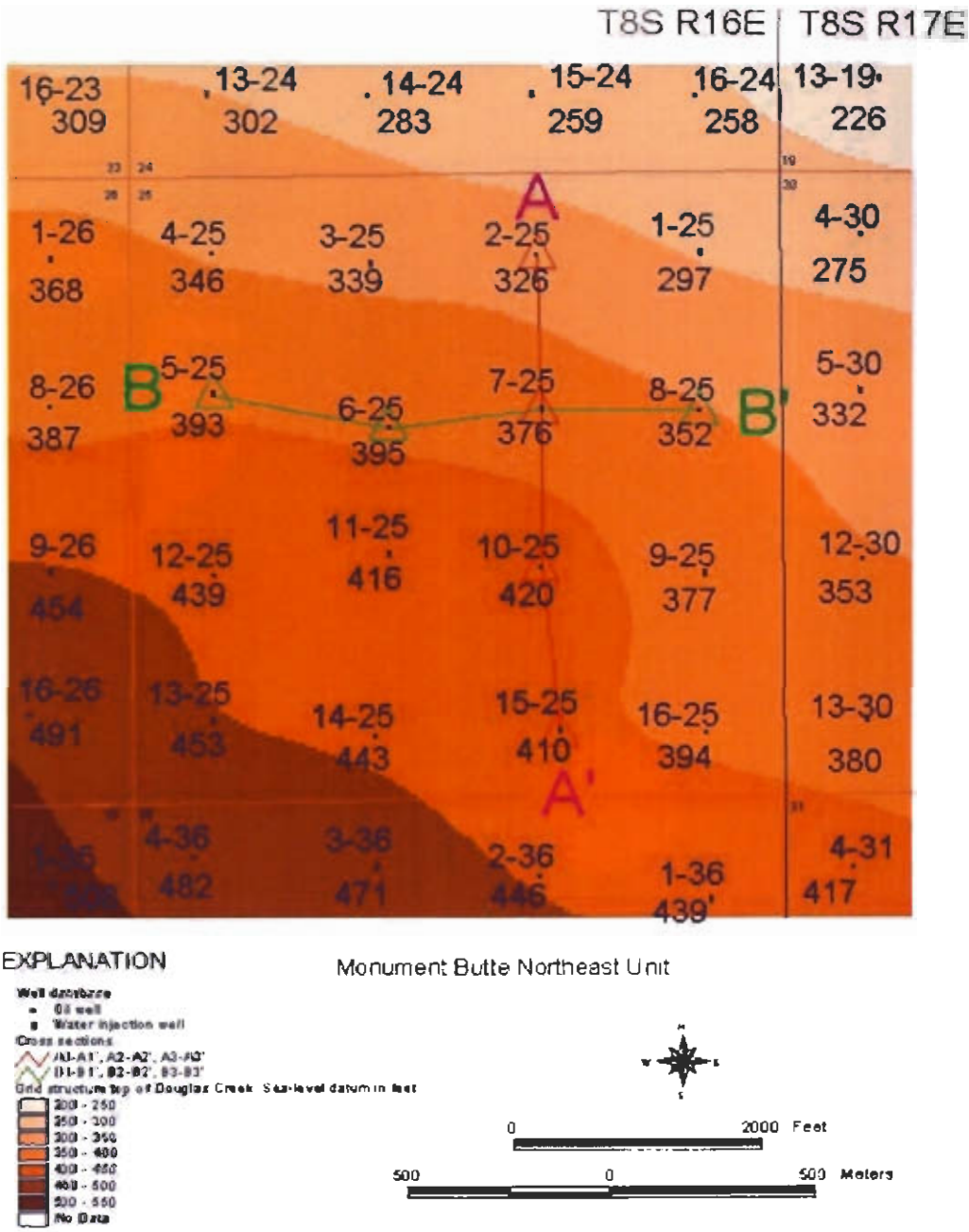

Figure 31. Map of the Monument Butte Northeast unit showing wells, well numbers, cross section locations, and gridded structure of the top of the Douglas Creek reservoir. Grid interval is 50 feet, sea-level datum. Cross sections A - A' and B - B', refer to A1 - A1' (plate 23), A2 - A2' (plate 25), A3 - A3' (plate 27), and B1 - B1' (plate 24), B2 - B2' (plate 26), B3 - B3' (plate 28), respectively. The number designation of the cross sections relate to the same wells but at different stratigraphic horizons and drill depths.

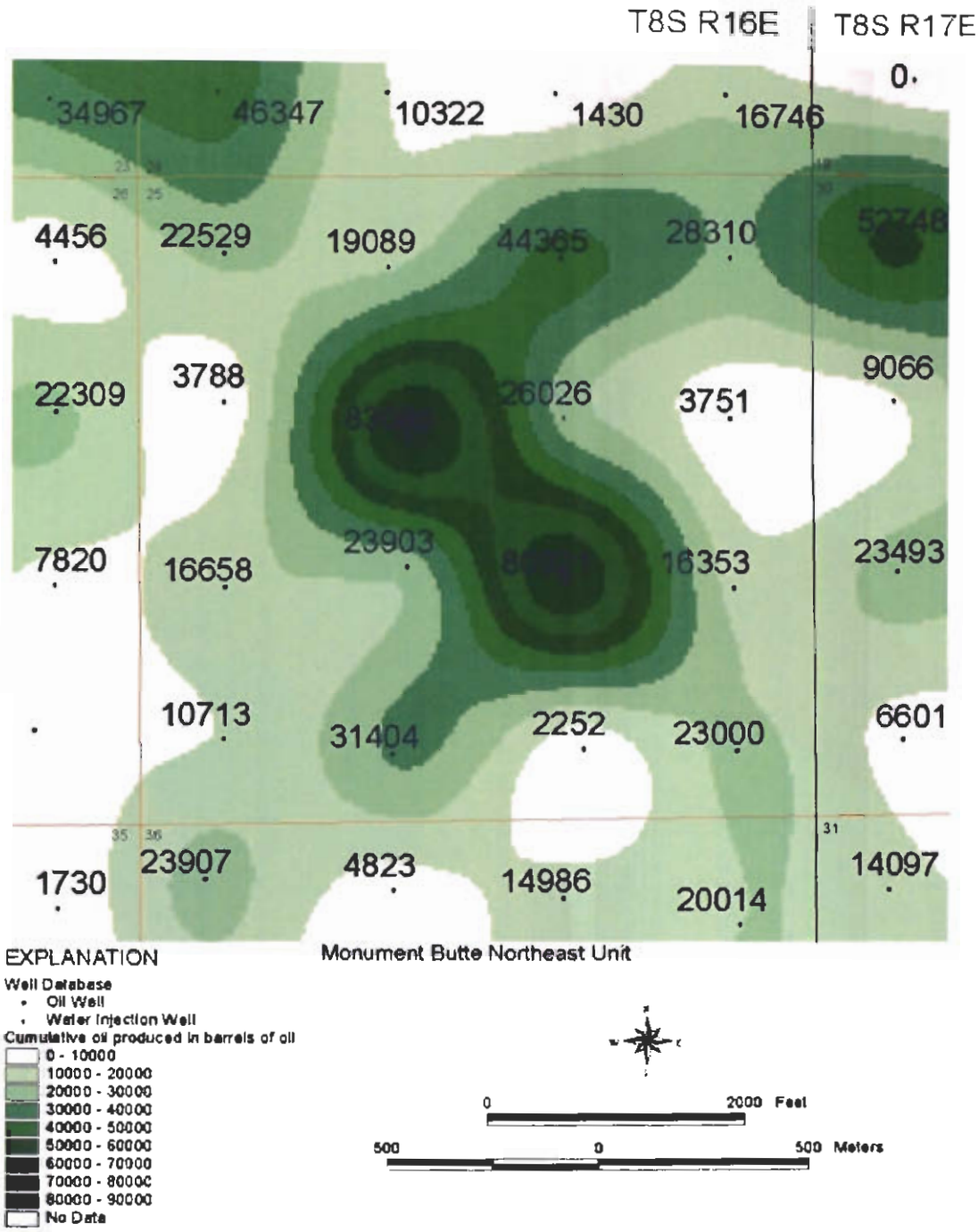

Figure 32. Gridded distribution of cumulative oil produced from each well in the Monument Butte Northeast unit, grid interval is 10,000 barrels of oil. The upper Douglas Creek is the primary oil-producing reservoir. Data source: Utah Division of Oil, Gas and Mining (October 31, 1999).

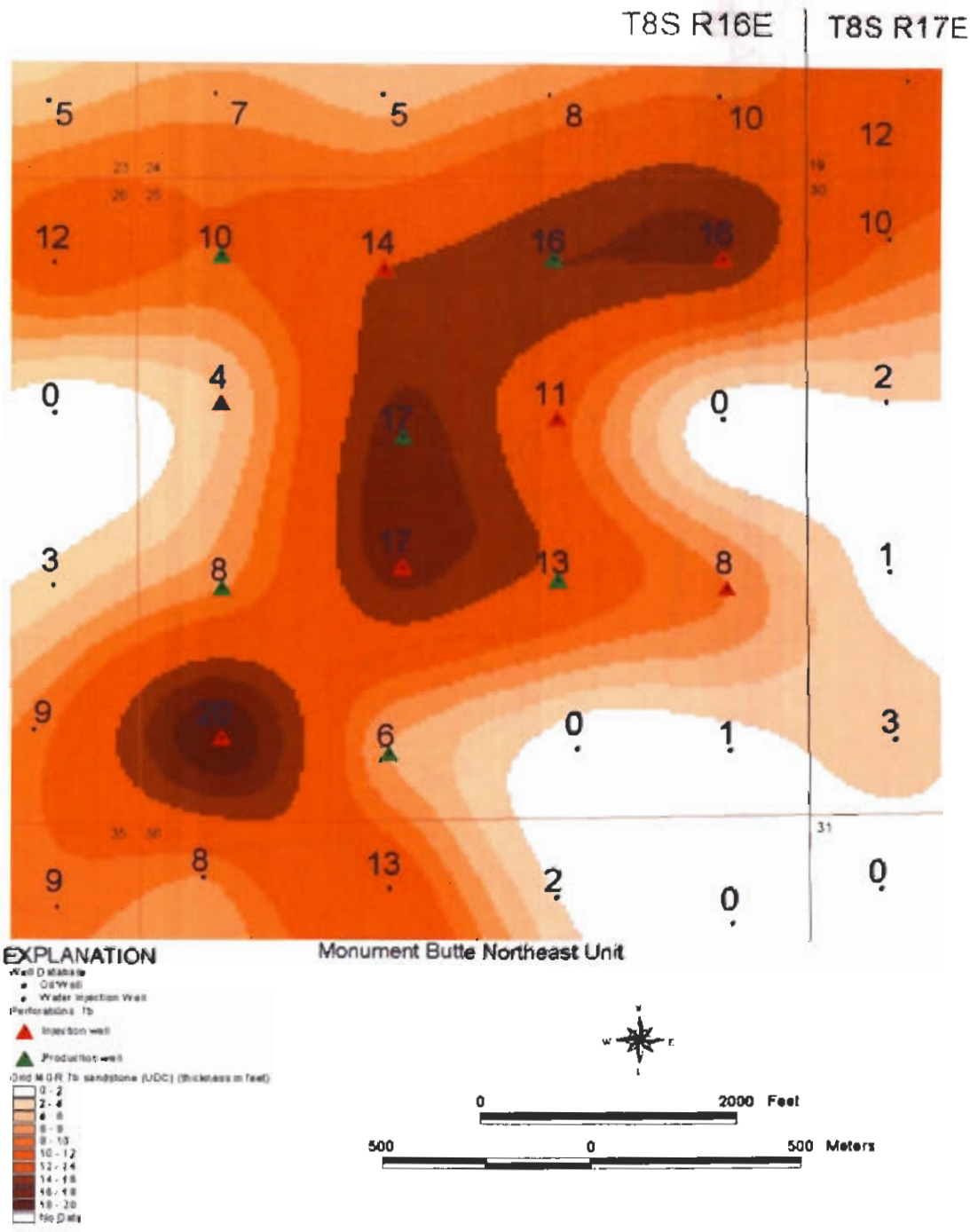

Figure 33. Gridded thickness map of the MGR 7b sandstone in the Monument Butte Northeast unit. Grid interval is 2 feet.

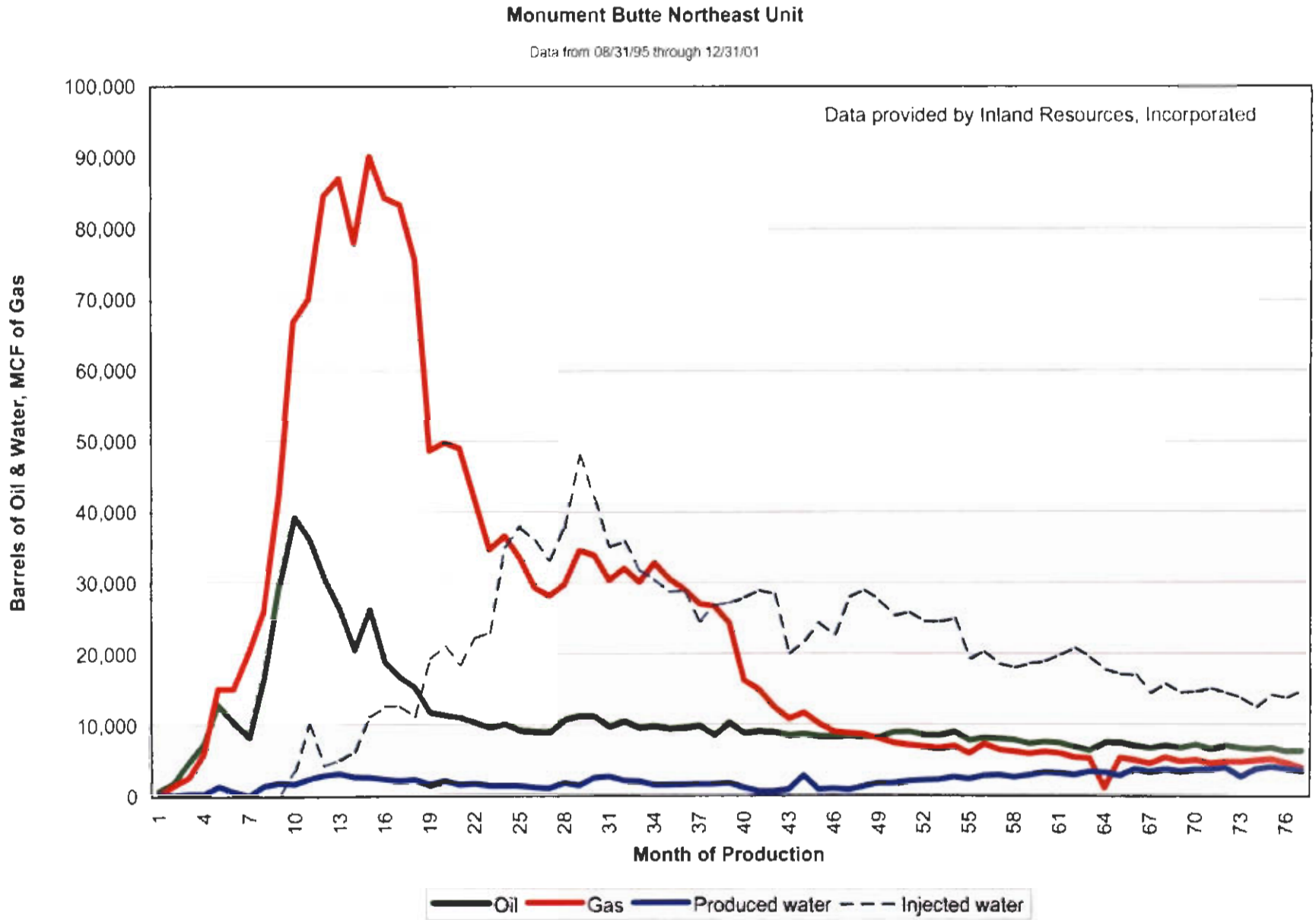

Figure 34. Monthly production of oil, gas, and water, and monthly volumes of water injected, in the Monument Butte Northeast unit. Water injection has reduced gas production and slowed the oil-production decline.

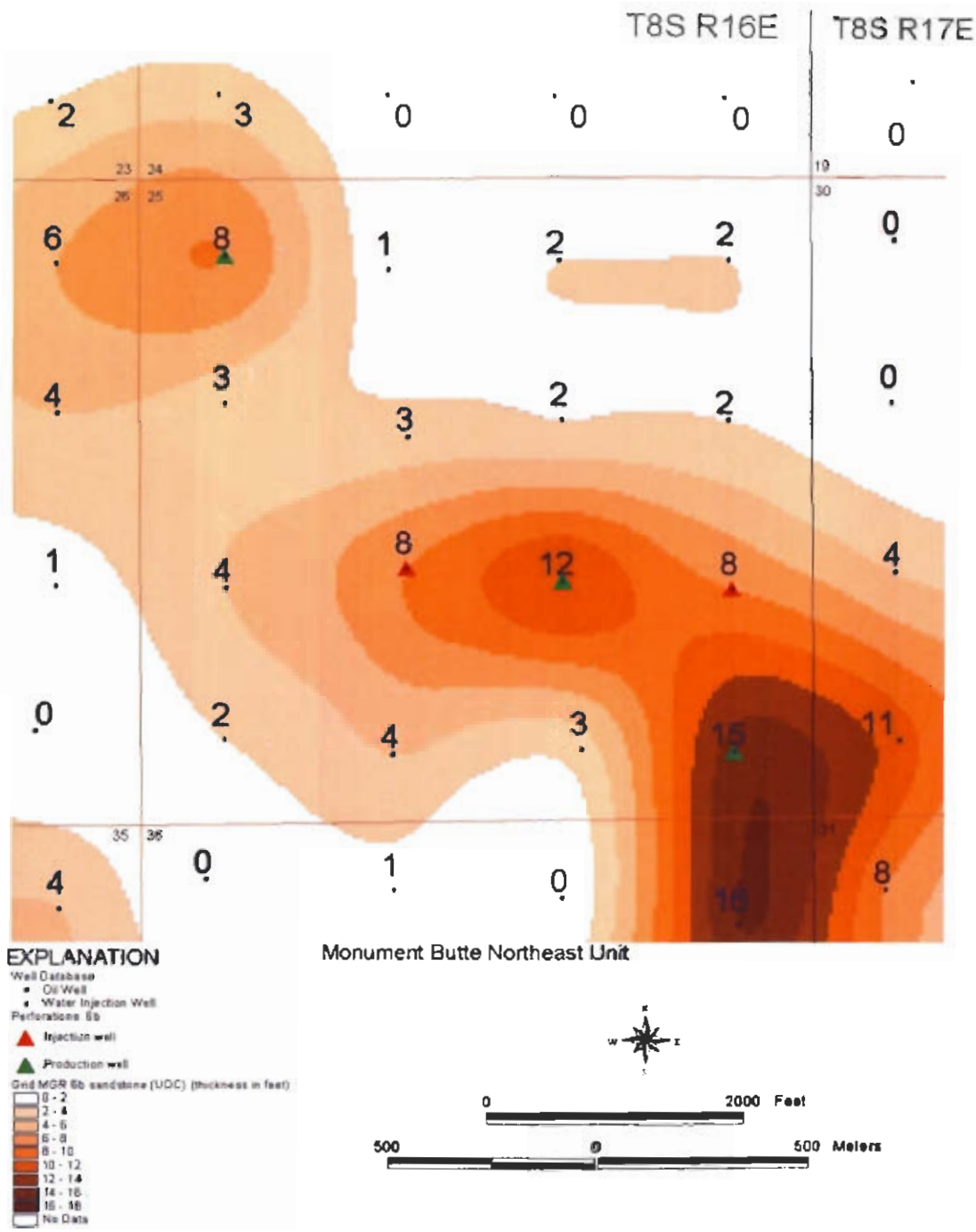

Figure 35. Gridded thickness map of the MGR 6b sandstone in the Monument Butte Northeast unit. Grid interval is 2 feet.

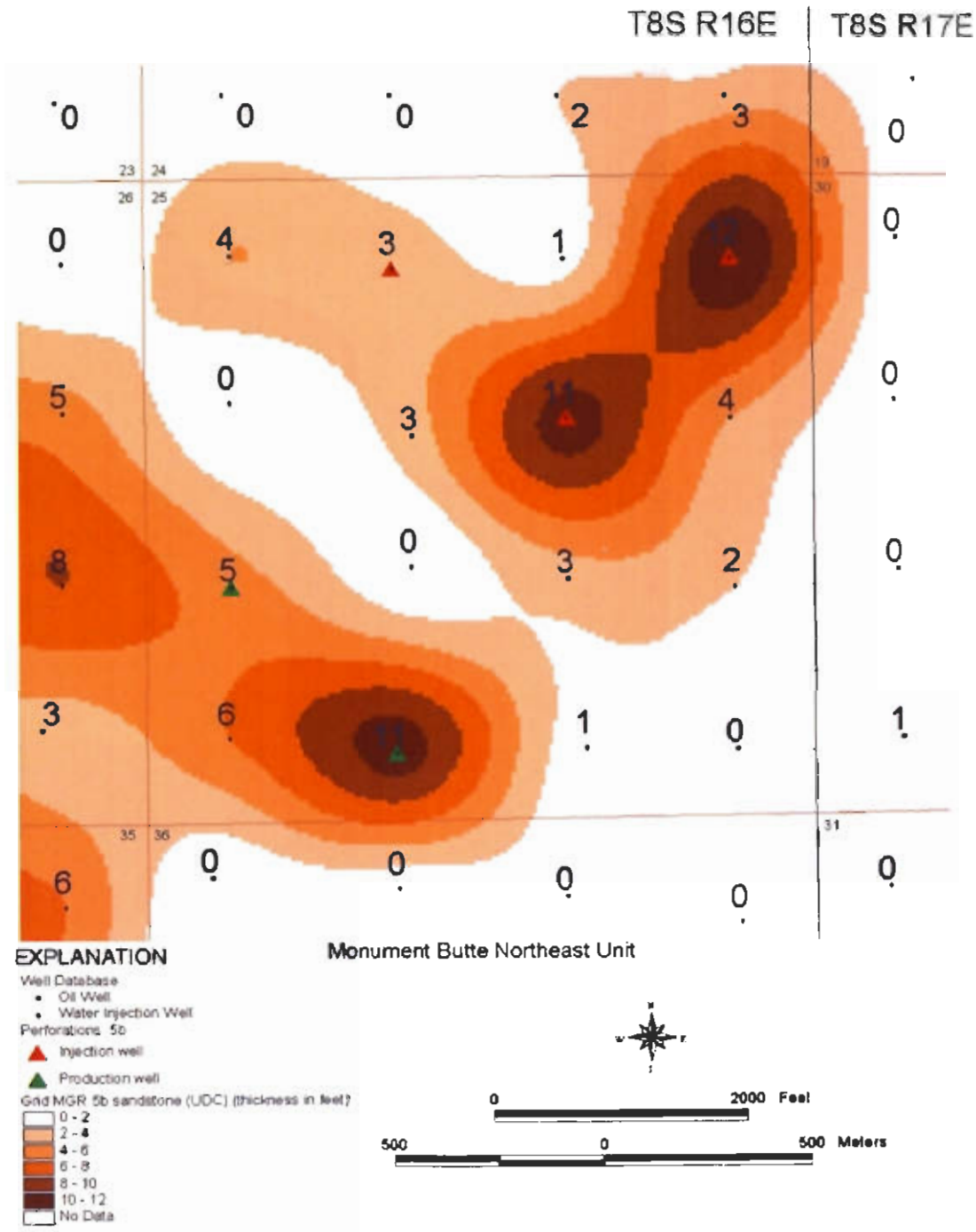

Figure 36. Gridded thickness map of the MGR 5b sandstone in the Monument Butte Northeast unit. Grid interval is 2 feet.

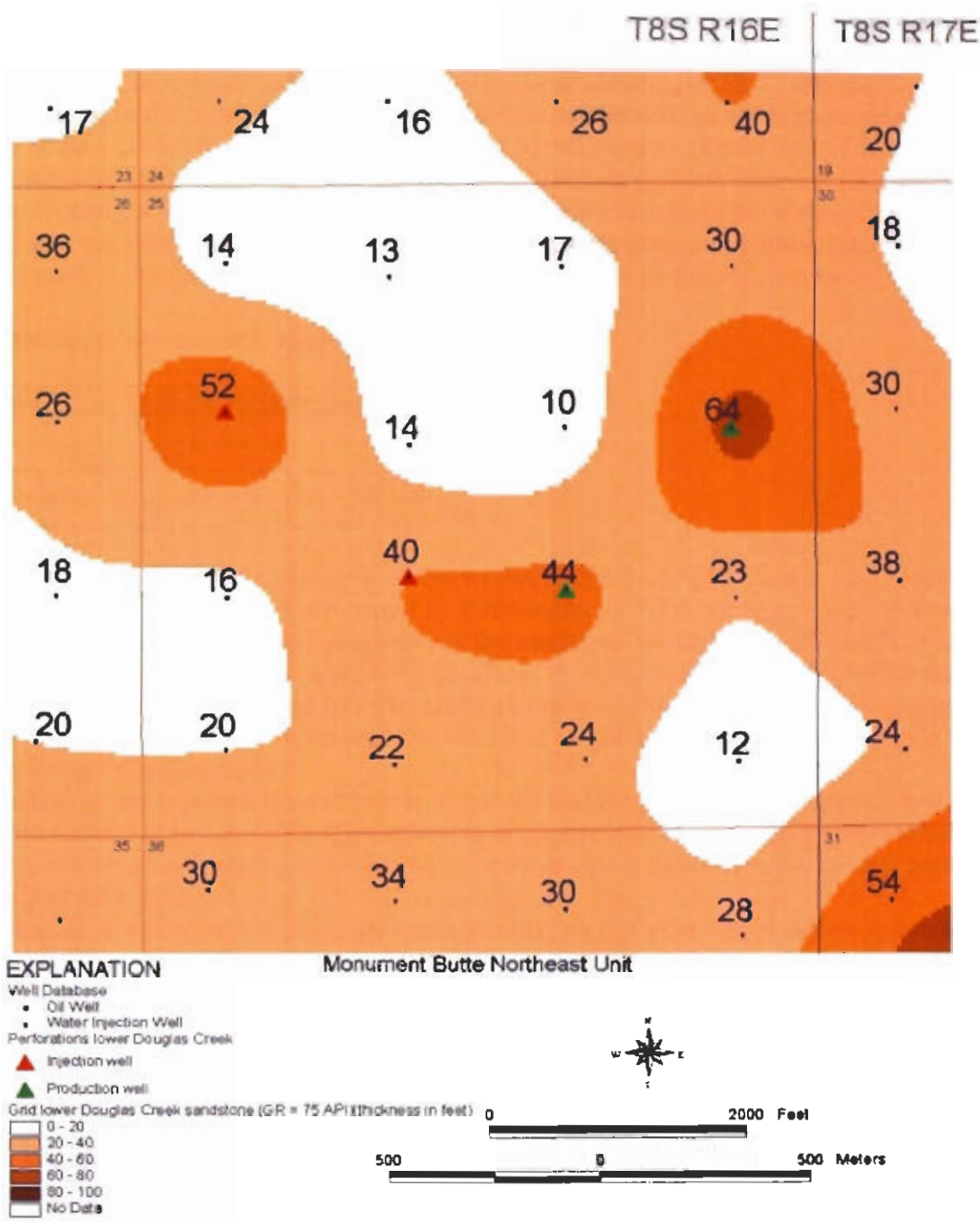

Figure 37. Gridded thickness map of the lower Douglas Creek sandstone using a 75 API unit gamma-ray cutoff, in the Monument Butte Northeast unit. Grid interval is 20 feet.

GENERATION OF GEOSTATISTICAL RESERVOIR MODELS

To create a geological model for the fluid flow simulations the spatial distributions of porosity, permeability and water saturation are required. The geological model for the MBNE unit was created using Heresim3D® (Heterogeneities of Reservoir Simulations), an integrated computer–aided reservoir description program by BEICIP-FRANLAB® Petroleum Consultants.

Petrophysical properties were generated for the D sandstone (MGR 7) and the C sandstone (MGR 6) in the upper Douglas Creek reservoir, in the sixteen wells in section 25, (T. 8 S., R. 16 E., SLBL), a portion of the Monument Butte Northeast unit (figure 21). The well log information included porosities and water saturations at 0.5-foot (0.1-m) intervals. Figure 38 shows the wells and the reference grid used, which was twenty blocks in the x-direction and twenty blocks in the y-direction. The block dimensions in both the x and y directions were 264 feet (80.5 m) each. Lithofacies were defined based on porosities and are shown table 2.

Table 2. Lithofacies assignments based on porosity.

Porosities in percent	Lithofacies Designation
0 to 12.5	10
12.5 to 15	20
15 to 17.5	30
17.5 to 20 +	40

The lithofacies designations in four of the wells (10-25, 11-25, 12-25 and 13-25) are shown in figure 39. The lithofacies are bound by three surfaces. The two upper and the lower surfaces are the upper and the lower boundaries of the sandstone while the middle surface was chosen at the middle of each sand as a reference surface. A northwest-to-southeast cross section through section 25 is shown in figure 40. The surfaces for the defined cross section are shown in figure 41. The entire D sandstone reservoir was modeled as one litho unit. A parallel grid was used in describing the stratigraphy.

Elevation of the top surface is shown in figure 42 and the corresponding elevation map for the bottom surface is in figure 43. The reservoir is constrained between these two surfaces. The thickness distribution is shown in figure 44. The reservoir is thickest in the central portion and tapers off at the edges.

Permeability was modeled using the cross plot shown in figure 45. A semi-logarithmic correlation between permeability and porosity was found to fit most measured porosity-permeability values across the field. The equation for the permeability-porosity cross-plot was:

$$\log(k) = 0.218\phi - 2.225$$

where, k was in millidarcies and ϕ was in percentage. The general statistics for the entire data set for permeability and porosity is shown in table 3.

Using the appropriate variogram parameters, lithotypes were simulated over the entire field. Litho unit distribution in the same cross section (as in figure 40) is shown in figure 46. Corresponding porosities and permeabilities are shown in figures 47 and 48.

We chose a resolution that was composed of about 250 half-foot layers (0.1-m), which would yield a total of 100,000 grid blocks. It is possible to build a reservoir model with these many blocks; however, the awkward aspect ratios of grid blocks would cause numerical instabilities. Therefore, the first series of reservoir models were built by upscaling the blocks vertically. A

Table 3. General permeability and porosity statistics for section 25, T. 8 S., R. 16 E. (SLBM), Monument Butte Northeast unit.

	Lithofacies 40		Lithofacies 30		Lithofacies 20		Lithofacies 10	
Attribute	ϕ (%)	K(md)	ϕ (%)	K(md)	ϕ (%)	K(md)	ϕ (%)	K(md)
Number of samples	86	86	114	114	121	117	91	80
Minimum	15.93	17.7	15.03	11.2	12.28	2.8	10.01	0.9
Maximum	20.3	158.7	17.49	38.7	16.34	21.8	12.51	3.2
Mean	18.6	74.02	16.2	21.1	13.9	6.992	11.5	2.085
Standard Deviation	0.854	33.24	0.71	7.7	0.79	2.78	0.71	0.63

ϕ = porosity in percent
K(md) = permeability in millidarcies

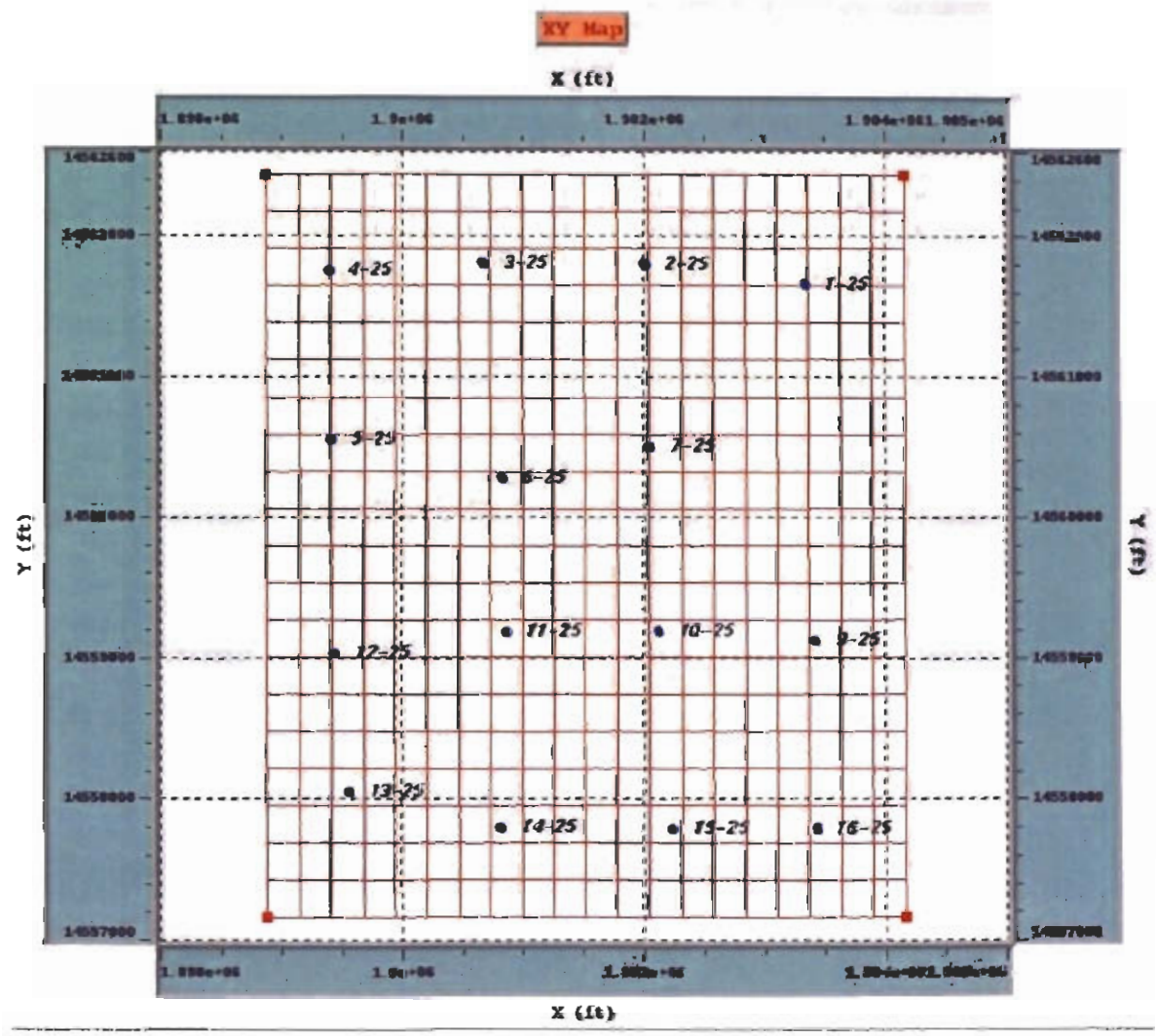

Figure 38. The map of section 25 showing the grid and all the wells.

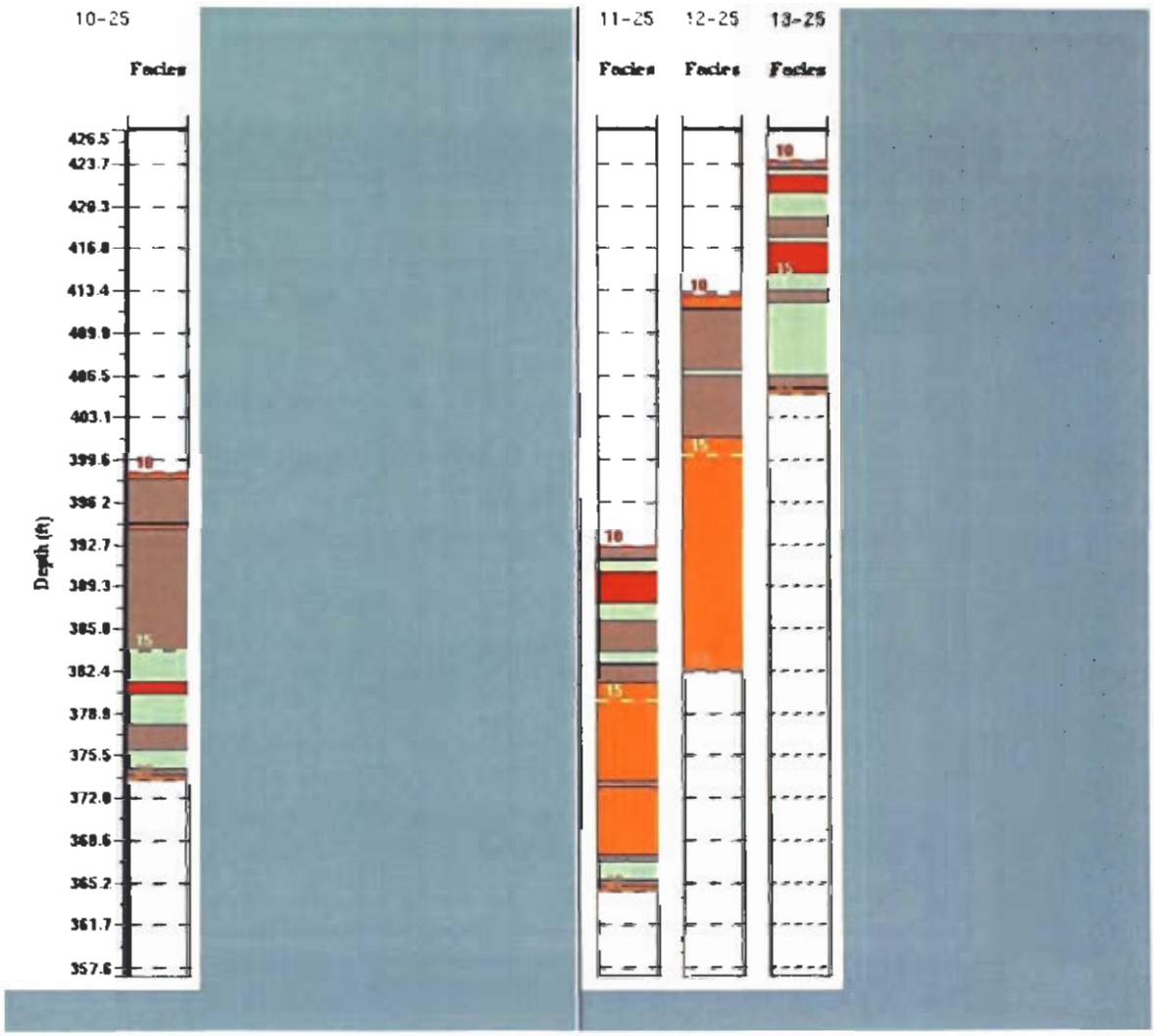

Figure 39. Lithofacies in some of the wells.

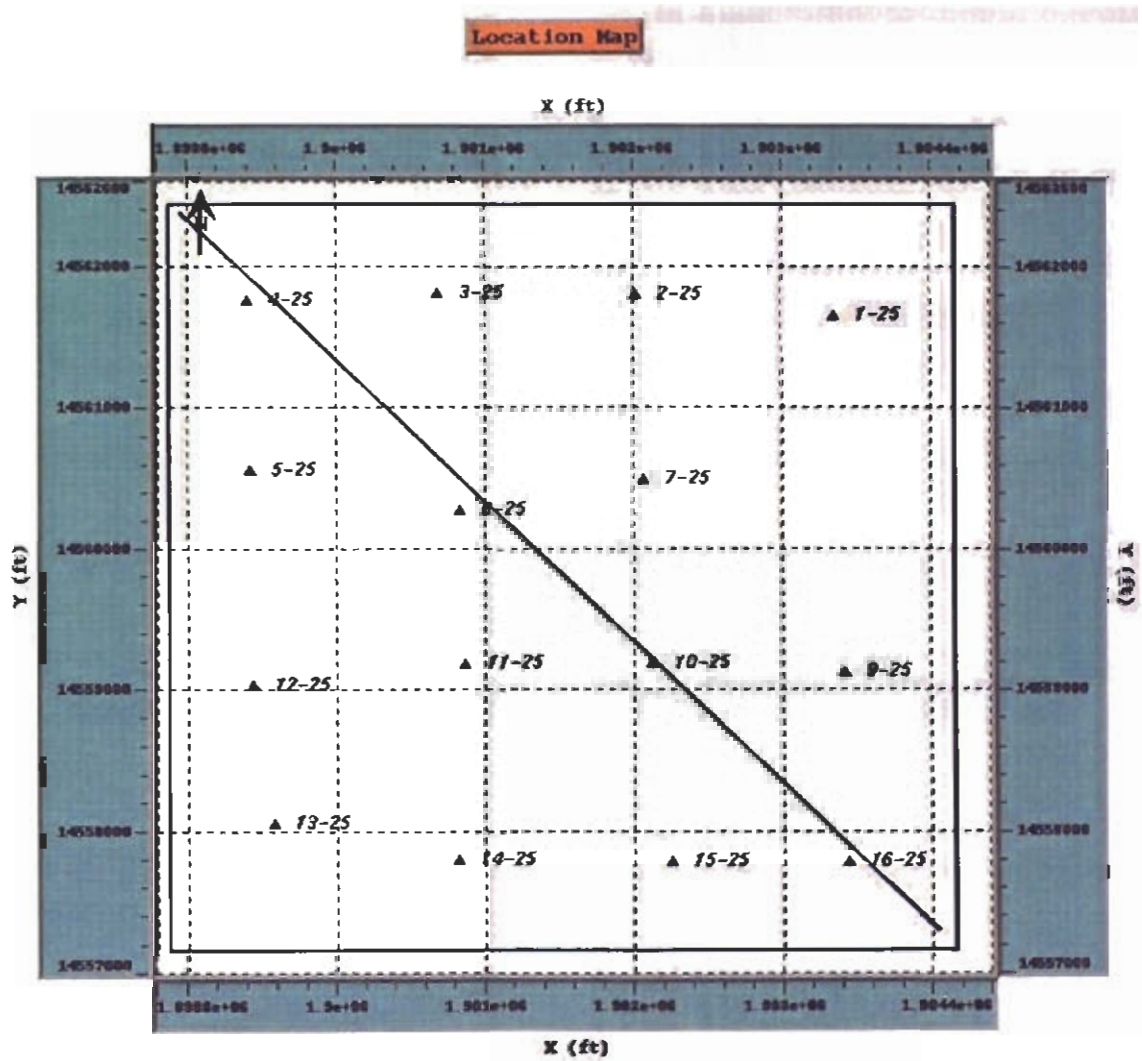

Figure 40. Location of the northwest-to-southeast cross section (figure 41) through section 25.

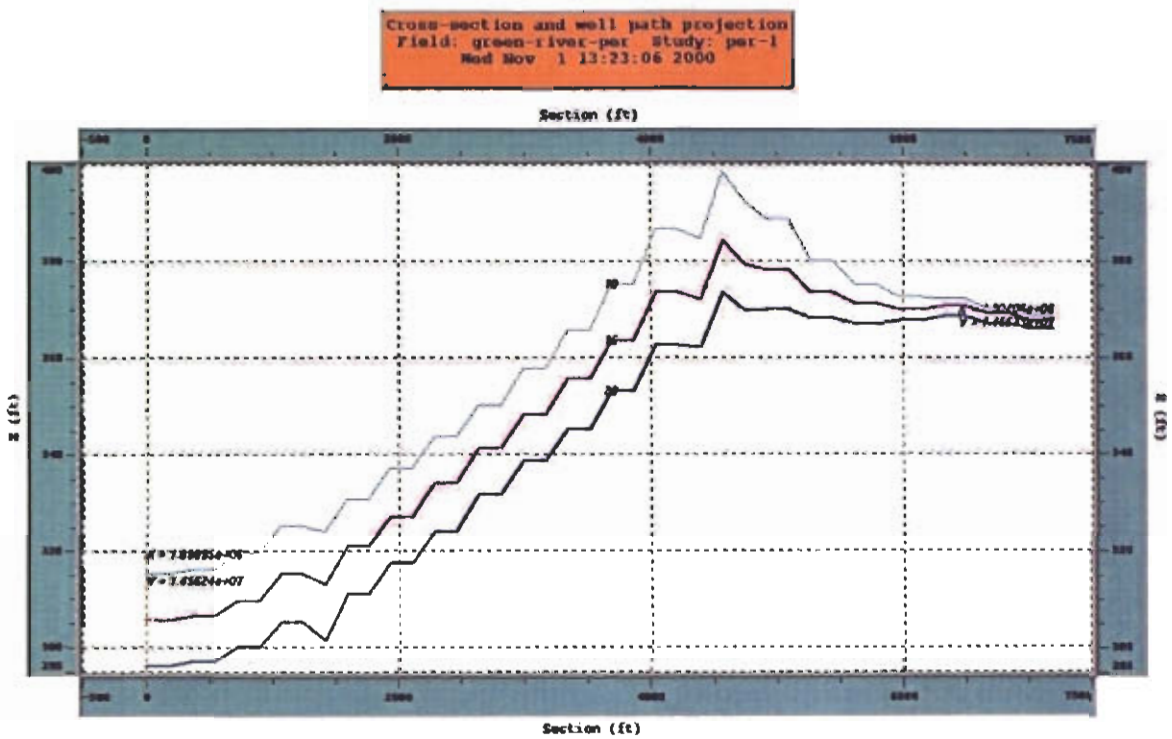

Figure 41. The three D sandstone surfaces along the cross section. See figure 40 for location of cross section.

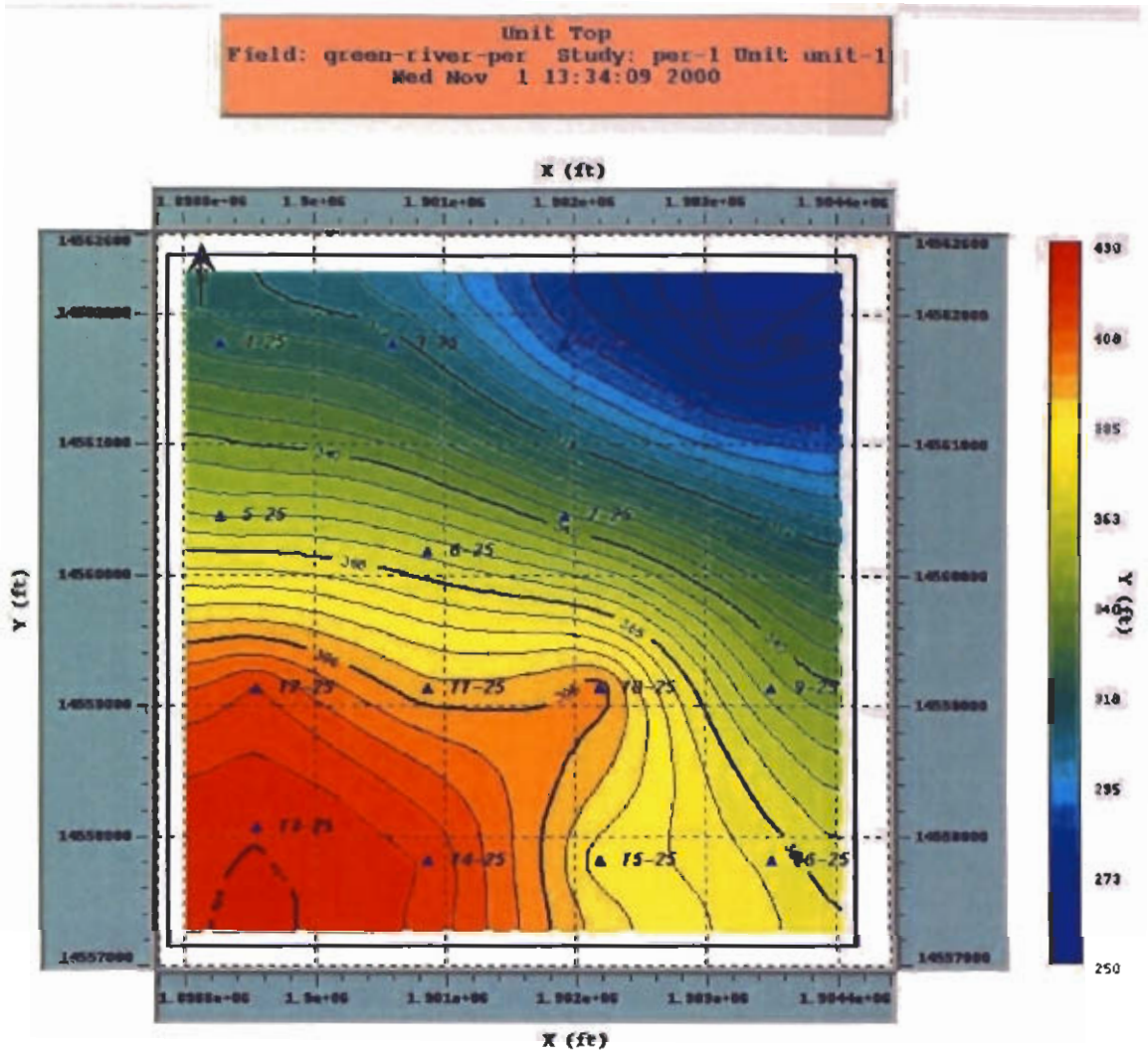

Figure 42. Contour map of the top surface of the D sandstone. Elevations are in feet, sea-level datum.

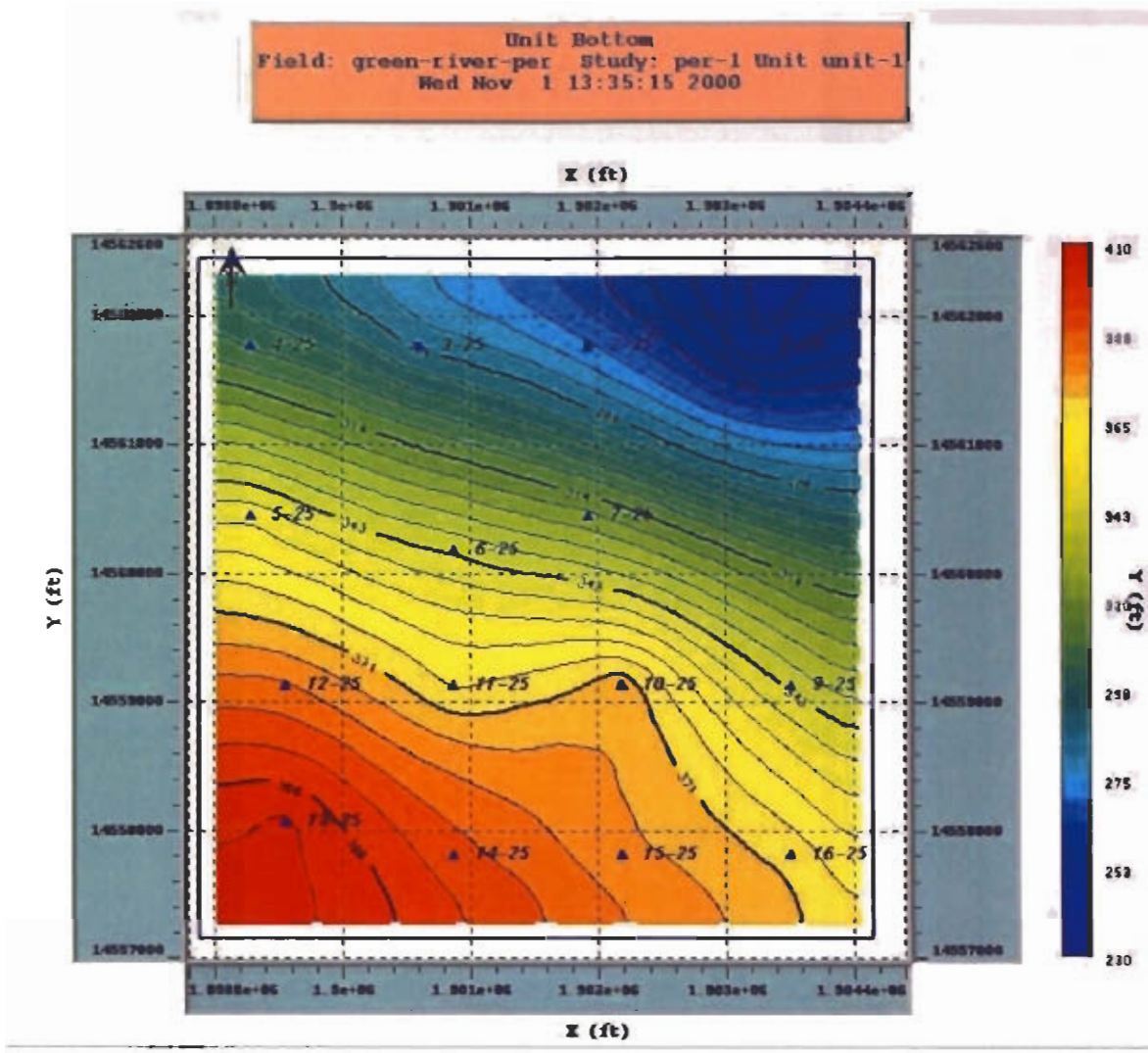

Figure 43. Contour map for the bottom of the D sandstone. Elevations are in feet, sea-level datum.

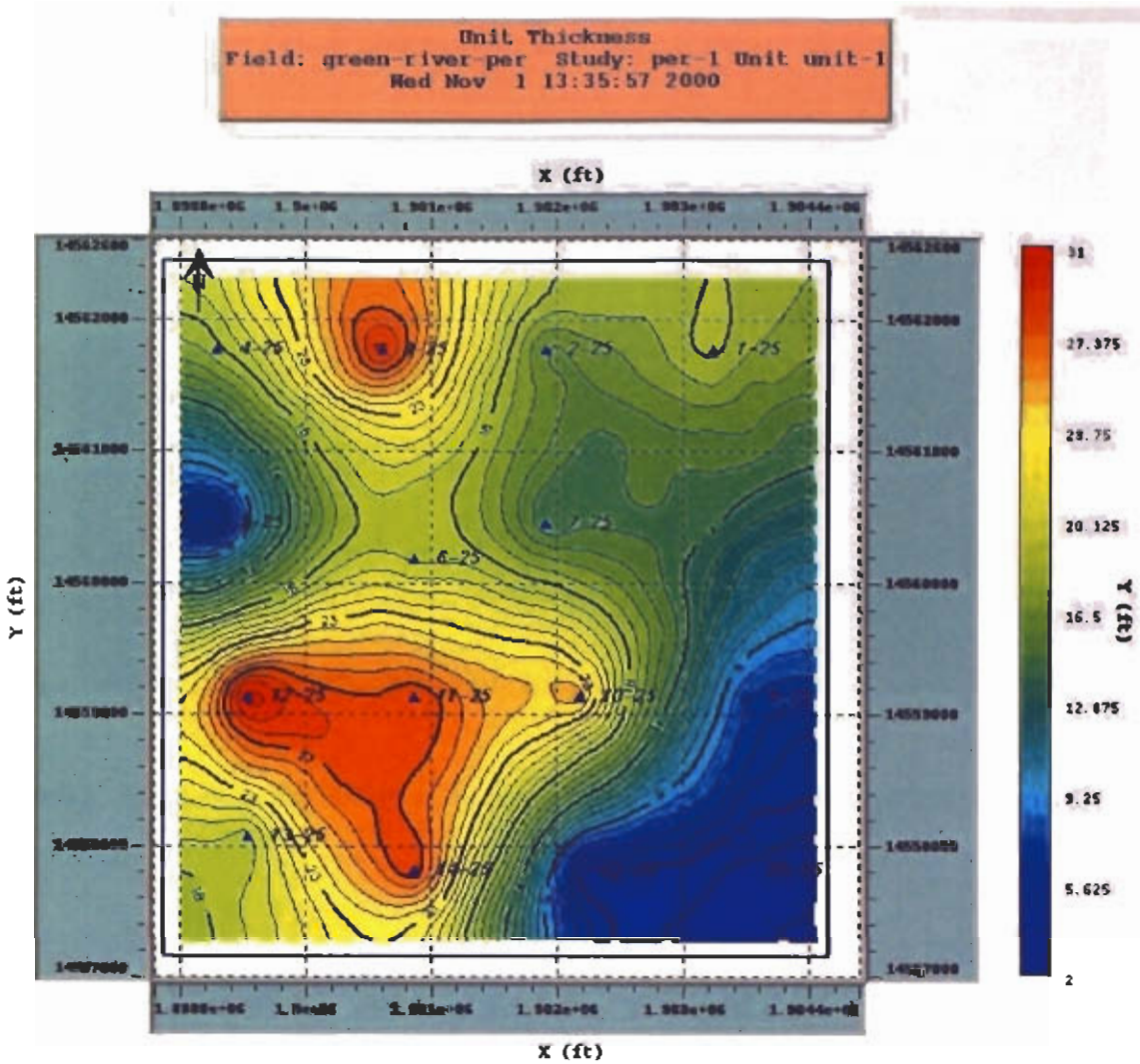

Figure 44. D sandstone thickness map in feet.

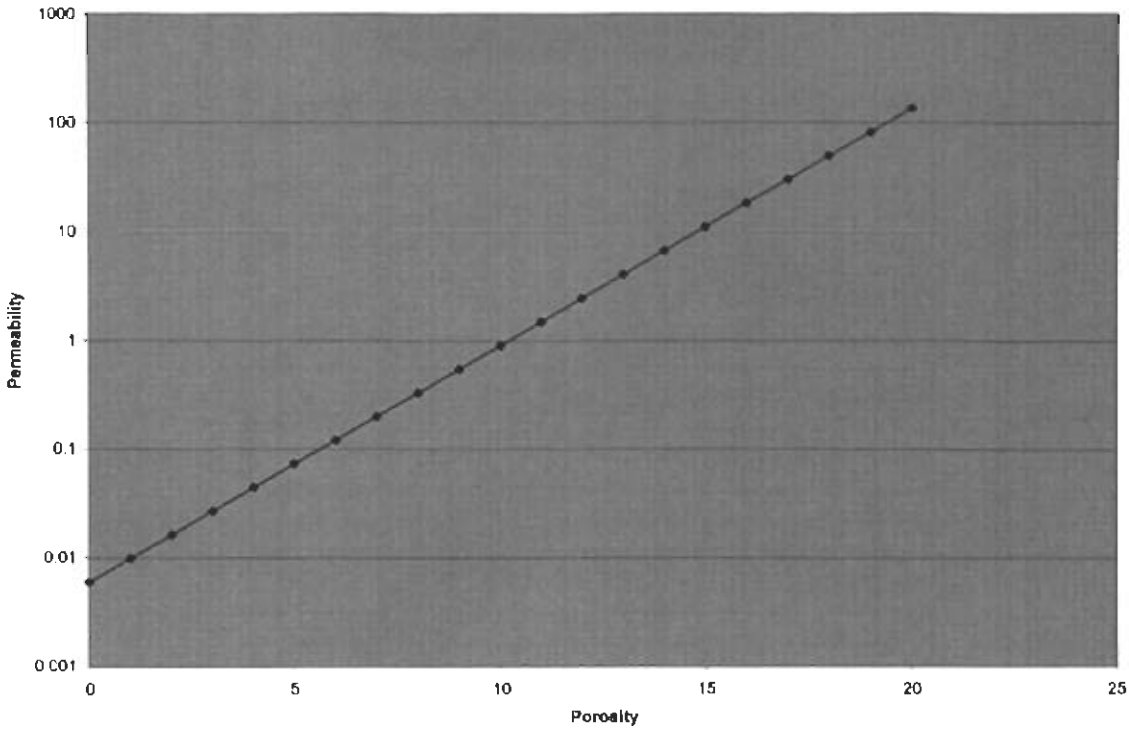

Figure 45. Porosity-permeability cross plot used in creating the petrophysical properties.

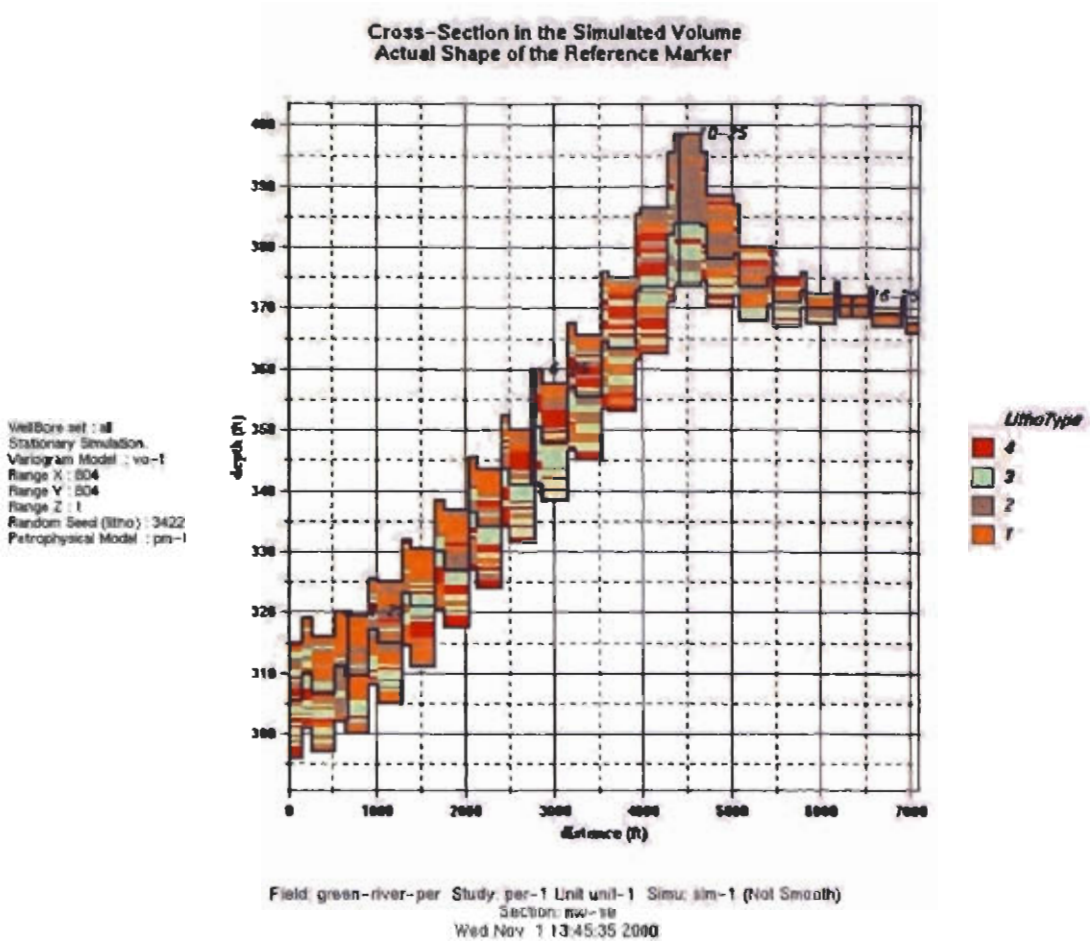

Figure 46. D sandstone lithotype distribution in the cross section shown in figure 40.

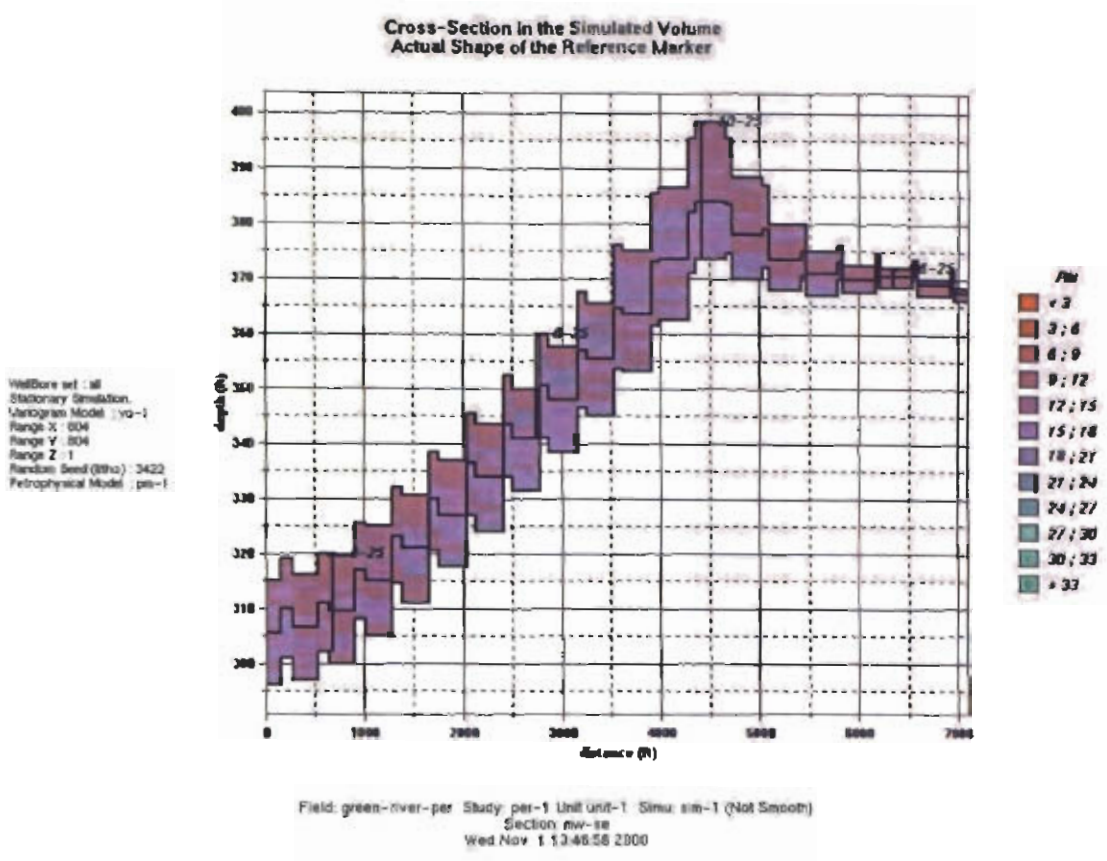

Figure 47. D sandstone porosity distribution in the cross section shown in figure 40.

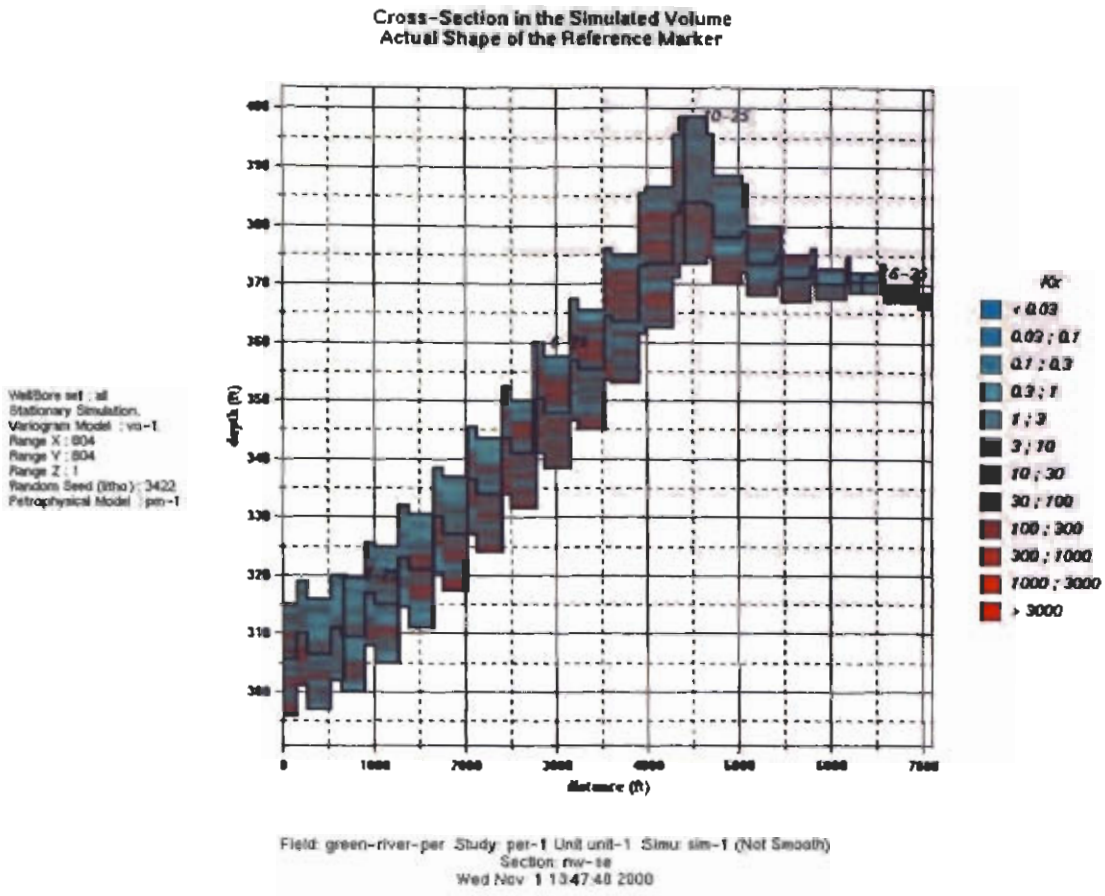

Figure 48. D sandstone permeability distribution in the cross section shown in figure 40.

total of 13 vertical blocks were created. The proportion of porosity as a function of elevation is shown in figure 49. This diagram is used to select locations of upscaled layers, which were selected at regular intervals. A reservoir model that was suitable for simulation was built using the upscaled information. The reservoir grid (plan view) is shown in figure 50.

The upscaled cross sections for section 25 (figure 40) are presented in figures 51 (porosity), figure 52 (permeability) and figure 53 (water saturation). The basic quality of petrophysical property distribution is preserved in the upscaling process. The upscaled models were later modified to accommodate the incorporation of hydraulic fractures.

The same methodology was used in generating petrophysical models for C sandstone. The thicknesses, porosities, permeabilities, and water saturations for the C sandstone are shown in figures 54-57. The thicknesses for the C sandstone are generally much lower than for D sandstone. The porosities, permeabilities and water saturations for the C sandstone and D sandstone, are comparable.

The conventional well-log data was effectively used to create detailed reservoir images based on geostatistics. The geostatistical models had be appropriately upscaled for use in reservoir simulation. The reservoir model was used to simulate production in section 25 and is discussed in the reservoir simulation chapter.

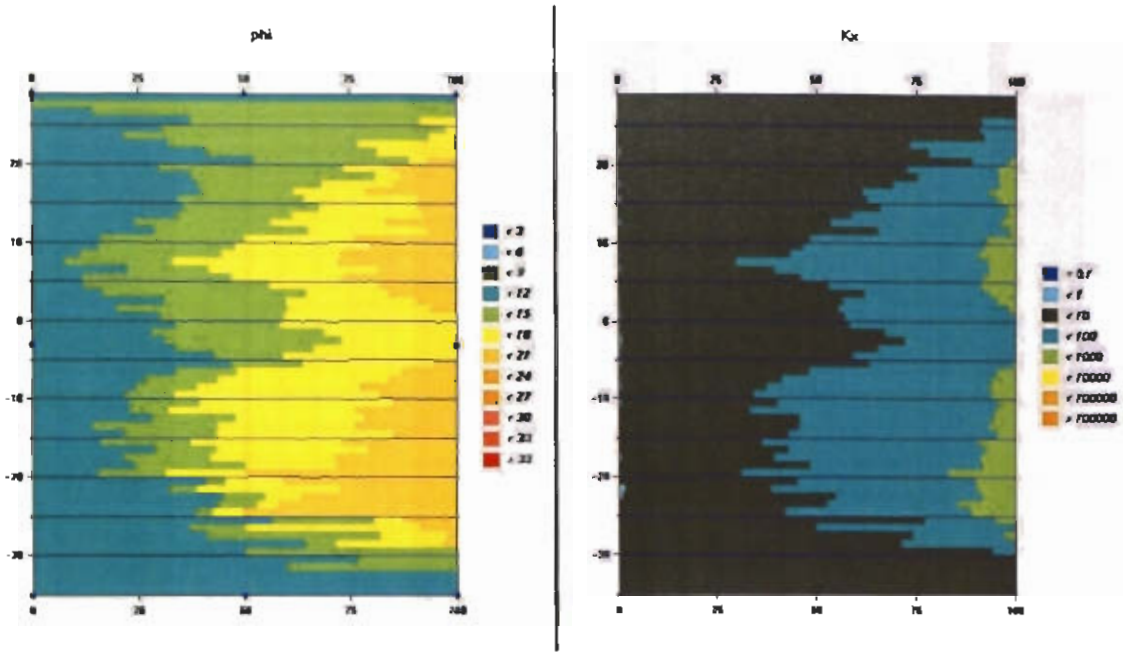

Figure 49. D sandstone porosity and permeability proportion curves and locations of upscaled layer boundaries.

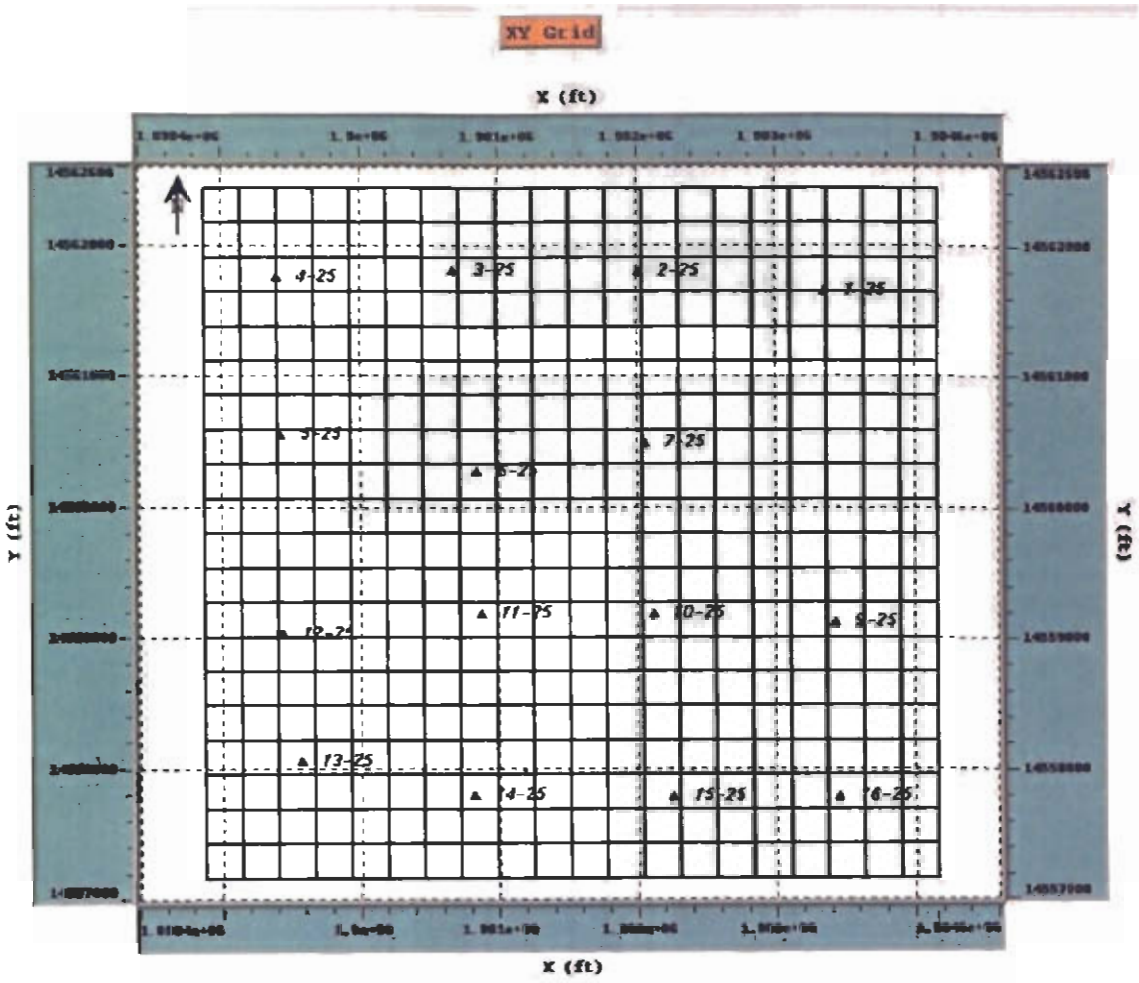

Figure 50. The plan view of the upscaled reservoir grid.

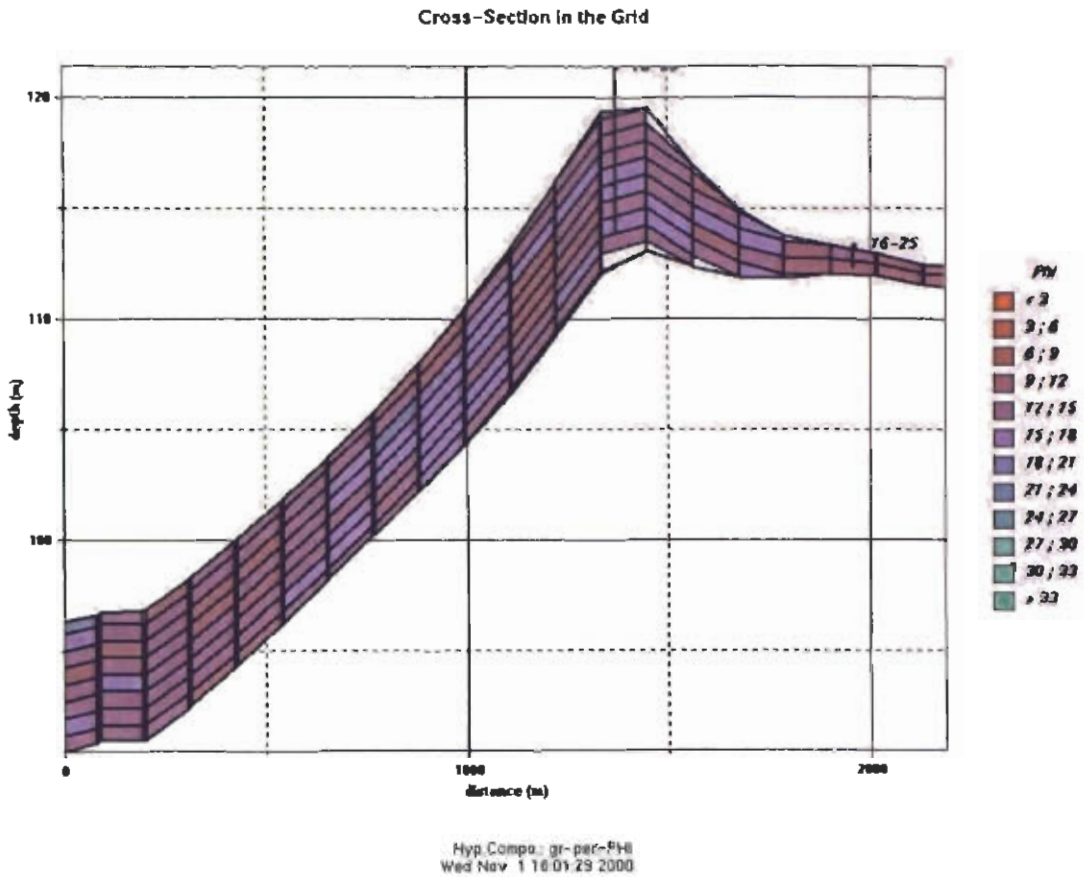

Figure 51. D sandstone porosity distribution in the cross section shown in figure 40 for the upscaled reservoir.

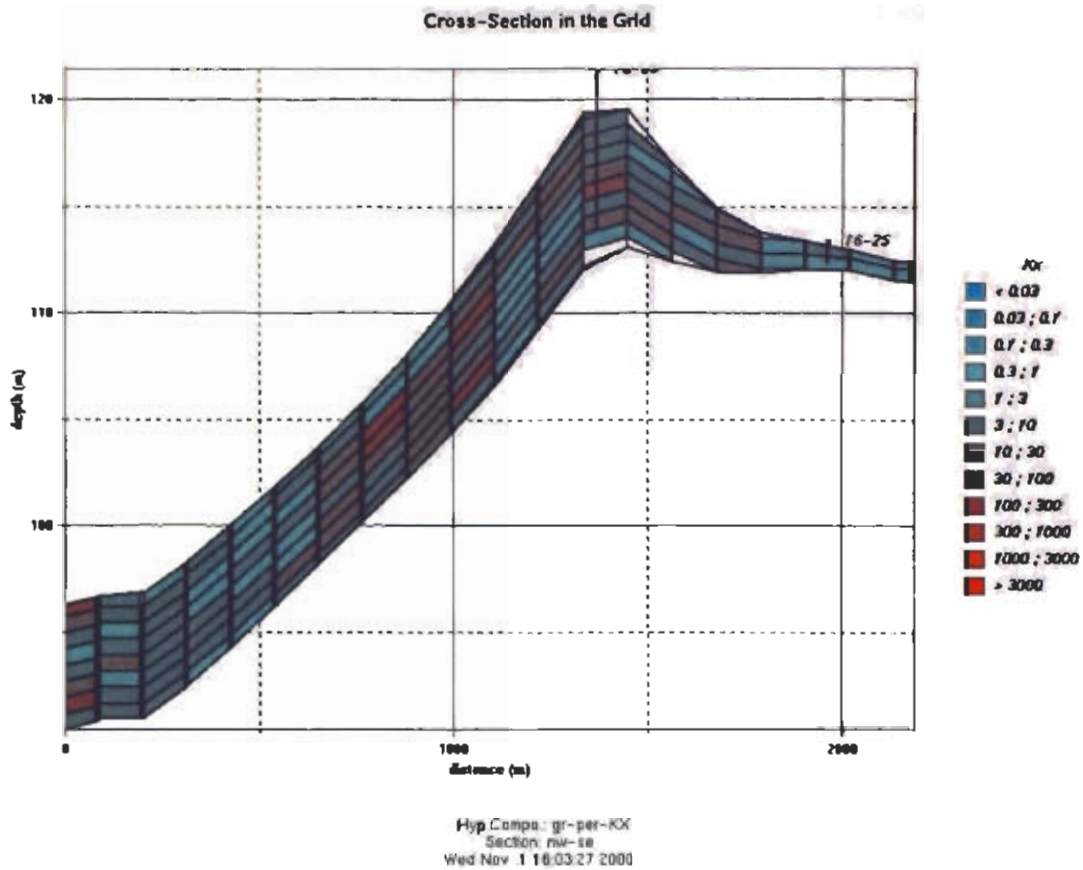

Figure 52. D sandstone permeability distribution in the upscaled reservoir for the cross section shown in figure 40.

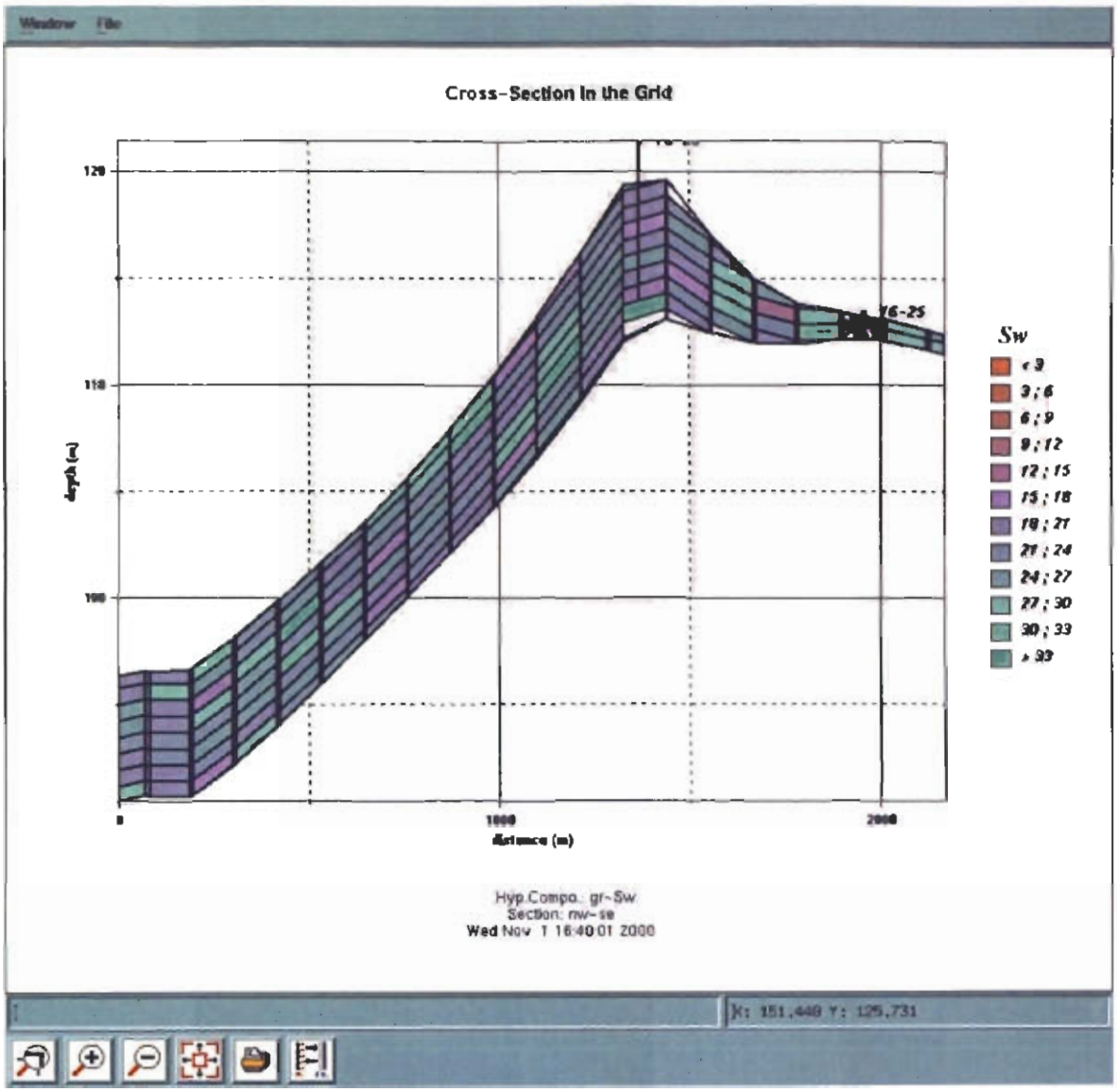

Figure 53. D sandstone water saturation distribution in the upscaled reservoir for the cross section shown in figure 40.

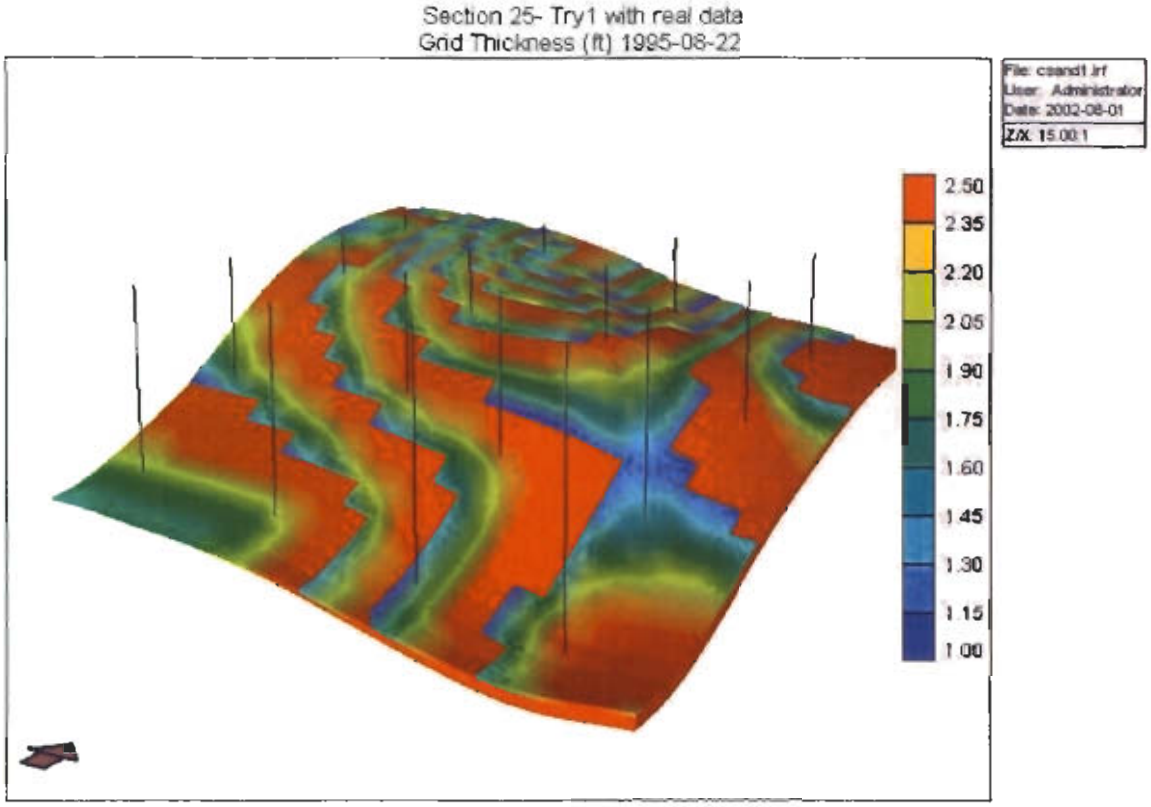

Figure 54. The C sandstone thickness map in feet.

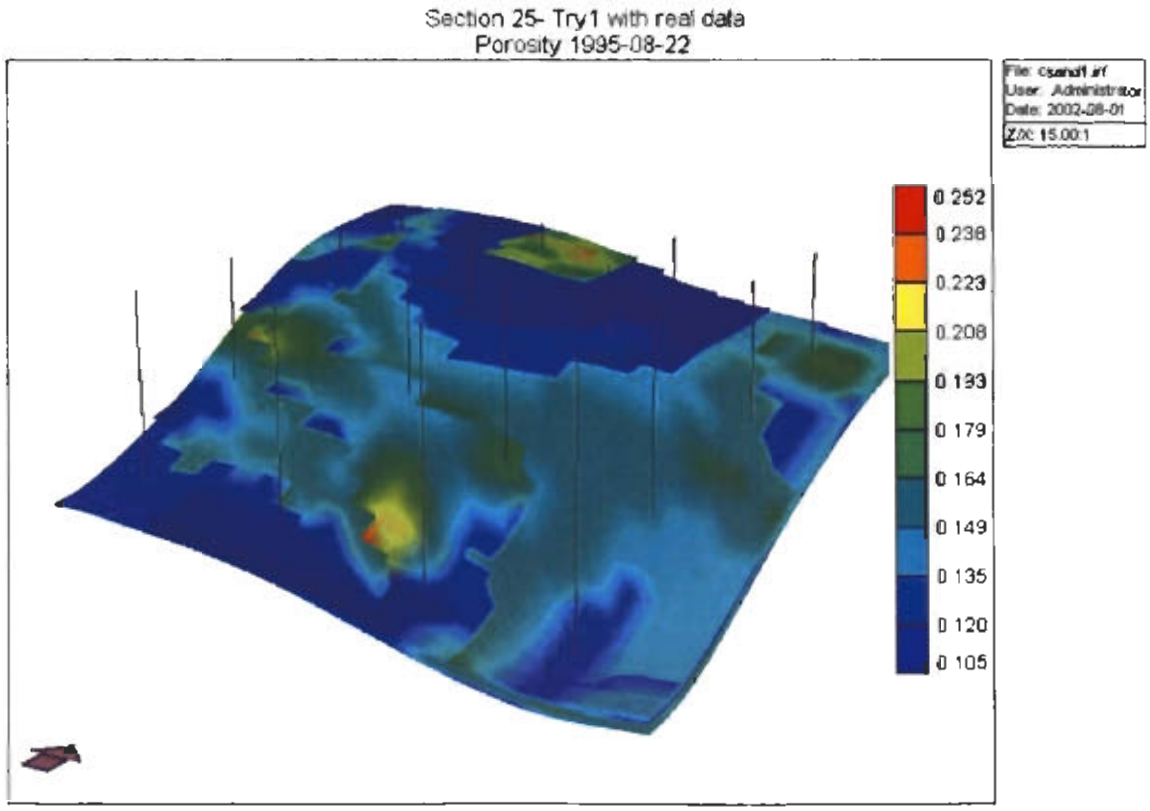

Figure 55. The C sandstone porosity map, dimensionless.

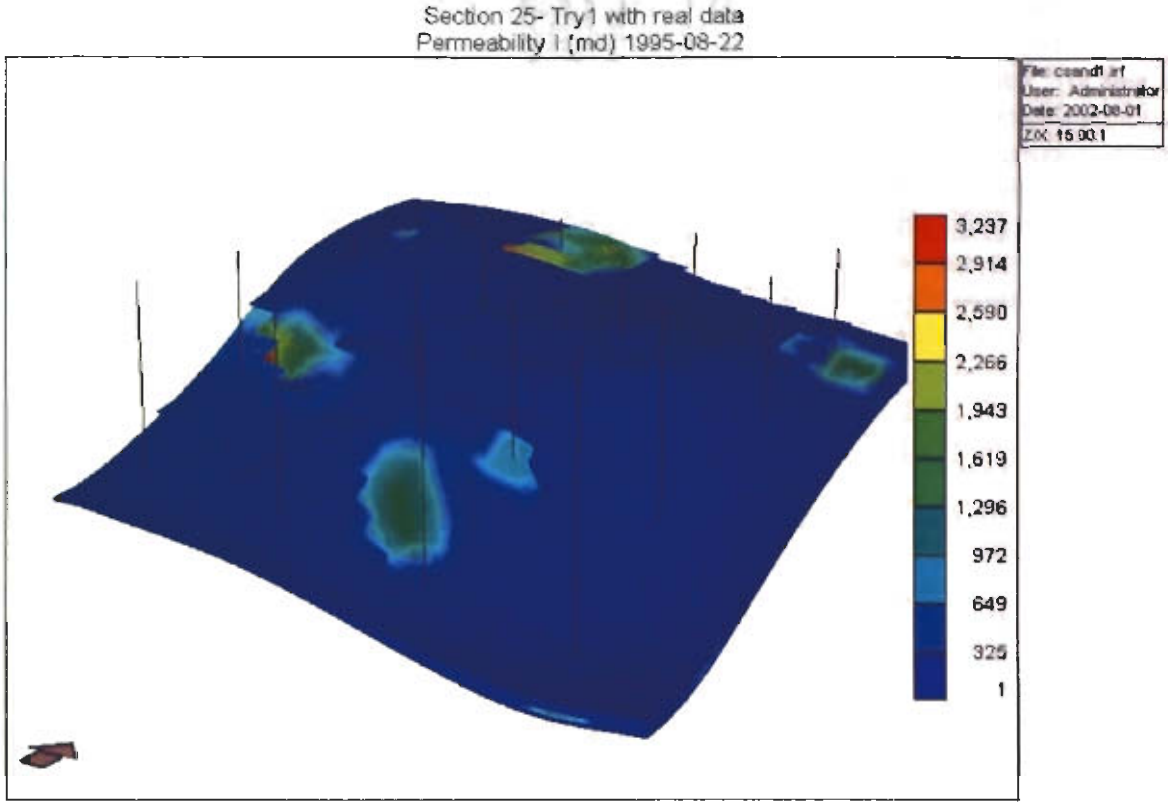

Figure 56. The C sandstone permeability values in millidarcies.

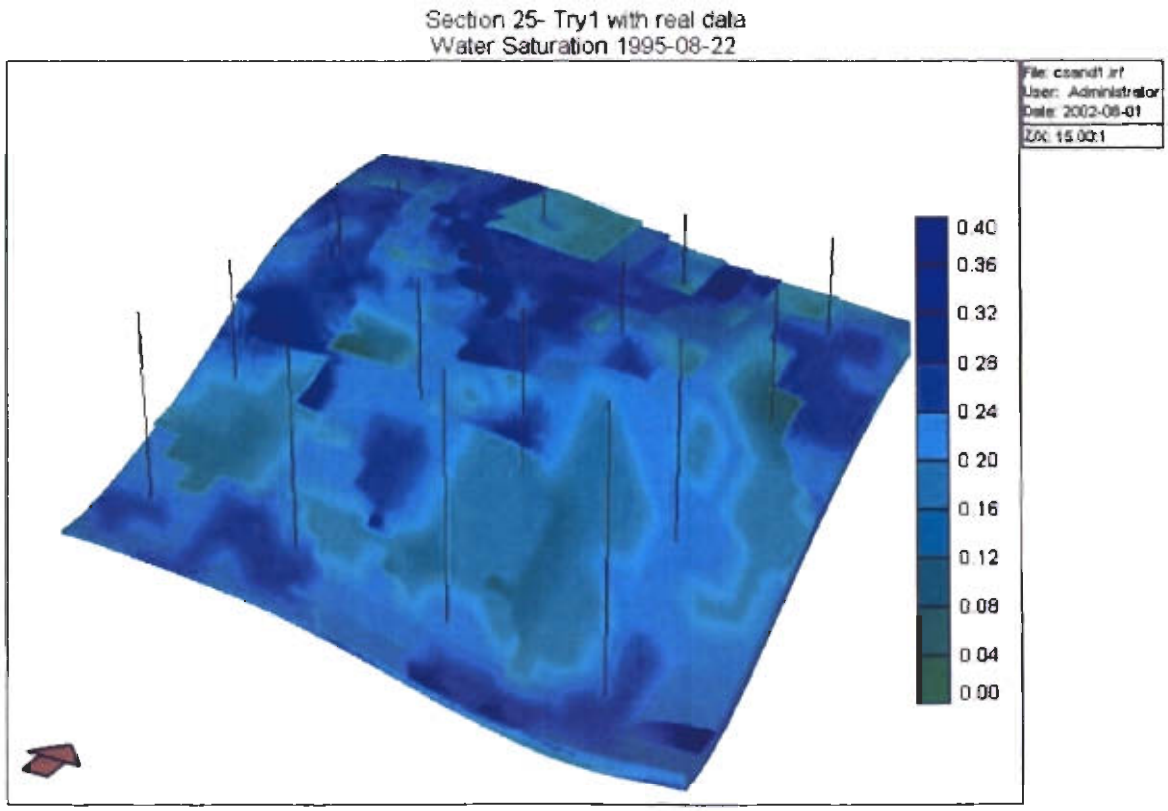

Figure 57. C sandstone water saturations, dimensionless.

NUMERICAL SIMULATION MODELS OF THE UPPER DOUGLAS CREEK, CASTLE PEAK, AND UTELAND BUTTE RESERVOIRS

Numerical simulation models were constructed for the Monument Butte Northeast unit (upper Douglas Creek reservoir), Brundage Canyon field (Castle Peak reservoir) and, Uteland Butte field (Uteland Butte reservoir). The Monument Butte Northeast is a secondary-recovery water-flood unit but the Brundage Canyon and Uteland Butte fields are in primary production. Porosity, permeability, and oil saturations were determined from geophysical well logs and core data. Geostatistical models of the porosity, permeability, and oil saturation for each of the fields were upscaled to obtain a reasonable number of grid blocks for reservoir simulation. All simulations were conducted using the Implicit-Explicit Black Oil Simulator® (IMEX), developed by the Computer Modeling Group Limited®.

Monument Butte Northeast Unit

The Monument Butte Northeast (MBNE) unit consists of 16 wells, eight injectors, and eight producers in section 25 (T. 8 S., R. 16 E., SLBL) (figure 21). The MBNE unit includes parts of the neighboring sections 24 and 26, but only section 25 was modeled. The MBNE unit produces from all of the reservoirs in the lower and middle members of the Green River Formation but the majority of the oil is produced from the upper Douglas Creek reservoir in the middle member. Section 25 has about 10 million stock-tank barrels (MMSTB) (1.6 MMm^3) of original oil in place (OOIP) in two major sandstone beds and several minor ones. The major oil-producing sandstone beds are the D (MGR 7) and the C (MGR 6) sandstone beds, of which the D sandstone has nearly 75 percent of the oil in place and was studied in the most detail.

A geological model, structure, and sandstone thickness was developed using geophysical well logs. The thickness of the sandstone beds were assigned based on the mapped thickness and the perforated interval data for each well. The composition of the oil from specific wells was analyzed by simulated distillation on a capillary gas chromatographic column. The reservoir fluid properties such as the viscosities and gravities, were measured in the laboratory. The bubble points and oil formation factors at different gas-to-oil ratios were also measured. The reservoir was modeled using a variable thickness, variable depth option with several layers present. The model resulted in an excellent match between the simulated production and actual field production.

Simulation Results

A Cartesian coordinate system was used to describe the Monument Butte unit with a multilayer, 20 by 20 grid to represent the reservoir. The total dimension of the field was 5,200 feet (1,584.9 m) by 5,200 feet (1,584.9 m). The reservoir was modeled using a variable thickness, variable depth option with 13 layers present. Porosity, permeability and water saturation computed in the geological model were used in constructing the model for flow simulations. Since there was no free gas present in the reservoir initially, the oil saturations are just the difference between total saturation 1.0 and the water saturation. With the aforesaid reservoir description, the D sandstone was determined to contain 7.52 MMSTB (1.20 MMm^3) of OOIP. Reservoir fluid properties were the same as those computed and used in the previous work. The properties are summarized in table 4. The initial pressure in the reservoir was estimated to be between 2,200 and 2,300 pounds per square inch (psi) (15,000 to 16,000 kPa).

Table 4. Thermodynamic properties of Monument Butte fluids.

p	rs	bo	eg	μ_o	μ_g
14.7	0	1.0018	4.73	14.1	0.0055
500	115.128	1.0625	168.8	12.248	0.0057
1000	230.256	1.125	350.803	7.245	0.0061
1200	276.307	1.15	426.603	6.21	0.0062
1500	345.383	1.1875	541.8	5.348	0.0065
2000	450.511	1.25	850.991	4.14	0.0071
2500	575.639	1.3125	950	3.45	0.0077
3000	690.767	1.375	1140	3.105	0.0842
4000	921.022	1.5	1500	2.415	0.0907
6000	1370	1.75	2200	1.5	0.092
9000	2025	2.1	3200	1	0.093

p = pressure in psi
rs = gas oil ratio in SCF/STB
bo = oil formation volume factor, reservoir barrel/stock tank barrel
eg = gas formation volume factor SCF/reservoir barrel
μ_o = oil viscosity in cp
μ_g = gas viscosity in cp

The bubble–point pressure of the reservoir crude at the initial GOR of about 450 to 500 standard cubic feet/stock-tank barrel (SCF/STB) (80 to 90 m^3/m^3) was around 2,200 psi (15,000 kPa), close to the reservoir pressure. As the first well was placed on production, the reservoir pressure began to drop, resulting in the formation of free gas in the reservoir. Gas being less viscous than oil, was preferentially produced and the production GOR increased. The average pressure had dropped to 2,140 psi (14,800 kPa). As water was injected into the reservoir, the reservoir was pressurized and the production GOR declined to the current value of 488 SCF/STB (86.9 m^3/m^3). The reservoir pressure was almost equal to the bubble–point pressure in most parts of the reservoir and well above the bubble point in the areas adjoining the injectors.

All the producer wells were operated at a bottom hole pressure of 650 psi (4,480 kPa). Since injecting as much water into the reservoir as possible is important for a successful water flood, water injection was started early in the MBNE unit. The important deviation from conventional water floods is the injection strategy. Some of the largest producers were converted to injectors. To ensure a five–spot pattern, alternate producers were converted to injectors.

The field cumulative oil production and that predicted by the simulator are shown in figure 58. The D sandstone contains nearly 76 percent of the OOIP and the remaining is in the C sandstone. To account for the production from D sandstone, simulations with different water injection rates were performed. Simulation runs with water injection rates of 60 percent and 40 percent of the original rates in each of the wells were performed. The cumulative oil production, as predicted by the simulations with 60 percent water injection (figure 59) rate did not match the field oil production well.

The run with 40 percent water injection rate (figure 60) matched approximately 82.8 percent of the total production from the field and the cumulative oil production profile matched the field results closely. This is approximately the production contribution expected from the D sandstone. The production match from individual wells was not matched well, though a satisfactory matched was obtained for some of the wells.

Figures 61 and 62 show the cumulative water and gas production profiles along with the corresponding field results. A pronounced variation between the field and simulation profiles was observed.

Figure 63 shows the water injection profile along with the field values. An excellent match was obtained between the simulation and the field results. However, the injection rate of 40 percent was lower than the amount that would have been injected into the D sandstone.

Inclusion of Hydraulic Fractures in the Reservoir Model

Introduction: All the wells in the field and most of the greater Monument Butte area are hydraulically fractured but the initial simulations did not include the effects of hydraulic fractures. Hydraulic proppant fracturing and gravel packing are common stimulation and stabilization treatments during completion, testing, and exploration of hydrocarbon reservoirs in the oil and gas exploration and production industry. Hydraulic fracturing is a method for increasing well productivity by fracturing the producing formation, and thus, increasing well drainage area. Thus, it can be defined as the process of creating a fracture or fracture system in a porous medium by injecting a fluid under pressure through a well bore in order to overcome the native stress and to cause material failure of the porous medium. Briefly, it is the creation and preservation of the fracture in a reservoir rock. Fluid is pumped down the well and injected into the formation, generating the energy needed to fracture the rock.

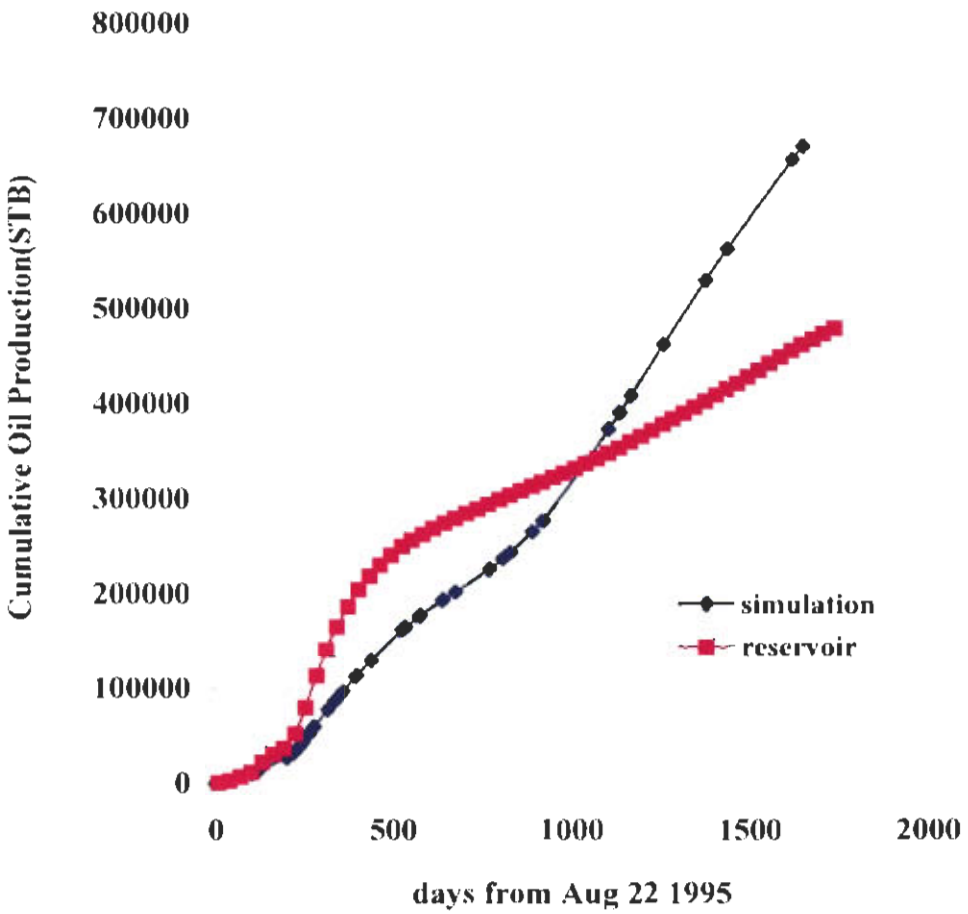

Figure 58. Comparison of cumulative oil production in the MBNE unit with total water injection into the D sandstone.

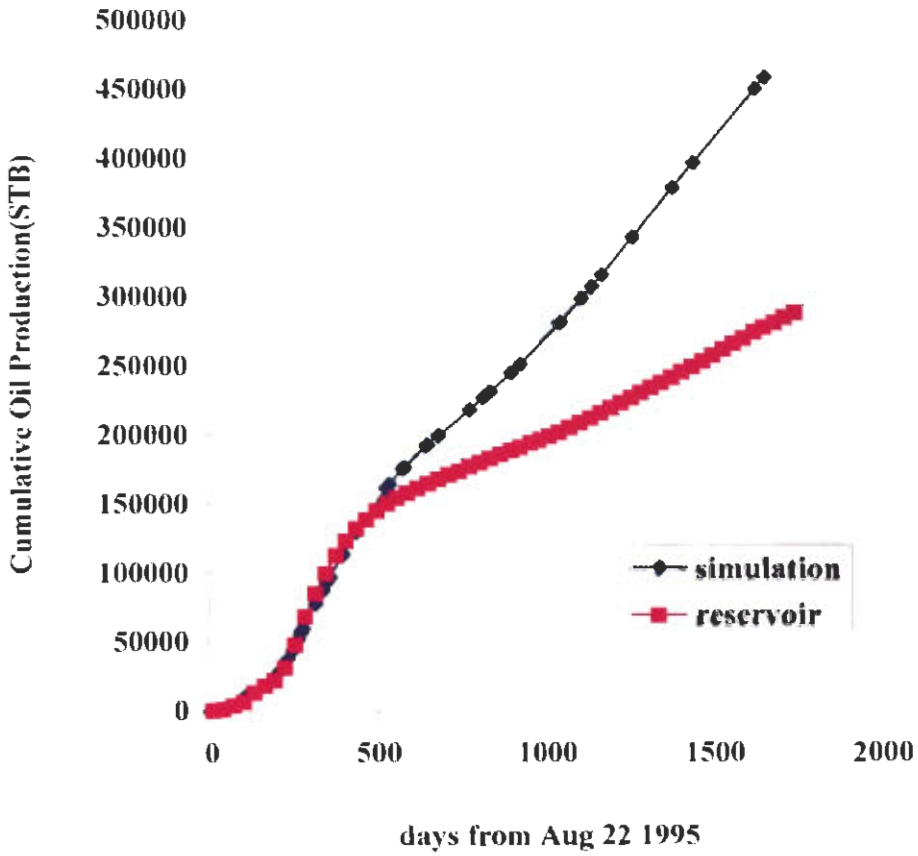

Figure 59. Comparison of cumulative oil production in the MBNE unit with 60 percent water injection into the D sandstone.

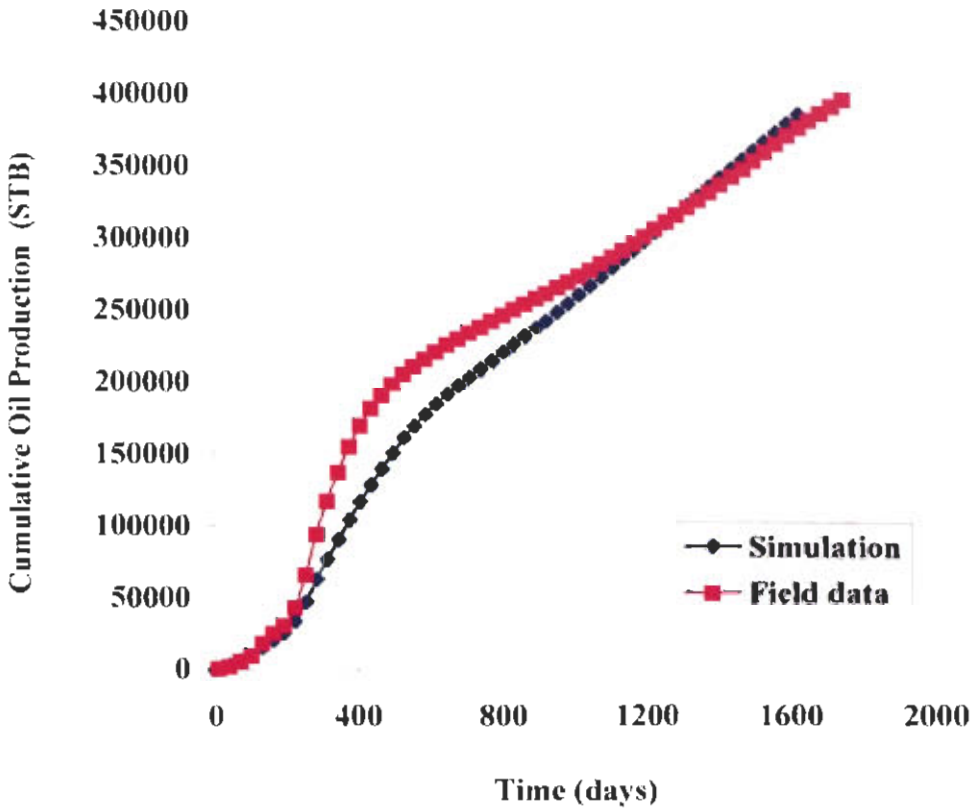

Figure 60. Comparison of cumulative oil production in the MBNE unit with 40 percent water injection into the D sandstone.

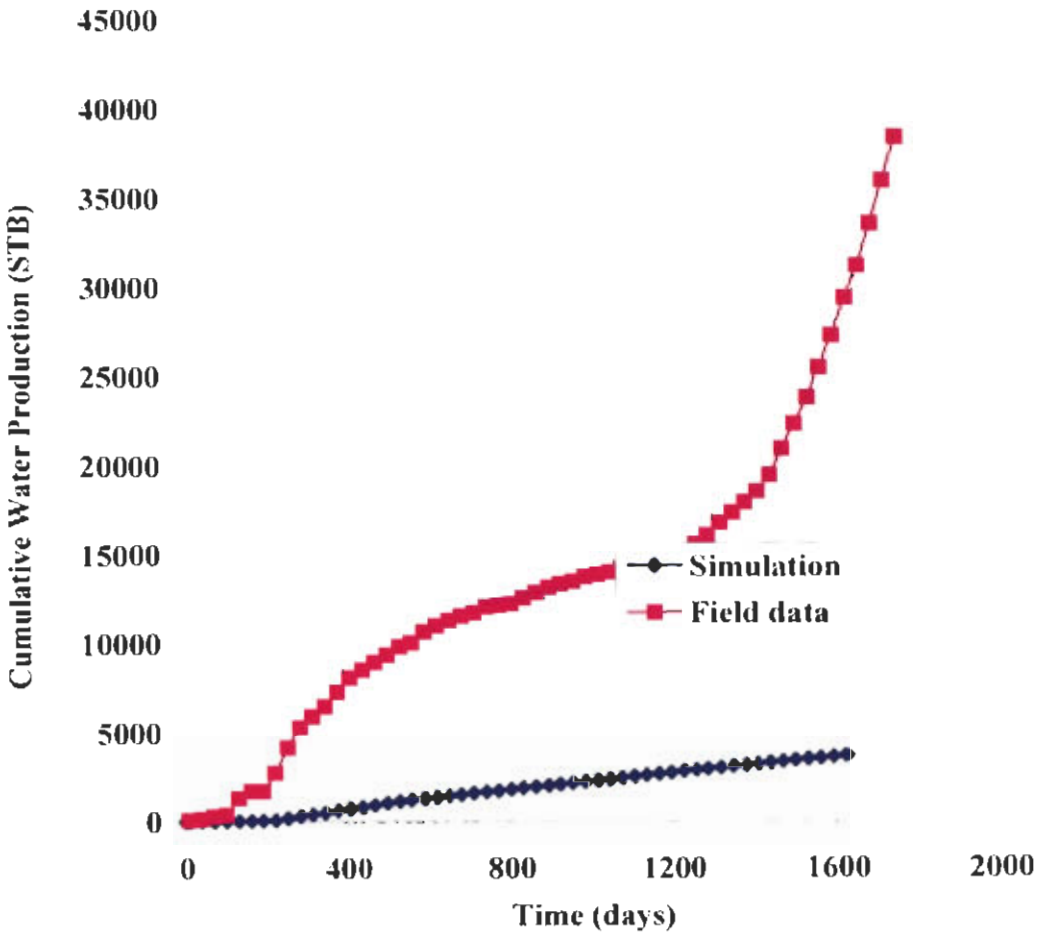

Figure 61. Comparison of cumulative water production in the MBNE unit with 40 percent water injection into the D sandstone.

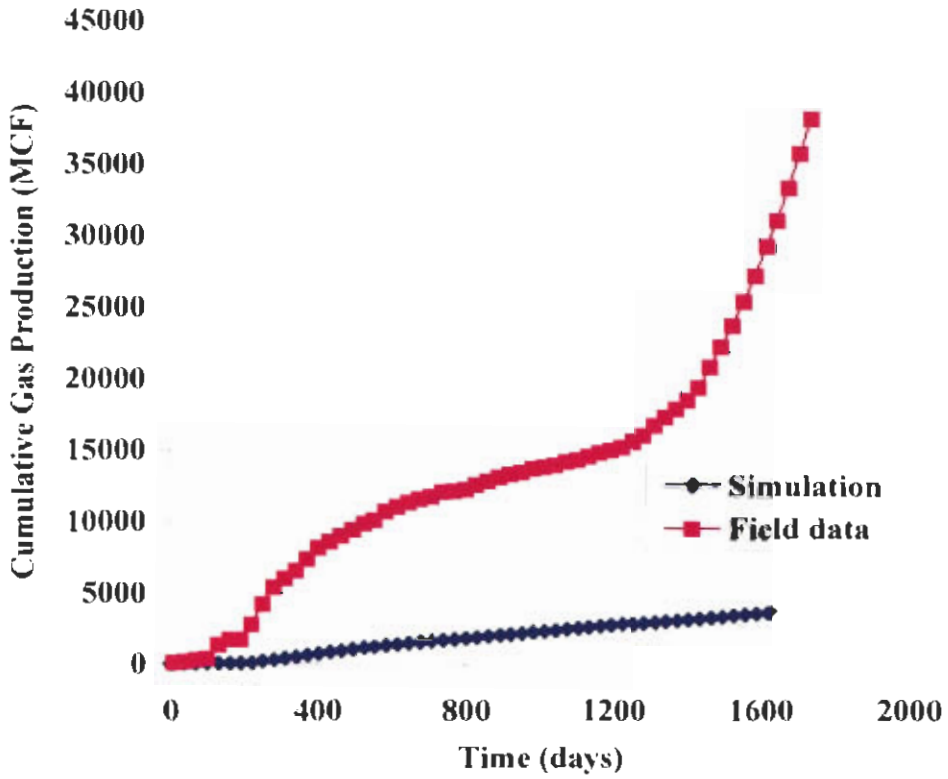

Figure 62. Comparison of cumulative gas production in the MBNE unit with 40 percent water injection into the D sandstone.

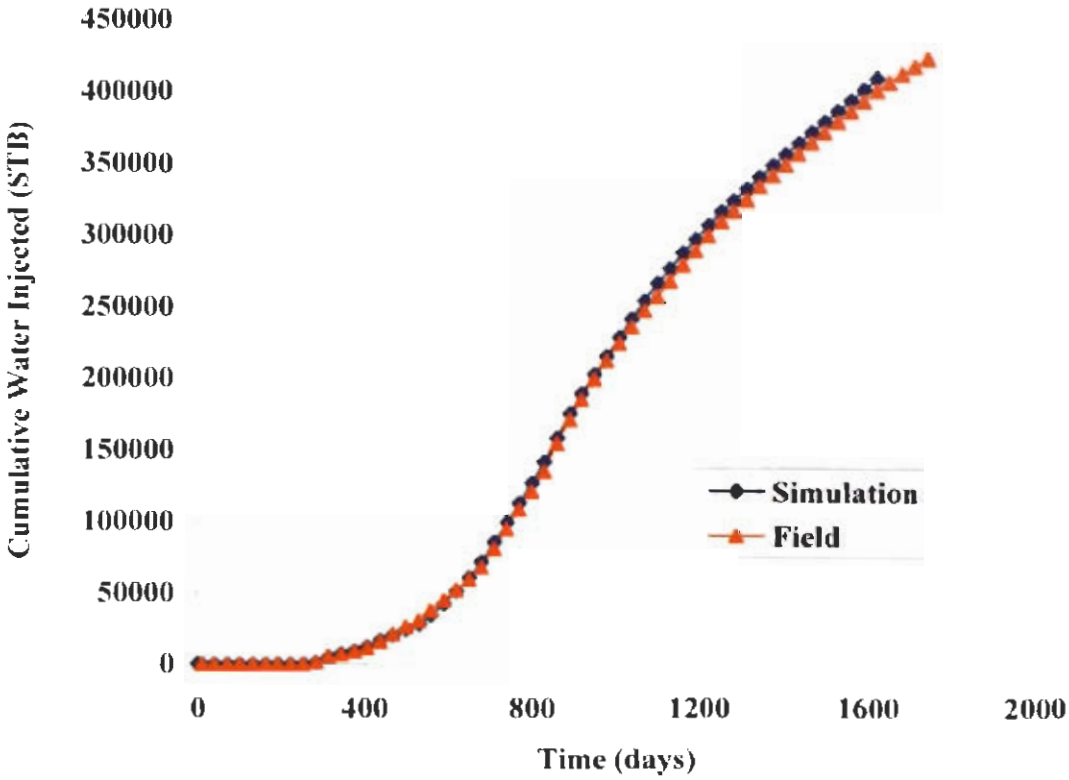

Figure 63. Comparison of cumulative water production in the MBNE with 40 percent water injection into the D sandstone.

The purpose of natural sand or synthetic proppants of different type and grain size in hydraulic fracturing is to support the crack in order to keep it open against the closure stress acting in pay zone depth and to maintain a highly conductive drainage path through the tight reservoir rock matrix for oil and gas flowing to the well bore, and in gravel packing to plug the perforation tunnels and to build a gravel mantle along the well bore wall in order to filter the hydrocarbons flowing into the well bore and prevent pay zone sand from moving. Hydraulic fracturing and gravel packing lead to enhanced oil and gas recovery from low permeability and weakly cemented to loose friable sandstones.

Incorporating Hydraulic Fractures: All wells in this field and in most of the greater Monument Butte belt are hydraulically fractured. The objective of this study was to examine the impact of the presence of hydraulic fractures in the reservoir. The hydraulic fractures were inserted in blocks containing the wells. It is known (from stimulation simulations and through rock-mechanics considerations) that the hydraulic fractures are vertical, circular shaped, and extend about 200 feet (60 m) beyond the well bore on either side and span the entire thickness of the reservoir.

The following procedure was used to incorporate hydraulic fractures in the reservoir model. The grid blocks containing the wells were refined by local grid refinement. The hydraulic fracture was approximately 158.5 feet (48.3 m) in length and its height spanned the perforated sand thickness. The fracture block was about 0.45 feet (0.137 m) in width. This was the finest refinement that the simulator would allow. The width of the hydraulic fracture cannot be set to a finite value and is based upon the local grid refinement of a grid block approximately 264 feet (80.5 m) in length and width. The block was refined into five blocks each in the x and y direction. The second, third, and the fourth blocks in the middle row in the j direction were further refined to five blocks in the i direction. The middle row of the resulting blocks was further refined and this procedure was carried out until the smallest refinement was slightly greater than the diameter of the well. With this refinement, there were a total of 12,900 grid blocks. A fracture spanning nearly 200 feet (60 m) on either side of the well bore would have represented a more realistic picture, but the total number of resulting blocks would exceed the limits of the simulator.

The smallest refinement thus obtained was nearly 0.45 feet (0.137 m) in width. All layers in which the wells were completed were refined to the dimensions stated above. We represented the fracture with the smallest refined block containing the well and one refined block on either side of the block containing the well. A high permeability zone represented the fracture and a permeability of 1,000 md was assigned to each of the refined blocks representing the fracture. It should be noted that the matrix permeability varied over a range of about 0.1 to 150 md. The porosity was the same as the original refined block. All other properties were identical to the original simulation.

Simulation Results

Comparison at the End of Primary Production: The initial pressure of 2,300 psi (15,900 kPa) dropped to around 2,100 psi (14,500 kPa) at the end of primary production. The presence of hydraulic fractures increased production in comparison to the model without fractures. The gas production rose significantly from 33.50 MMSCF (0.95 MMm^3) to 770.78 MMSCF (21.83 MMm^3). The average oil production rate increased to 533.46 STB/day (84.8 m^3/day) from 273.47 STB/day (43.5 m^3/day). The cumulative oil production increased to 77.09 MSTB (12.257 m^3) from 59.20 MSTB (9,413 m^3) in the model without the fractures. The gas saturation

had increased to nearly 2 percent. The oil production rate increased to 641.88 STB/day from the previous value of 491.08 STB/day. The total water production had increased nearly tenfold from 0.266 MSTB to 2.99 MSTB, with the production rate increasing tenfold from 3.66 STB/day to 32.158 STB/day. Table 5 summarizes the primary production from the field and simulation models with and without fractures. In comparison to the field values, oil and gas production values were less than the corresponding field numbers. The water production matched quite well.

Table 5. Comparison of cumulative production at the end of primary.

Fluids	Field	Simulation	
		With fractures	Without fractures
Oil (MSTB)	99.97	77.093	59.209
Water(MSTB)	2.2926	2.9928	0.2668
Gas(MMSCF)	148.96	70.782	33.5

The difference in values of the oil and gas production may be due to relative permeability data used in the model. The values used are the ones experimentally determined in the laboratory and used in previous work on the Monument Butte field, as stated earlier. Different sections of the reservoir may have different relative permeabilities, which have not been accounted for in the model. Another plausible reason is the size of the hydraulic fractures. Hydraulic fractures usually extend to around 200 feet (60 m) on either side of the well bore, but the ones represented in the model is only 158.5 feet (48.3 m) in length. This was due to the limitation on the total number of blocks allowed by the simulator. To incorporate the required size, nearly 25,000 blocks would be necessary which is far more than that allowed by the simulator. The permeability of the fractures was assigned a value of 500 md. This value depends on the packing material and the packing pattern in the fracture.

Further Comparisons and Analysis: Water injection started on May 24, 1996. As water was injected into the reservoir, the reservoir pressure started to increase. The significant increase in gas production during primary production continued nearly at the same rate until about 600 days of production before more and more gas was driven into the solution, as only half of the injecting wells were opened by then. The production GOR reached a maximum of about 7,000 SCF/STB (1,200 m^3/m^3) before declining to the current value of around 600 SCF/STB (100 m^3/m^3) as the reservoir continued being pressurized. The gas saturation increased to nearly 5 percent before starting to decrease. The reason for this was some of the biggest producers had just been opened and some producers were opened after water injection had started in couple of wells. The gas saturation decreased to the current value of 1.33 percent at the end of simulation period. The average oil saturation at the end of the period decreased to about 70 percent. As expected, the reservoir shows a large variation in oil saturation, ranging from 25 percent in the vicinity of the injectors to 70 percent in regions farther from the injectors.

Figure 64 shows the comparison of the field cumulative oil production and that predicted by the reservoir simulator. When some the producers were switched to injectors, the production profile started to flatten out, but when all the injectors were functional, the water flood rejuvenated oil production. The production from D sandstone matched nearly 88 percent of the total production from the field. Hereafter, all comparisons are made between 88 percent of the field value and that from the simulator. The remaining is attributed to the C sandstone. The cumulative production at the end of the simulation period was 408,690 STB (64,981.7 m^3) and

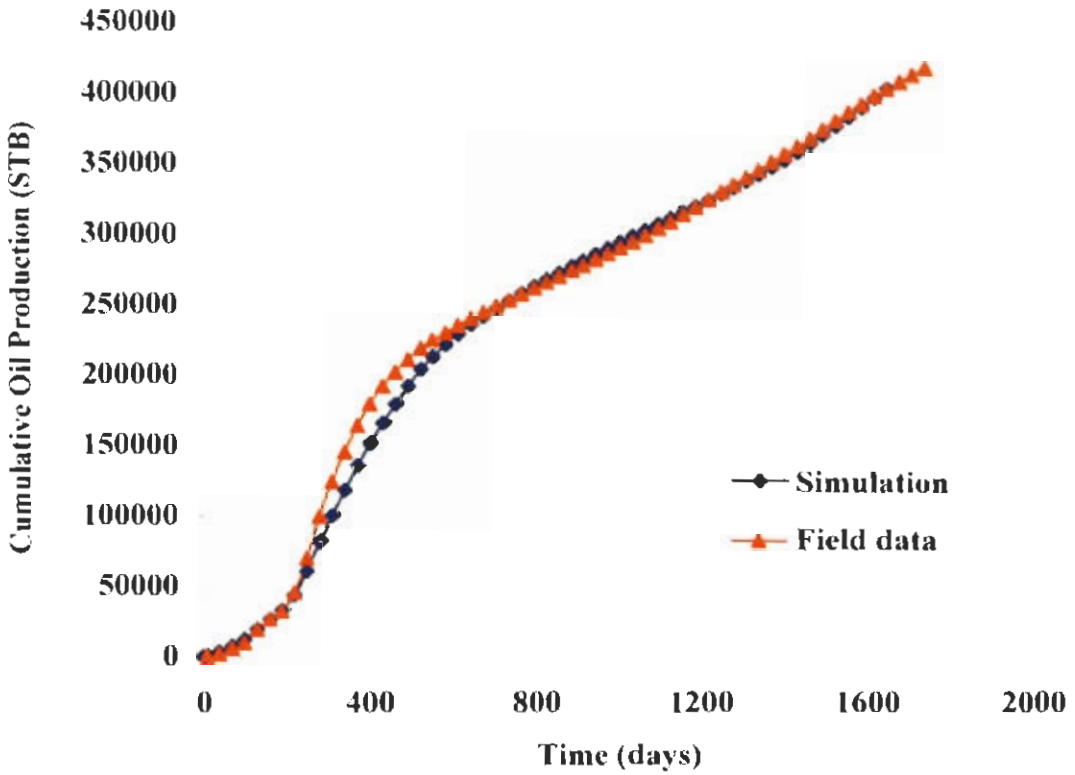

Figure 64. Comparison of actual cumulative oil production with simulated oil production in the MBNE unit.

nearly 7.5 percent of the mobile oil had been recovered. Figure 65 shows the comparison of the field average rate of oil production and that from the simulations. A close match is obtained. The simulator does not do a good job of predicting the quick response to water flood observed in the field without fractures, but the response is closer in the model with hydraulic fractures. Thus, the inclusion of hydraulic fractures in the wells is very important in matching history and cannot be neglected. The simulator matched the actual water injection profile well. Figure 66 shows the water injection for the MBNE field.

The mechanism of water flooding can be clearly understood by examining the instantaneous GOR as a function of time. The GOR is around 450 SCF/STB (80 m^3/m^3) at the beginning of primary production. The reservoir pressure falls below the bubble–point pressure and the instantaneous GOR increases rapidly. As more and more free gas is produced in the reservoir and this gas is preferentially produced, the production GOR continues to increase reaching a value of about 7,000 SCF/STB (1,200 m^3). When all the injectors are functional, the reservoir is slowly pressurized; gas is driven back in to the reservoir and the production GOR declines.

Figure 67 shows the field production GOR and those predicted by the simulations. The simulator lags behind the field response to water flood. It takes more time in the simulation for the GOR's to decline than in the field. This decline continues to the current value of around 600 SCF/STB (100 m^3) as stated earlier. Matching instantaneous GOR by reservoir simulation is complex since the value depends not only on the thermodynamics of oil and gas but also on the three–phase flow aspects of oil, water, and gas. Figure 68 shows the cumulative gas production is fairly tracked by the simulator. The simulator does a poor job matching the initial increase in gas production, as the reservoir initially declines below the bubble point. Once water flood was initiated, a close match in gas production is observed. As discussed earlier, a more realistic representation of the hydraulic fracture is bound to have a major effect on the amount of gas produced and an even closer match could be obtained.

The simulator does an excellent job of matching the cumulative water production. Figures 69 and 70 show the cumulative water production and the water cut as a percentage respectively. The water cut is much higher and closer to the field values in the model with hydraulic fractures. Figure 71 illustrates this point. There is a large variation in the water production and hence the water cut at the end of the simulation period. One reason may be due to existence of different regions with varying relative permeabilities. The relative permeability data used were the ones measured in the laboratory. The relative permeability data were altered to obtain a satisfactory match between the simulation and the field results. Another reason for variation in water production may be due to the use of bottom hole constraint to model the data rather than respecting the individual water injection rates. This had to be followed because the local grid refinement used to model the hydraulic fractures gave rise to backflow problems. The size of the grid block was too small to inject the given rate of water.

To obtain a realistic representation of hydraulic fractures, and to overcome the limitations of the simulator, the length of the grid blocks containing the wells was changed to nearly 392 feet (119.5 m), quite close to the actual size of the fractures. The simulator does not allow the representation of grid blocks with different lengths for a given position in any coordinate direction. To circumvent this problem, the position of some of the wells had to be shifted by one block, so that position in the x direction was the same. Simulations were performed with this representation. The relative permeabilities were adjusted and refined to match the total water production.

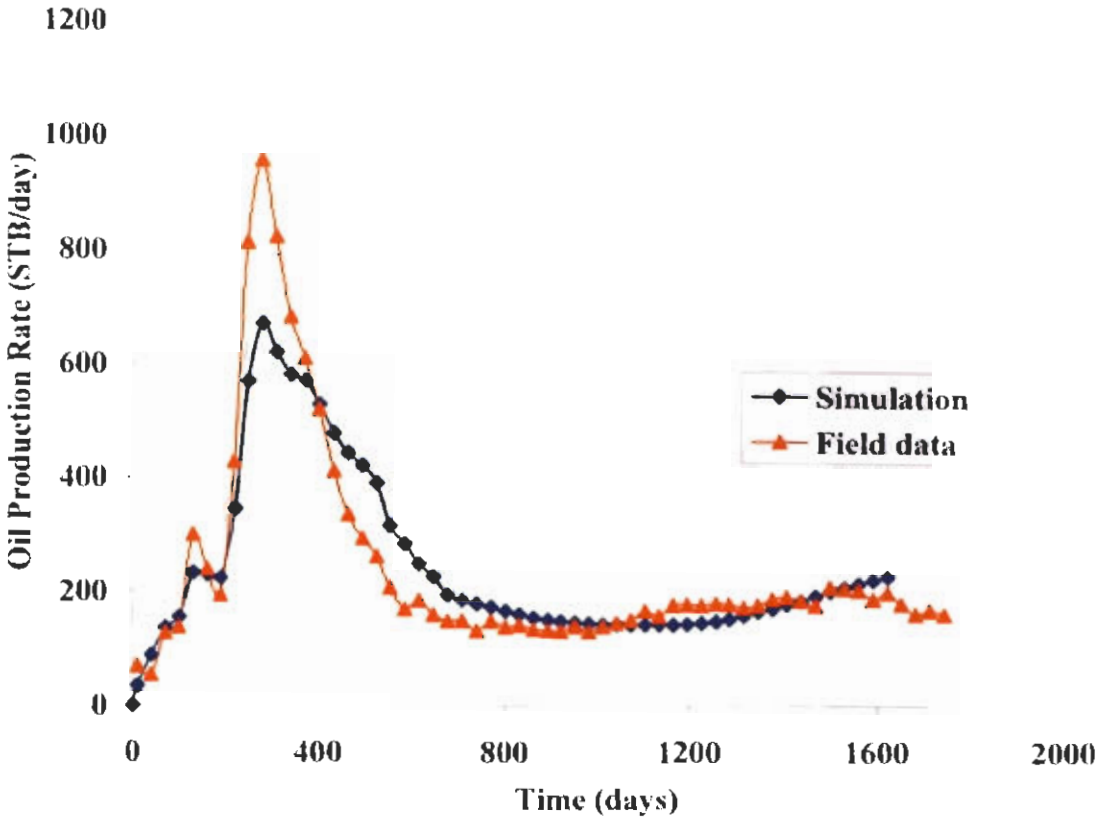

Figure 65. Comparison of actual average rate of oil production with simulated average rate of oil production in the MBNE unit.

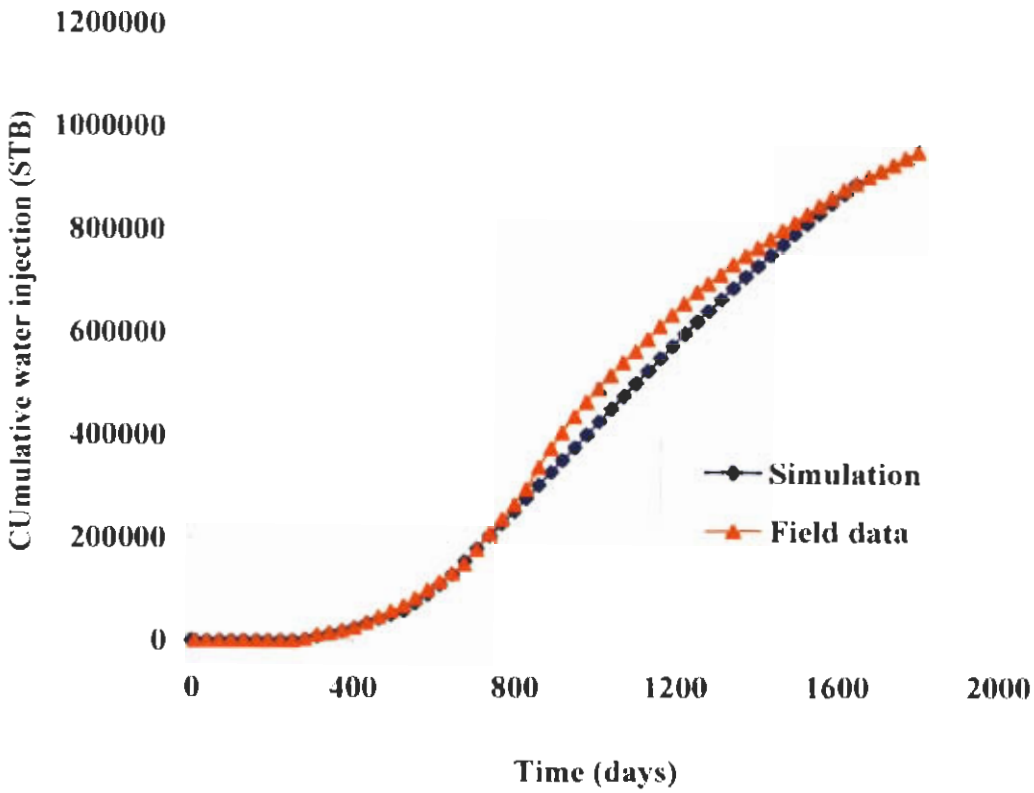

Figure 66. Comparison of actual cumulative water injection to simulated cumulative water injection in the MBNE unit.

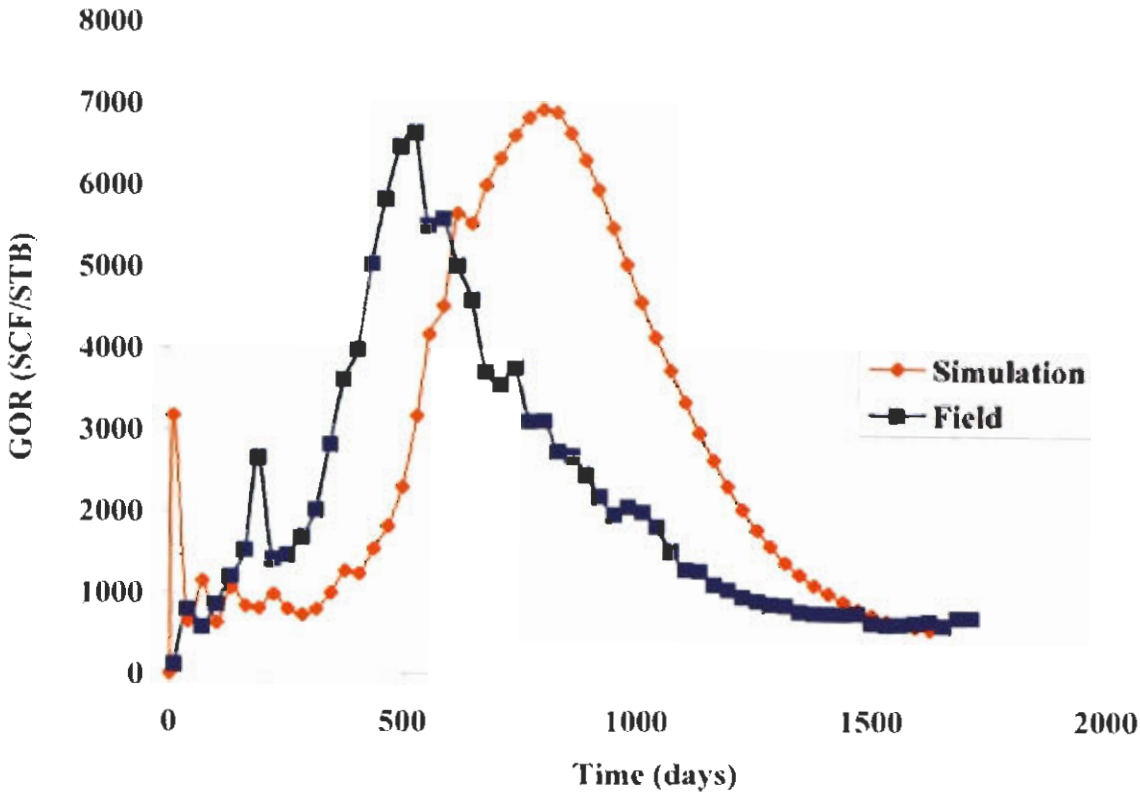

Figure 67. Comparison of producing gas-to-oil ratio to simulated gas-to-oil ratio in the MBNE unit.

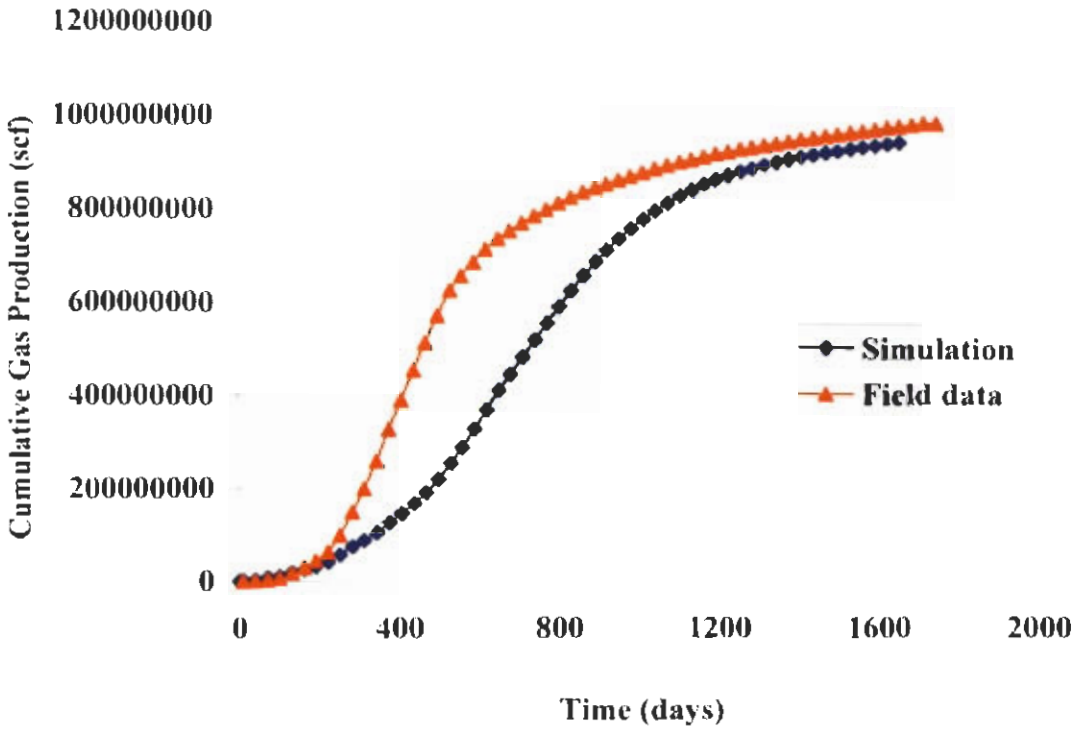

Figure 68. Comparison of actual cumulative gas production to simulated cumulative gas production in the MBNE unit.

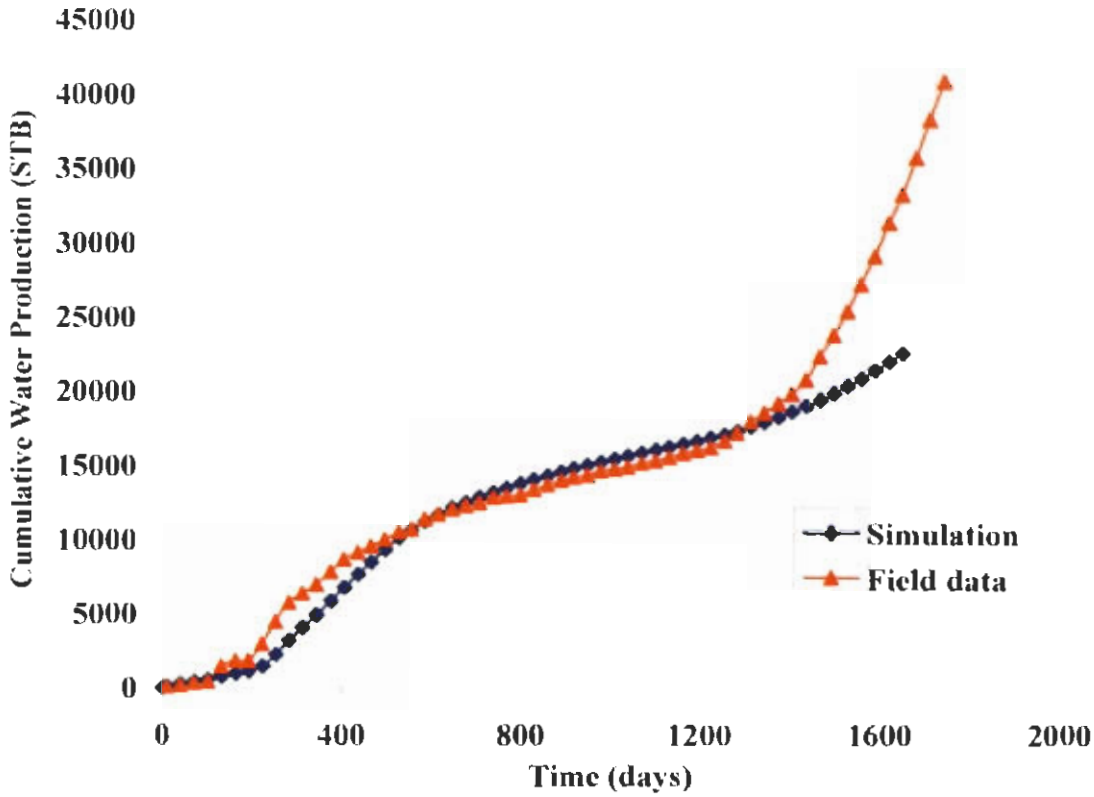

Figure 69. Comparison of actual cumulative water production to simulated cumulative water production in the MBNE unit.

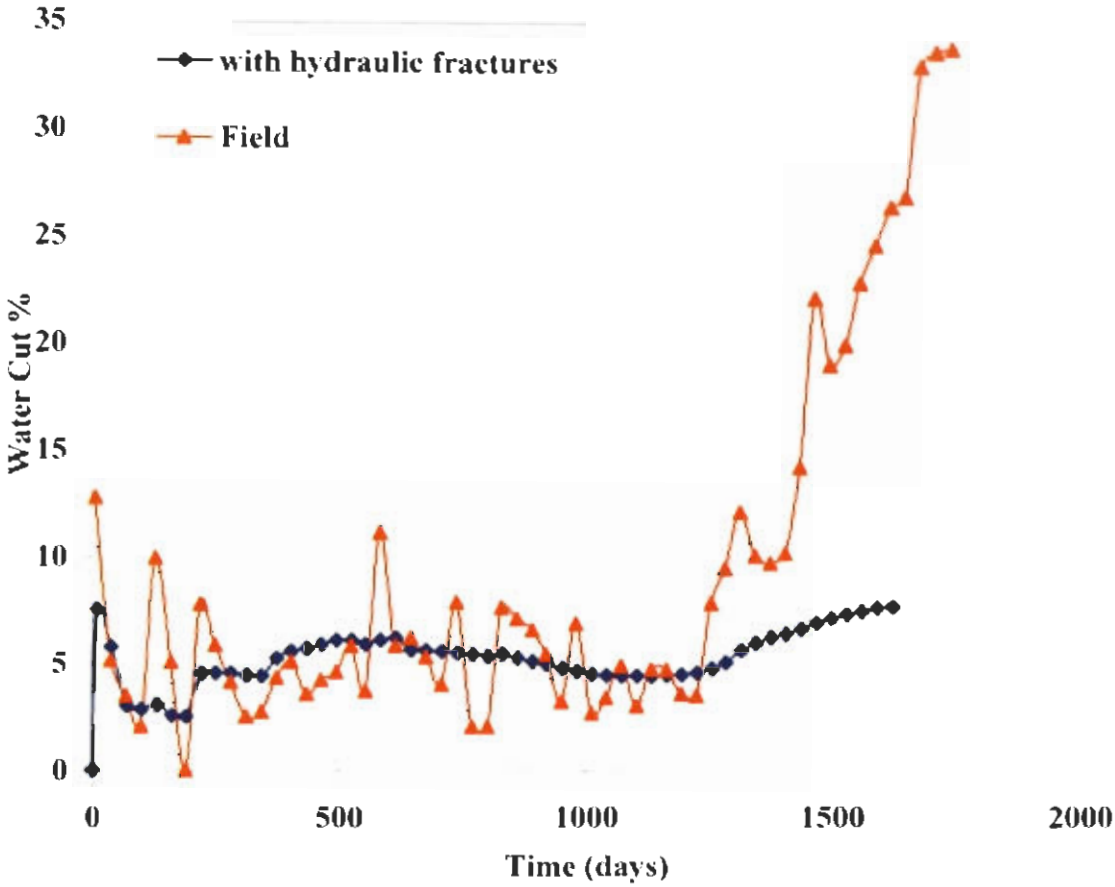

Figure 70. Comparison of actual water cut to simulated water cut in the MBNE unit.

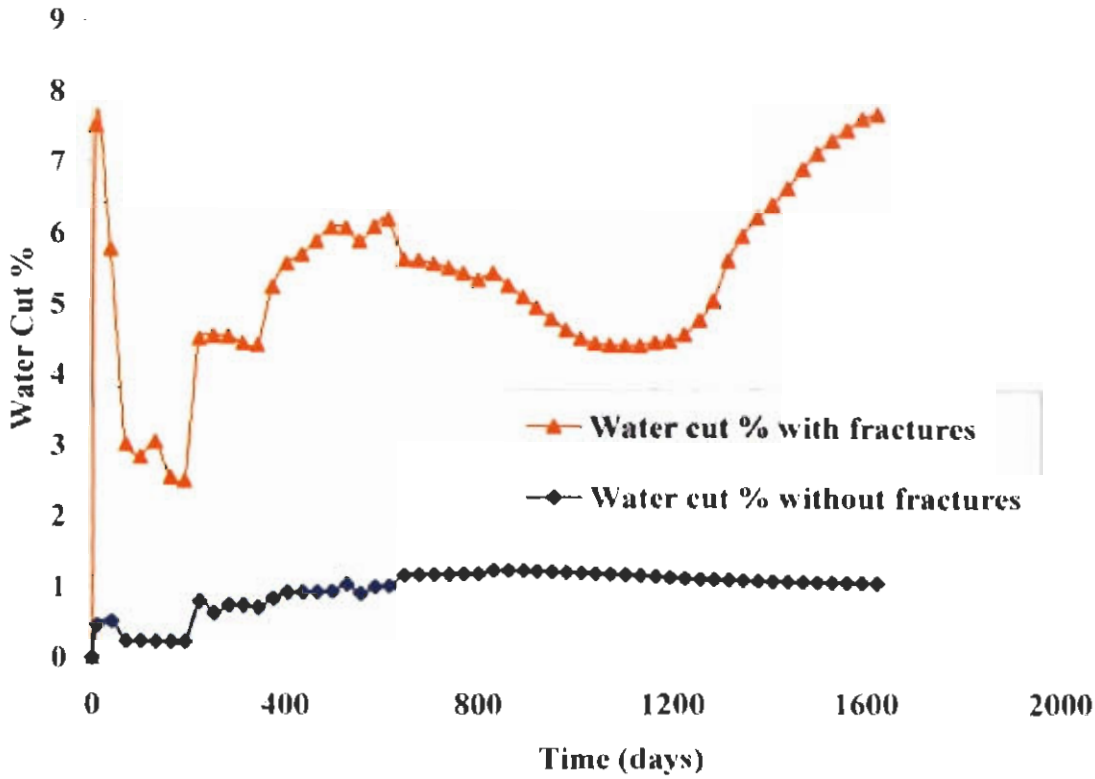

Figure 71. Comparison of simulated water cut with and without fractures, in the MBNE unit.

The cumulative oil production during primary production had increased to nearly 85 MSTB (14 Mm^3). Water and gas production had increased significantly to about 6 MSTB (950 m^3) and 100 MMSCF (2.8 MMm^3) respectively. At the end of the time period, roughly the same amount of oil as in the previous case had been produced, but the water and gas production had increased significantly. Nearly 43 MSTB (6.8 Mm^3) of water and 1,300 MMSCF (36.8 MMm^3) of gas had been produced and 1,110 MSTB (176.5 Mm^3) of water had been injected. The cumulative water production profile (figure 72) did not match the field results well, the total water produced at the end of simulation matching field data notwithstanding. The water cut profile is shown in figure 73.

Thus, the inclusion of hydraulic fractures increased oil production predominantly during primary production, but once water injection had started, there was not any pronounced influence on oil production. However, the water and gas production both increased phenomenally during primary production and at the end of the time period. The runs with more realistic representation of the fractures had decreased oil and water production while increasing gas production. The relative permeabilities had to be tuned to match oil and water production, but gas production and water injection increased slightly. Hence, the relative permeabilities play an influential role in obtaining a good history match.

While the simulator does an excellent job of matching the overall reservoir performance, it doesn't do so in matching individual well performance. Heterogeneities and local production constraints play larger roles in individual well performances. Most of the individual well productions were matched within about 40 percent margin.

The simulator does a good job in matching all the field quantities, but the overall contribution of 88 percent from the D sandstone appears to be higher than expected from that layer. Since the OOIP is nearly 75 percent of the total field and the D sandstone layer being the most productive one, a contribution of nearly 75 to 80 percent is reasonable. The primary reason for this being the fluvial reservoir modeled in this work is a subsystem that is a part of a much larger geologic system. The injected water may be leaving through the boundaries of the unit through sands channeling out of the unit. This is also the reason why the production rate predicted by the simulator is slightly higher than the ones observed in the field. Another reason is attributed to the paraffin deposition around the vicinity of injection and production wells, which is not accounted for in the model. Thus, even though the simulator in matching reservoir performance obtains a reasonably good match, it should be used with caution to predict future performance.

Extended Predictions

The simulations were extended to the year 2010 using the same reservoir representation. Results are tabulated in table 6. The simulations predict that 1.53 MMSTB (243 Mm^3) of oil would have been produced from the unit by the year 2010. This amounts to a recovery of 20 percent of the OOIP. The simulations project the water cut would have increased to 34 percent. With better representation of relative permeabilities, it is expected that the water cut would increase to around 60 to 70 percent and recover nearly 40 to 45 percent of the OOIP before the unit waters out. The model would have to be constantly monitored with field data and calibrated at a later time to ensure good prediction.

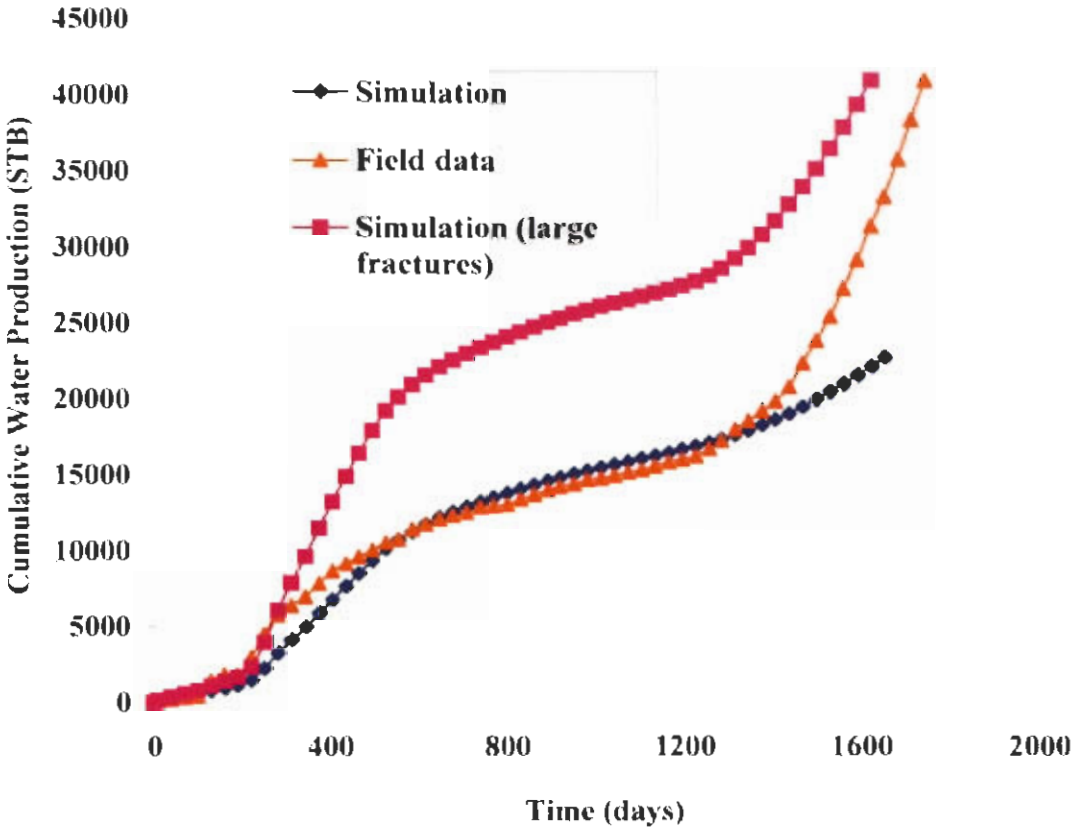

Figure 72. Comparison of actual cumulative water production to simulated cumulative water production without large fractures and without fractures, in the MBNE unit.

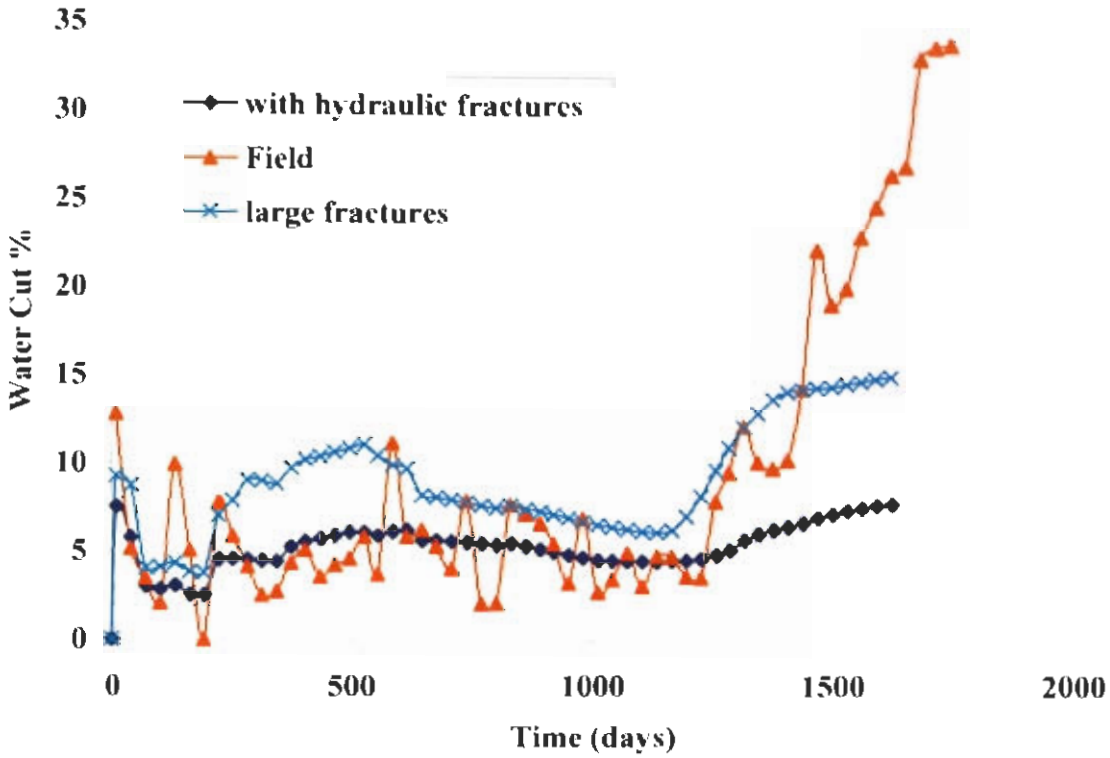

Figure 73. Comparison of actual water cut to simulated water cut with hydraulic fractures and with large fractures, in the MBNE unit.

Table 6. Extended simulation predictions.

Year (March of)	Cumulative Oil Production (MSTB)	Recovery % OOIP
2001	514	6.84
2002	626	8.32
2003	744	9.89
2004	864	11.49
2005	984	13.09
2006	1091	14.51
2007	1206	16.04
2008	1318	17.53
2009	1440	19.15
2010	1532	20.37

Simulations of the Uteland Butte Field

The purpose of this project was to make a baseline oil production prediction from the Uteland Butte oil field. The IMEX® program enabled us to break up the oil field into a grid system and assign values of porosity, permeability, and pressure for each individual block. The grid was simplified in the x and y plane into 15 x 15 matrix of equal size. Each of these blocks was approximately 225 feet (68.6 m) by 225 feet (68.6 m).

The next step was to determine the thickness of each block. In this instance, the case was greatly simplified. It was assumed that the grid had only one block in the z direction, and the thickness of the block was dependent upon how deep the wells were in the field. Most of the thickness values had to be estimated since there were only 19 wells with given thickness while 225 blocks needed to be assigned a thickness. If, for example, a well had a thickness of 10 feet (3 m), then the blocks around it that did not have wells would have thickness values close to that of 10 feet (3 m). To make reasonable estimations, some interpolation was done, and it was also assumed that the thickness at the edge of the grid eventually went to zero. After these calculations and estimations were performed, thickness values could be assigned. Figure 74 is the thickness grid generated by the simulator for the Uteland Butte field.

Now that the grid had been constructed, initial conditions had to be set. Several assumptions had to be made in this case, since it was not known at the time of this analysis what the initial conditions were. The assumptions that were made were a constant porosity of 13 percent for all of the blocks. The permeability was set to a constant of 5 md. The initial reservoir pressure was set to 3,000 psi (20,700 kPa), while the bubble point was set to 3,500 psi (24,100 kPa). The initial oil saturation was 78 percent, which meant that the initial water saturation was set to 22 percent for each of the blocks. Other values were assumed for well geometries and other important geometries and initial conditions.

The next part was to run simulations using the IMEX® program. In order for a baseline to be constructed, a simulation had to be run for each well. In each case, only one well was opened and oil was collected for a time period from 1989 to 2005 (16 years). The amount of oil collected was different than for the other wells. The cumulative oil collected from each well is shown in figure 75.

This figure shows that the program does indeed work and obtains reasonable working values of oil collected. In comparison with the actual oil collected, some of the values are quite close, while there are some values that are not that close. These errors are expected however, since there was no time frame given when the wells were open and when they were closed. In conclusion, a reasonable baseline was obtained from the field.

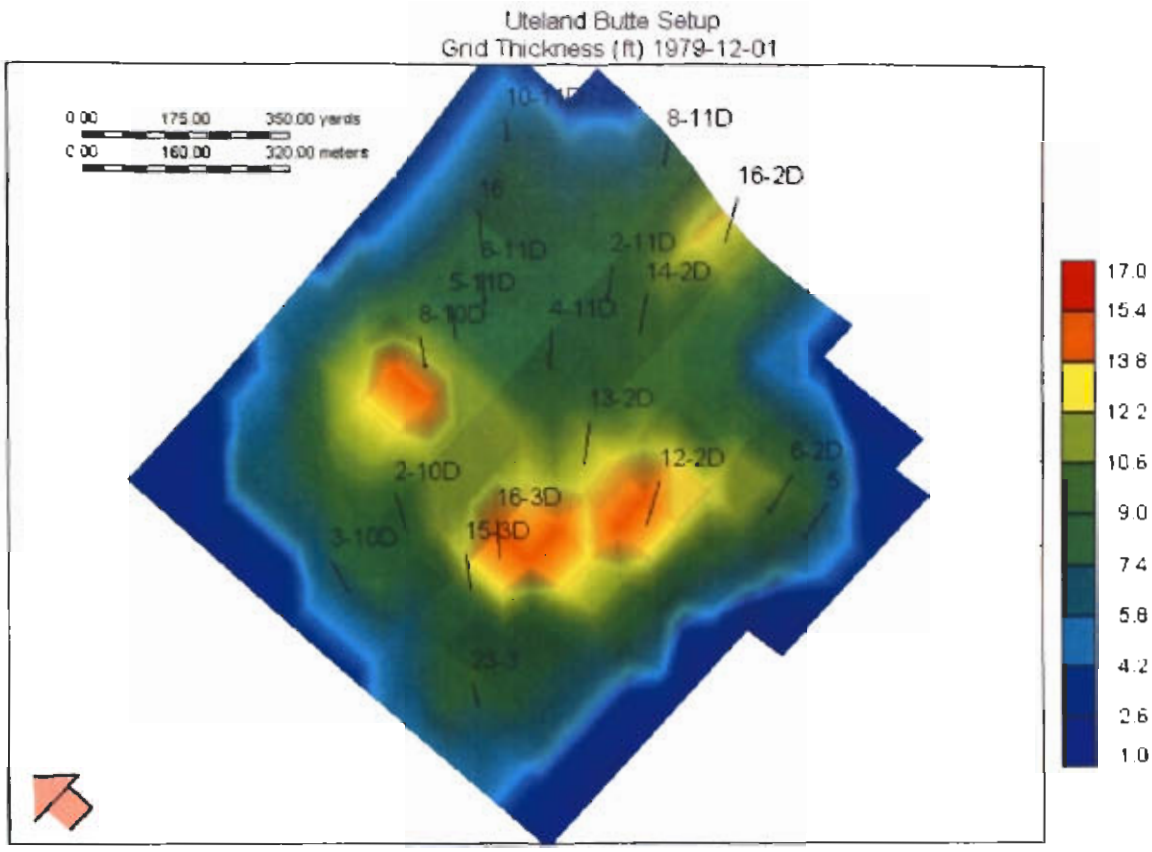

Figure 74. Sandstone thickness grid in feet, in the Uteland Butte field.

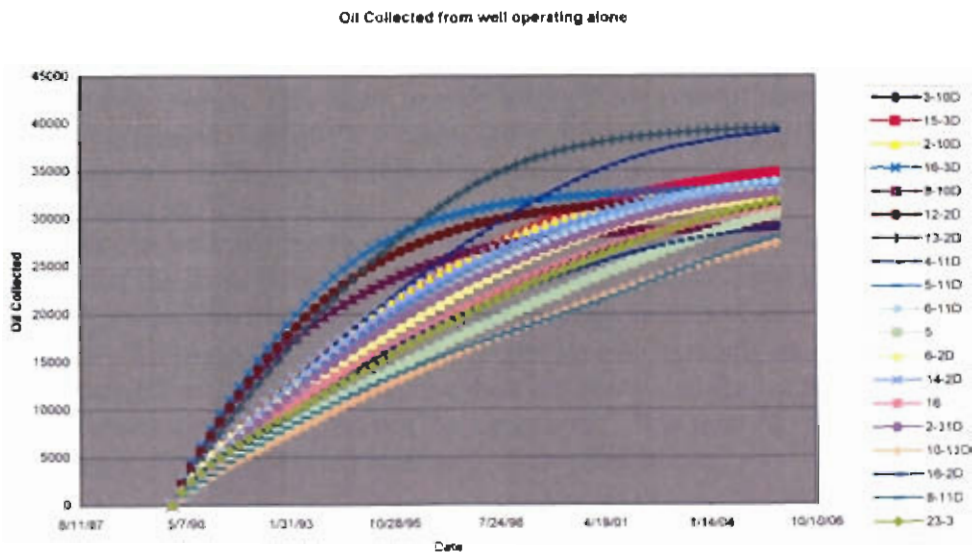

Figure 75. Cumulative oil production curves for all 16 wells in the Uteland Butte field.

Simulations of the Brundage Canyon Field

The purpose of this simulation was to compare the results of the computer simulation to the actual data that was collected from Brundage Canyon field. For purposes of simplification, the field was considered to be two layers on a 16 by 16 grid. Also from actual well data, porosity, and thickness were assigned to each block. The grid is shown in figure 76.

For this simulation, several simplifications needed to be made. One of these simplifications was that all of the blocks in the grid started with the same initial oil saturation. While this is not one hundred percent true, it is a fairly accurate assumption. The pressure versus temperature (PVT) table was also not altered for the experiment. Once again, for this simulation, only times were given when the wells were opened, but no data was supplied as to when the wells were shut in. This will lead to issues concerning well pressure, which will be discussed later.

The simulation was run with an initial oil pressure of 3,000 psi (20,700 kPa) and a bubble point of 2,300 psi (15,900 kPa). The initial oil concentration was constant throughout the whole grid and was at the value of 70 percent. When the simulation was run until the year 2006. The total oil collected is shown in figure 77.

A good deal of oil is collected from the well, with an extra push of oil collected in about 1998. This can be accounted for several new wells being opened during that time period. However, as time goes on, less oil is collected and eventually the oil production stops. This is due to the lack of pressure that is in the well, which is caused by the continuous operation of the wells. The pressure from the well reaches readings as low as 700 psi (4,800 kPa), which is a significant pressure drop compared to the initial pressure of 3,000 psi 20,700 kPa). Since there is not a considerable pressure gradient, no oil could be collected. One method to improve the computer simulation would be to have steam injected to the wells, or at least have the wells open and close when they actually did. Unfortunately, the data of when the wells were opened, not closed, was provided. If this information was given, the results could have been much more accurate.

Another major problem with the simulation was the initial conditions. It was not known what all of the initial conditions were. What were only known were the depths, porosity, and location of the wells. This leads to only a rough estimate of how much oil is collected. If proper data was given and correct PVT tables were provided, then a much better simulation could have been produced. In the case of this simulation, the output was not very close to the actual field data as shown in figure 78.

As can be seen, the shape of the curves are similar (oil production increases and decreases at the same time for both graphs), but the curve from the simulation shows a much lower oil production than the oil that was actually collected, and then at the end of the simulation, it slowly declines and the oil production virtually stops. This error is due to what has been discussed earlier. However, the data did show that the increase and decrease of oil rate was predicted reasonably well, but not the magnitude. It is possible that the field is fractured, allowing gas to segregate and maintain reservoir pressure.

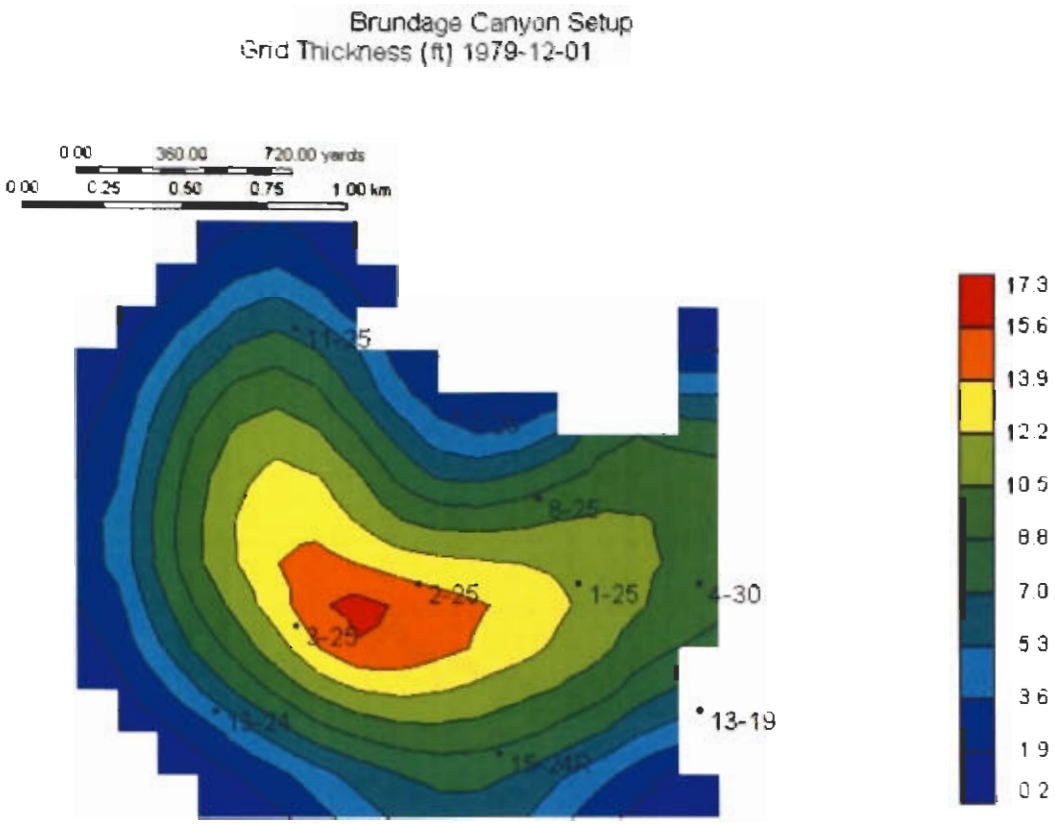

Figure 76. Sandstone thickness grid in feet, for the Brundage Canyon field.

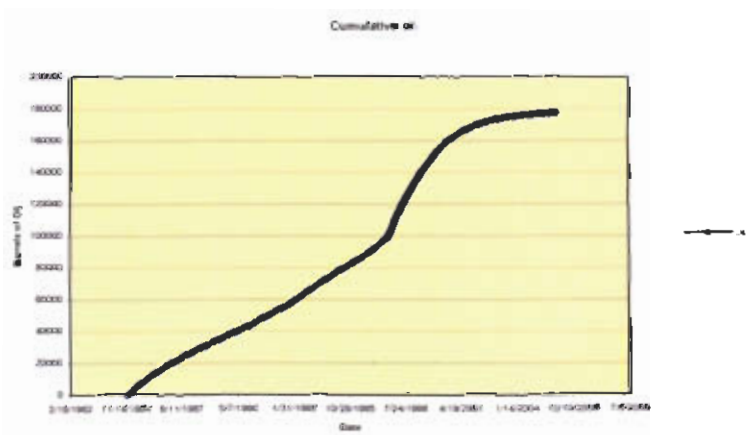

Figure 77. Cumulative oil produced from the Brundage Canyon field.

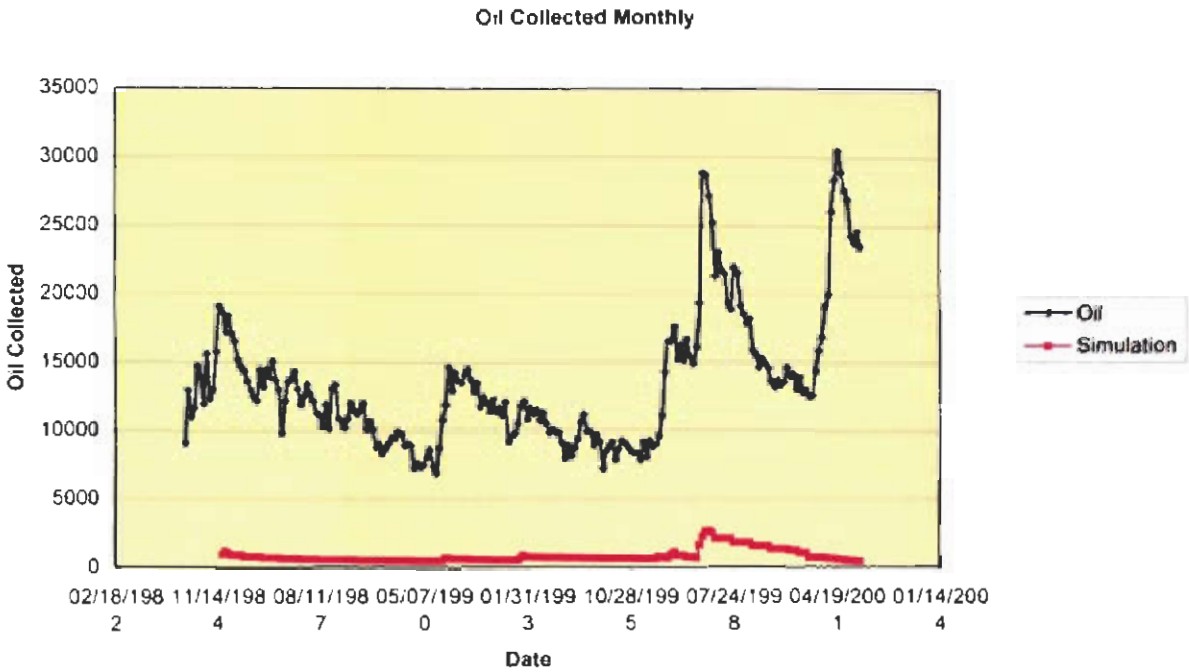

Figure 78. Comparison of actual oil produced to the simulated oil produced in the Brundage Canyon field.

TREND SURFACE ANALYSIS FOR VITRINITE REFLECTANCE DATA

Vitrinite reflectance data were analyzed using trend surfaces. Trend surfaces are created by multiple regression analysis where spatial coordinates are used as independent variables (Davis, 1984).

Data

The location of 211 samples selected for the trend surface analysis is shown in figure 79. The 211 data records (table 7) were selected from 246 published records (Nuccio and Johnson, 1986; Pitman and others, 1988; Anders and others, 1992; Rice and others, 1992; Schmoker and others, 1992; Johnson and Nuccio, 1993;). About 40 percent the selected records are for coal samples and the remainder are for kerogen, which was presumably obtained by acid digestion of whole rocks and cuttings. Reflectance values for five, newly collected samples (table 7) are used to verify results from the trend surface analysis.

Note that some published data are not included in the selected data. Four records are ignored where the reported vitrinite reflectance is considered doubtful. Thirty records are ignored where the reflectance assay is based on less than 30 measured readings or has a standard deviation greater than 0.1 percent. One data record is ignored where the reflectance is 2.4 percent. Although the reflectance value for this record is probably accurate, the value is more than four standard deviations from the median reflectance value of the selected data. Consequently, the record is not included in the regression analysis since it would have a disproportionately large influence on the result.

Method

Multiple regression analysis, where the spatial data are used to predict vitrinite reflectance, shows that a second-order trend surface gives the most satisfactory fit. Two independent variables in the second-order equation are omitted since they do not significantly improve the prediction. The resulting equation is shown below:

Eq. 1 $$Ro = -243.506 - 7.569E^{-7}UTME + 1.132E^{4}\,UTMN - 1.314E^{-11}(UTMN)^2 + \frac{1.960E^{4}}{(EL + 20{,}000)}$$

where, Ro is the percent vitrinite reflectance,
UTME is the NAD27 Universal Transverse Mercator easting coordinate,
UTMN is the NAD27 Universal Transverse Mercator northing coordinate and,
EL is elevation in feet relative to mean sea level.

The equation shows an adjusted R^2 equal to 0.70 and a standard error of 0.14 percent reflectance. This precision is reasonably good since the reproducibility of reflectance analysis of coal samples is about 0.06 percent reflectance (ASTM, 2001). Analytical precision for reflectance analysis of kerogen samples has not been established in national standards but is probably not as good as that for coal samples.

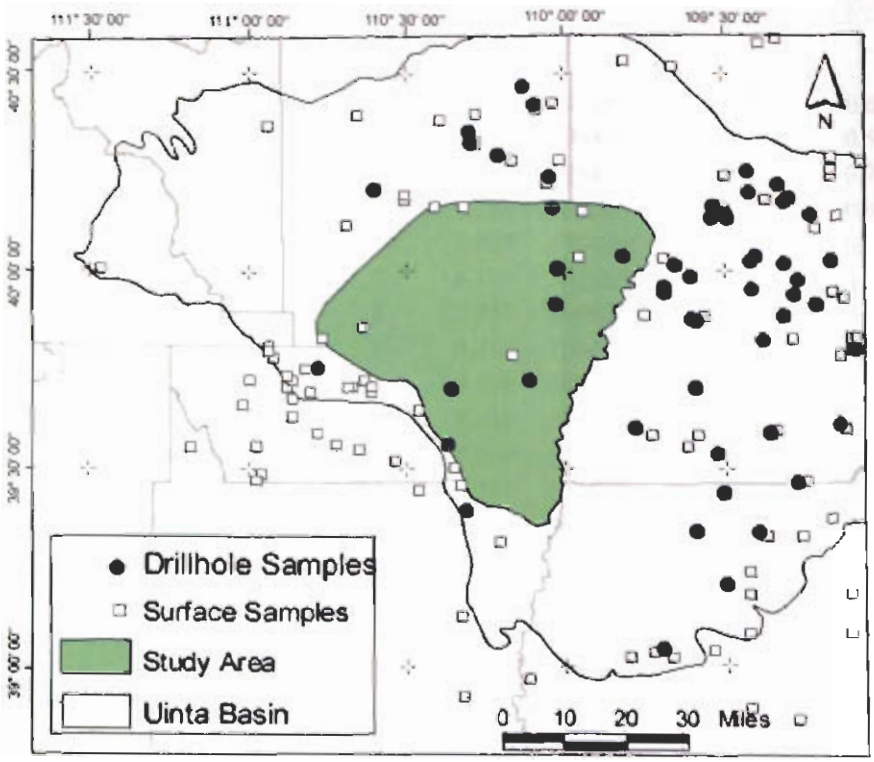

Figure 79. Location of 115 surface samples, and 96 subsurface samples from 52 drill holes, used to construct regional trends of vitrinite reflectance for the study area and surrounding Uinta Basin, Utah.

Table 7. Data used for trend surface analysis.

ID or Well Name	API Number	Depth (feet)	Elevation (feet)	UTME (meters)	UTMN (meters)	Ro (measured)	Ro** (calculated)
1 Bartles	4300710752	7,550	1,703	554889	4394753	0.68	0.72
1 Bitter Creek	4304710477	6,855	-963	638415	4409497	0.69	0.75
1 Govt-Dial (Carter Oil Govt.)	4300710480	1,665	5,761	518368	4400865	0.54	0.59
8 Peters Point	4300710481	8,505	-1,645	576109	4397424	1.03	0.87
not identified		0	5,919	571188	4404515	0.61	0.54
not identified		0	6,644	503199	4370780	0.68	0.64
not identified		0	6,801	501538	4378959	0.65	0.63
not identified		0	5,508	523305	4379215	0.68	0.65
not identified		0	6,001	511492	4392052	0.72	0.61
not identified		0	7,001	501540	4369148	0.68	0.64
not identified		0	7,775	555488	4372887	0.73	0.57
not identified		0	6,821	553835	4379368	0.73	0.58
not identified		0	7,188	498216	4390412	0.69	0.59
not identified		0	6,893	516462	4393692	0.72	0.58
not identified		0	8,176	499871	4396948	0.57	0.55
not identified		0	6,608	514795	4400237	0.49	0.57
not identified		0	7,995	532874	4395487	0.52	0.54
86-5I		0	5,600	539394	4374420	0.61	0.64
86-5J		0	5,607	529737	4377617	0.58	0.64
86-5K		0	5,600	518144	4382254	0.58	0.64
86-5L		0	5,896	511499	4387146	0.59	0.63
U86-KF-1RC		0	7,835	545737	4389060	0.52	0.54

UGMS 594		0	6,653	532881	4393867	0.63	0.57
86-5M		0	6,801	509824	4395323	0.55	0.58
UGMS 204		0	7,027	526462	4395462	0.70	0.57
UGMS 587		0	7,218	528065	4395468	0.61	0.56
86-5N		0	5,997	511484	4396957	0.61	0.60
UGMS 588		0	8,199	531265	4397101	0.59	0.53
86-5O		0	7,057	509820	4398597	0.49	0.57
86-5P		0	6,735	506499	4403499	0.54	0.57
U86-KF-1VR		0	7,798	504846	4405129	0.49	0.54
86-5Q		0	7,119	504845	4406761	0.49	0.55
1 Blanchard (1-3A2)	4301320316	10,456	-4,609	576971	4474891	0.85	0.81
1 Daniel Uresk	4301330113	5,035	211	581686	4445940	0.54	0.62
1 Daniel Uresk	4301330113	6,095	-849	581686	4445940	0.50	0.67
1 Daniel Uresk	4301330113	7,805	-2,559	581686	4445940	0.67	0.77
1 Daniel Uresk	4301330113	8,285	-3,039	581686	4445940	0.71	0.80
1 Daniel Uresk	4301330113	10,325	-5,079	581686	4445940	0.75	0.96
1 Daniel Uresk	4301330113	11,075	-5,829	581686	4445940	0.94	1.03
1 Dustin Etal	4301330122	8,695	-2,841	567075	4460313	0.77	0.75
1 Dustin Etal	4301330122	8,875	-3,021	567075	4460313	0.70	0.76
1 Dustin Etal	4301330122	10,525	-4,671	567075	4460313	0.74	0.88
1 Dustin Etal	4301330122	10,885	-5,031	567075	4460313	0.89	0.91
1 Dustin Etal	4301330122	11,005	-5,151	567075	4460313	0.84	0.92
1 Dustin Etal	4301330122	11,065	-5,211	567075	4460313	0.97	0.93
1 Dustin Etal	4301330122	11,665	-5,811	567075	4460313	0.92	0.99
1 Dustin Etal	4301330122	12,745	-6,891	567075	4460313	1.14	1.10
1 Dustin Etal	4301330122	13,285	-7,431	567075	4460313	1.26	1.16
1 Dustin Etal	4301330122	14,065	-8,211	567075	4460313	1.36	1.27
1 Miles	4301330029	12,195	-5,816	559401	4467053	1.10	0.96
1 Miles	4301330029	12,893	-6,514	559401	4467053	1.12	1.04
1 Miles	4301330029	12,918	-6,539	559401	4467053	1.15	1.04
1 Miles	4301330029	12,928	-6,549	559401	4467053	1.30	1.04
1 Senor Mortansen	4301311087	5,200	81	581107	4454393	0.50	0.59
1 Senor Mortansen	4301311087	6,300	-1,019	581107	4454393	0.61	0.65
1-11B4 Brotherson	4301330052	9,300	-3,121	559639	4463882	0.79	0.76
1-11B4 Brotherson	4301330052	10,700	-4,521	559639	4463882	0.94	0.86
1-11B4 Brotherson	4301330052	11,980	-5,801	559639	4463882	1.08	0.98
1-11B4 Brotherson	4301330052	13,180	-7,001	559639	4463882	1.23	1.10
1-11B4 Brotherson	4301330052	16,300	-10,121	559639	4463882	1.60	1.58
1-20Z2 Ute	4301330378	9,000	-2,624	573466	4479798	0.42	0.64
1-20Z2 Ute	4301330378	10,700	-4,324	573466	4479798	0.45	0.77
1-20Z2 Ute	4301330378	11,400	-5,024	573466	4479798	0.50	0.82
1-20Z2 Ute	4301330378	12,300	-5,924	573466	4479798	0.50	0.91
1-20Z2 Ute	4301330378	13,300	-6,924	573466	4479798	0.59	1.01
22-29 (1 Wilkin-RDG)	4301330327	12,185	-6,013	582770	4418763	1.60	1.14
22-29 (1 Wilkin-RDG)	4301330327	12,345	-6,173	582770	4418763	1.63	1.15
5 Book Cliffs	4301920065	1,515	4,479	629372	4340541	0.70	0.65
3 Cedar Rim	4301330040	8,202	-1,916	533790	4450601	0.68	0.75
85-73A		0	5,860	581583	4475085	0.45	0.29
85-74		0	5,138	580245	4452547	0.58	0.40

85-77		0	5,600	549826	4445847	0.48	0.44
85-97E		0	5,807	541787	4447408	0.47	0.43
85-97J		0	6,900	551144	4469998	0.45	0.30
U86-KF-2VR		0	7,995	519467	4408948	0.49	0.51
not identified		0	9,170	530759	4412137	0.50	0.47
not identified		0	8,973	504610	4468216	0.50	0.29
not identified		0	8,018	528651	4471477	0.45	0.29
not identified		0	6,801	525811	4440899	0.33	0.44
not identified		0	6,568	560749	4471668	0.30	0.30
not identified		0	6,096	560848	4463632	0.30	0.35
not identified		0	5,810	541761	4449017	0.36	0.43
not identified		0	5,807	576781	4473425	0.31	0.30
not identified		0	5,600	557857	4445904	0.30	0.43
not identified		0	5,600	570536	4458888	0.34	0.37
not identified		0	5,197	589973	4444608	0.30	0.42
not identified		0	5,194	583381	4459019	0.33	0.37
not identified		0	5,141	589065	4431887	0.55	0.47
U86-KF-3VR		0	7,401	557202	4367872	0.58	0.59
86-5H		0	5,367	545915	4366187	0.49	0.65
86-5D		0	4,600	557474	4330817	0.51	0.71
86-4Z		0	4,442	558095	4308704	0.53	0.72
not identified		0	9,035	484416	4378408	0.68	0.58
Forest 25-1 Arnold	4301510374	100	6,544	558895	4360787	0.56	0.62
not identified		0	6,174	567595	4352062	0.48	0.63
UB-86-KF-4VR		0	4,984	662667	4338588	0.65	0.61
2 EPR Sego Canyon	4301931232	656	5,184	612253	4322257	0.56	0.65
2 EPR Sego Canyon	4301931232	755	5,085	612253	4322257	0.57	0.66
1 Utah-Federal	4301915933	1,590	4,503	638082	4355486	0.69	0.63
1 Unit (PNGE 1 Segundo)	4301910805	5,490	2,851	620876	4355138	0.74	0.70
428-1 State	4301930169	5,140	2,173	628064	4366455	0.84	0.70
not identified		0	8,199	650236	4370138	0.52	0.49
not identified		0	6,998	657388	4359487	0.63	0.53
not identified		0	6,982	635061	4344524	0.64	0.57
not identified		0	6,630	649418	4354489	0.67	0.56
not identified		0	6,598	603067	4319795	0.63	0.62
not identified		0	6,099	614416	4319952	0.63	0.62
not identified		0	5,964	639738	4354309	0.63	0.58
not identified		0	5,197	635368	4326745	0.66	0.63
not identified		0	4,987	625731	4321745	0.57	0.65
not identified		0	4,268	662902	4327268	0.67	0.64
39-7		0	4,196	648618	4302738	0.60	0.66
39-15		0	4,396	635755	4305726	0.75	0.66
39-16		0	4,216	575862	4313693	0.57	0.71
UGMS 531		0	6,398	609529	4321503	0.59	0.62
UGMS 191		0	6,122	635173	4338065	0.70	0.60
86-5X		0	5,886	459780	4428186	0.40	0.56
84-56		0	5,600	663999	4459410	0.46	0.30
84-55A		0	5,600	663999	4459410	0.40	0.30
7 Southman Cyn	4304715882	5,971	-1,041	646839	4422379	0.7	0.71

4 Pariette Bench	4304715681	4,888	-141	600657	4432652	0.47	0.67
275 (31-26B) Red Wash	4304731077	5,413	138	645034	4449577	0.45	0.56
21 NBU	4304730255	4,495	355	634999	4423583	0.56	0.65
1-7 Federal Natural	4304730148	6,988	-1,454	619287	4415042	0.79	0.78
1-7 Federal Natural	4304730148	7,710	-2,176	619287	4415042	0.87	0.82
16 Chapita Wells	4304715061	5,512	-646	635934	4432812	0.58	0.67
128 Wonsits Valley	4304730798	5,315	-480	624203	4443257	0.48	0.63
117 Wonsits Valley	4304730238	5,545	-493	627835	4444537	0.49	0.62
11-17F River Bend UN	4304730584	8,300	-3,196	611878	4422267	0.83	0.87
1-1 Petes Flat-Federal	4304730558	8,202	-2,705	647758	4426263	0.91	0.80
Sunnyside		1,016	-1,016	553835	4379368	0.80	0.89
Oil Springs2		0	5,761	659989	4421545	0.26	0.43
Oil Springs1		0	6,004	662272	4407057	0.35	0.46
EX-1 Project Utah	4304700000	1,820	3,121	618624	4426866	0.37	0.53
EX-1 Project Utah	4304700000	2,340	2,601	618624	4426866	0.39	0.55
EX-1 Project Utah	4304700000	2,640	2,301	618624	4426866	0.40	0.56
EX-1 Project Utah	4304700000	2,800	2,141	618624	4426866	0.40	0.57
EX-1 Project Utah	4304700000	2,962	1,979	618624	4426866	0.40	0.58
Coyote Wash 1		2,674	2,416	643721	4431081	0.35	0.53
Coyote Wash 1		2,888	2,202	643721	4431081	0.45	0.53
Coyote Wash 1		3,423	1,667	643721	4431081	0.42	0.56
7 Southman Cyn Unit	4304715882	6,396	-1,466	646839	4422379	0.68	0.73
7 Southman Cyn Unit	4304715882	6,435	-1,505	646839	4422379	0.82	0.74
7 Southman Cyn Unit	4304715882	6,448	-1,518	646839	4422379	0.84	0.74
7 Southman Cyn Unit	4304715882	6,498	-1,568	646839	4422379	0.78	0.74
7 Southman Cyn Unit	4304711077	6,705	-1,323	652554	4419488	0.68	0.73
5 Chapita	4304715051	9,495	-4,550	634553	4431458	1.20	0.93
4 USA Pearl Broadhrs	4304715694	5,281	-101	642177	4453174	0.43	0.56
4 USA Pearl Broadhrs	4304715694	5,331	-151	642177	4453174	0.46	0.56
32 (32-22A) Red Wash	4304715159	10,003	-4,733	634197	4450791	0.74	0.87
32 (32-22A) Red Wash	4304715159	10,501	-5,231	634197	4450791	0.74	0.92
31-13 Federal	4304730097	3,445	4,815	648022	4369478	0.65	0.59
31-13 Federal	4304730097	5,200	3,060	648022	4369478	0.76	0.65
3 Pelilake	4304710876	5,782	-1,009	624755	4446926	0.42	0.64
3 Island Unit	4304715643	7,400	-2,440	611781	4423905	0.72	0.82
3 Island Unit	4304715643	10,875	-5,915	611781	4423905	1.12	1.09
288 (24-27B) Red Wash	4304731513	5,086	398	643462	4448388	0.45	0.55
2-8 Hope Unit	4304730189	9,195	-3,736	620299	4414474	0.94	0.93
23-2-1 Evacuation Cr	4304715675	3,575	2,211	663675	4407399	0.62	0.59
22-1 Conoco-Federal	4304730111	10,655	-5,822	614429	4430172	1.46	1.06
212 (41-8F) Red Wash	4304720014	8,705	-3,191	650721	4444909	0.67	0.77
212 (41-8F) Red Wash	4304720014	9,305	-3,791	650721	4444909	0.70	0.81
21 NBU	4304730255	7,402	-2,552	634999	4423583	0.72	0.81
21 NBU	4304730255	7,415	-2,565	634999	4423583	0.74	0.81
21 NBU	4304730255	7,459	-2,609	634999	4423583	0.77	0.81
21 NBU	4304730255	7,485	-2,635	634999	4423583	0.75	0.81
21 NBU	4304730255	7,491	-2,641	634999	4423583	0.76	0.81
21 NBU	4304730255	7,541	-2,691	634999	4423583	0.82	0.81
21 NBU	4304730255	8,449	-3,599	634999	4423583	0.89	0.88

21 NBU	4304730255	8,487	-3,637	634999	4423583	0.89	0.88
21 NBU	4304730255	8,496	-3,646	634999	4423583	0.90	0.88
21 NBU	4304730255	8,503	-3,653	634999	4423583	1.01	0.88
21 NBU	4304730255	8,563	-3,713	634999	4423583	1.00	0.89
108 Wonsits Valley	4304730026	5,552	-535	628237	4443400	0.52	0.63
1 Unit (1 Rainbow)	4304720512	6,772	-1,222	643816	4416429	0.69	0.74
1 Unit (Mid America)	4304710812	6,073	-620	656240	4432129	0.69	0.65
1 Uintah Oil Assoc	4304711120	6,635	-690	620255	4395922	0.89	0.78
1 Uintah Federal-219	4304711119	6,575	485	604520	4384316	0.77	0.76
1 Two Waters Unit	4304710692	2,435	4,225	659357	4386194	0.62	0.57
1 McLish Unit	4304710870	6,113	-996	633973	4456639	0.37	0.60
1 Kralovec	4301310227	10,205	-4,725	583222	4428631	1.39	0.99
1 Kralovec	4301310227	10,225	-4,745	583222	4428631	1.38	0.99
1 Crooked Canyon	4304730271	4,477	2,530	640533	4383424	0.83	0.65
1 Wolf Point Unit	4304730355	6,500	620	626467	4377301	0.76	0.75
not identified		0	5,699	646269	4409922	0.45	0.48
not identified		0	5,600	656573	4431335	0.39	0.41
not identified		0	5,469	656065	4455955	0.37	0.32
not identified		0	5,410	622281	4415873	0.58	0.49
not identified		0	5,200	651555	4441083	0.40	0.39
not identified		0	5,154	627402	4445568	0.30	0.39
not identified		0	4,800	611556	4432184	0.30	0.46
not identified		0	5,394	656031	4457598	0.30	0.32
not identified		0	5,236	656743	4423121	0.45	0.44
not identified		0	6,968	600395	4487004	0.59	0.19
not identified		0	6,772	613378	4485602	0.61	0.19
not identified		0	6,388	640771	4494019	0.52	0.14
not identified		0	5,600	635942	4492342	0.51	0.17
not identified		0	5,230	655963	4460883	0.48	0.31
not identified		0	7,559	661138	4384703	0.54	0.47
not identified		0	6,998	608430	4382195	0.52	0.53
not identified		0	6,801	618063	4379150	0.53	0.54
not identified		0	6,798	641964	4384326	0.54	0.51
not identified		0	6,398	621209	4382385	0.57	0.54
not identified		0	6,302	659111	4405392	0.50	0.46
not identified		0	6,197	663796	4410277	0.49	0.45
not identified		0	5,761	659989	4421545	0.28	0.43
not identified		0	5,577	662204	4410243	0.52	0.47
not identified		0	5,490	606149	4415986	0.35	0.50
not identified		0	5,469	638568	4449051	0.31	0.36
not identified		0	5,400	657904	4444499	0.35	0.37
not identified		0	5,000	627236	4455413	0.30	0.36
*Ute Tribal 2-25	4301331833	5,586	1,356	551758	4430251	0.74	0.64
*Grays Canyon		0	4,200	579570	4341343	0.50	0.70

* This study

**Calculated after equation 1

Results

Equation 1 can be used to estimate vitrinite reflectance at a given location and elevation within the Uinta Basin. For example, figure 80 shows the result from equation 1 for rocks at the surface, and figures 81, 82, 83, and 84 show predicted depths for buried sediments where reflectance is equal to 0.6, 0.8, 1.0, and 1.4 percent reflectance, respectively.

Projection of vitrinite reflectance gradients above the ground surface is sometimes used to estimate the thickness of eroded sediments (Dow, 1977). Although this approach is usually used with reflectance gradients observed in single wells, it is used here with equation 1 to examine the regional variation of sediments lost to erosion. Figure 85 shows the thickness of sediments eroded from the surface obtained by subtracting the current surface elevation from a hypothetical surface obtained by using reflectance value of 0.25 in equation 1 and solving for the elevation.

Equation 1 is perhaps most useful for estimating the maturity of buried source rocks where the depth of the source rock is known or can be estimated. For example, figure 86 shows the vitrinite reflectance for the top of the lower member of the Green River Formation in the study area. The figure shows that this potential source rock has not yet reached the onset of peak oil generation (0.8 percent Ro) suggested by Ruble and others (2001) for the type 1 kerogen found in the Green River Formation.

Limitation of the Trend Surface Analysis

The results presented here show a regional trend - local deviations from this trend are expected. Such deviations might be examined by constructing residual maps that show the difference between the predicted and measured vitrinite reflectance values. Although the selected data set (table 7) is reasonably comprehensive, an exhaustive literature search was not attempted and additional published data may be available. Clearly, additional data should improve confidence in the regression model. Finally, no attempt was made to correct the model for syn- and post-maturation structural deformation. Such corrections should improve the accuracy of the reflectance estimate, especially in areas with steeply dipping beds.

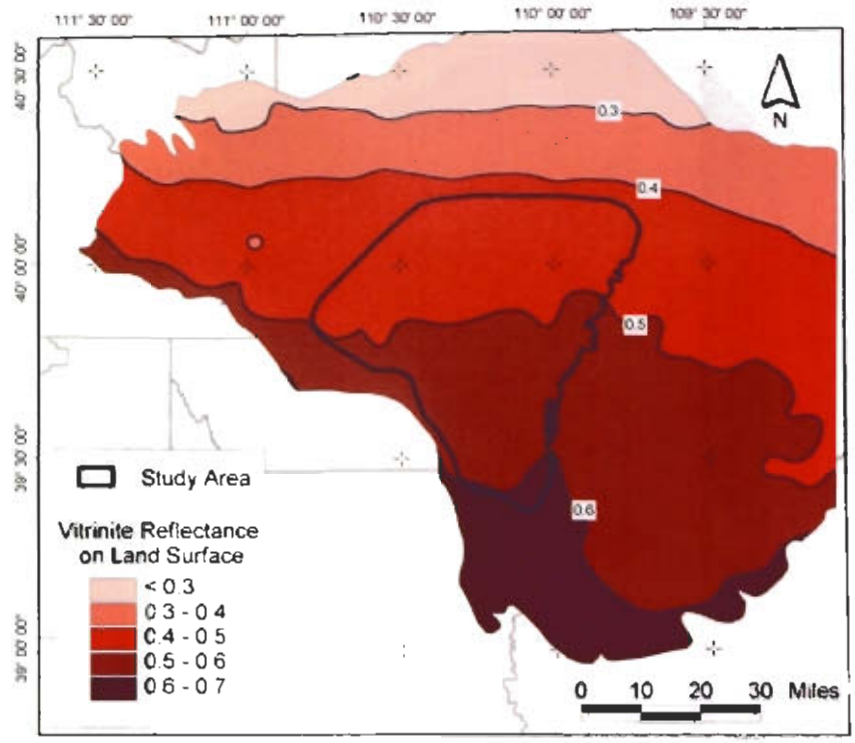

Figure 80. Regional trend of vitrinite reflectance on the land surface for the study area and surrounding Uinta Basin, Utah.

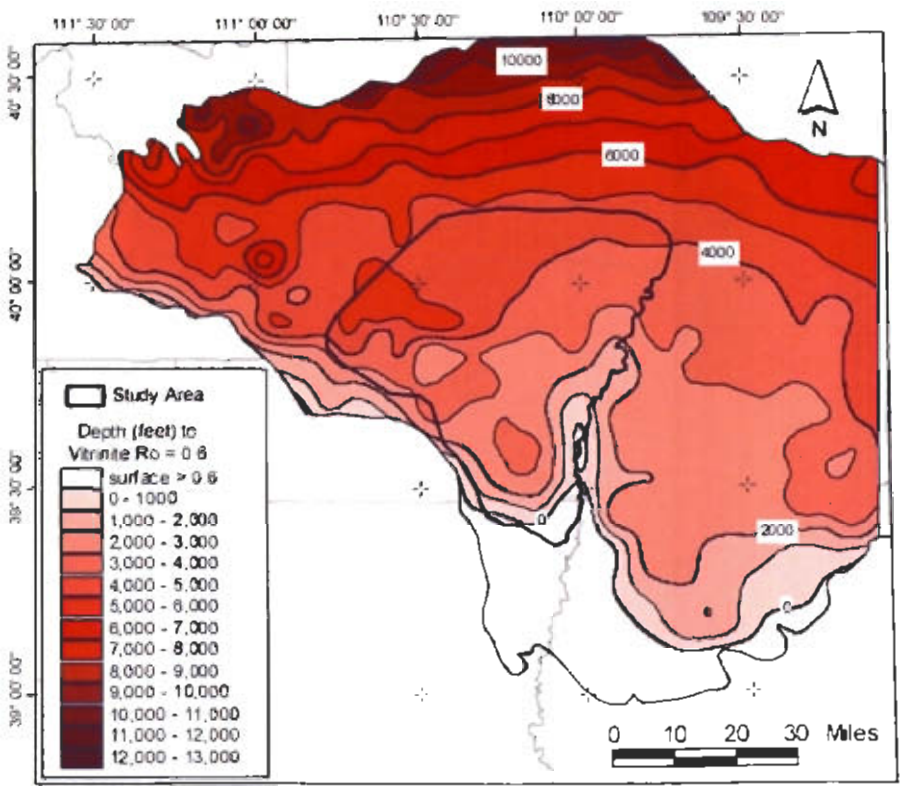

Figure 81. Estimated depth to sediments with a vitrinite reflectance equal to 0.60 (early oil window) in the study area and surrounding Uinta Basin, Utah.

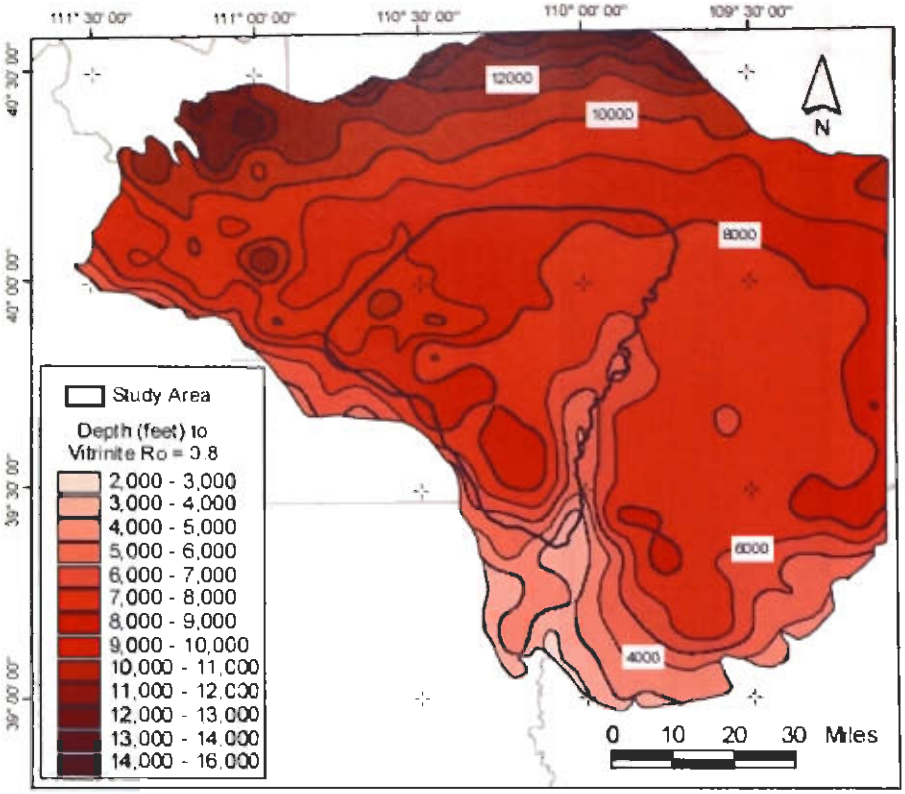

Figure 82. Estimated depth to sediments with a vitrinite reflectance equal to 0.80 in the study area and surrounding Uinta Basin, Utah. Ruble and others (2001) suggest that 0.80 percent reflectance marks the onset of peak oil generation from Green River kerogen.

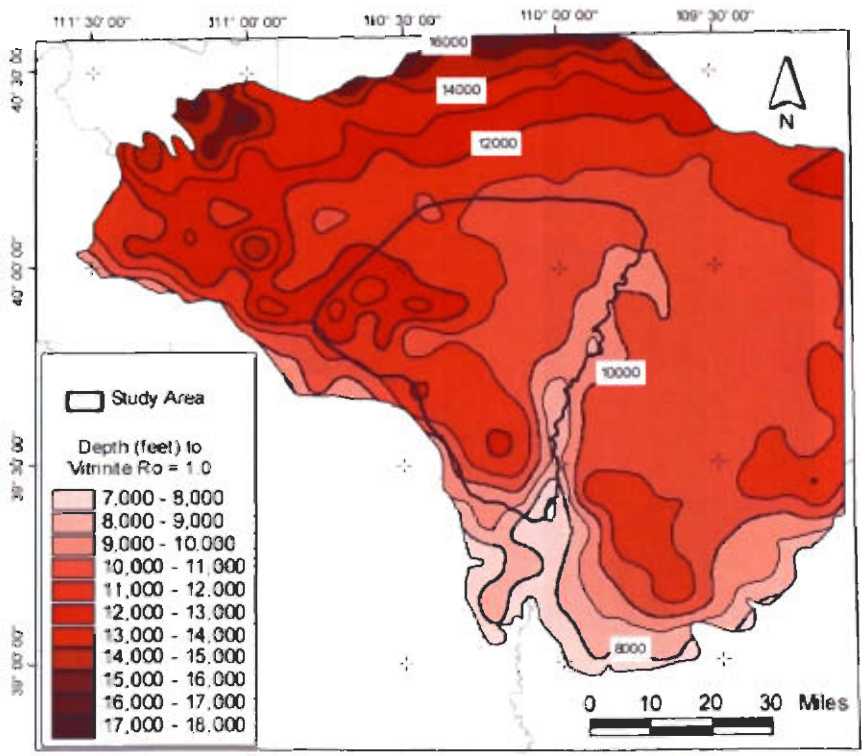

Figure 83. Estimated depth to sediments with a vitrinite reflectance equal to 1.0 in the study area and surrounding Uinta Basin, Utah. Ruble and others (2001) suggest 1.0 percent reflectance marks the end of peak oil generation from Green River kerogen.

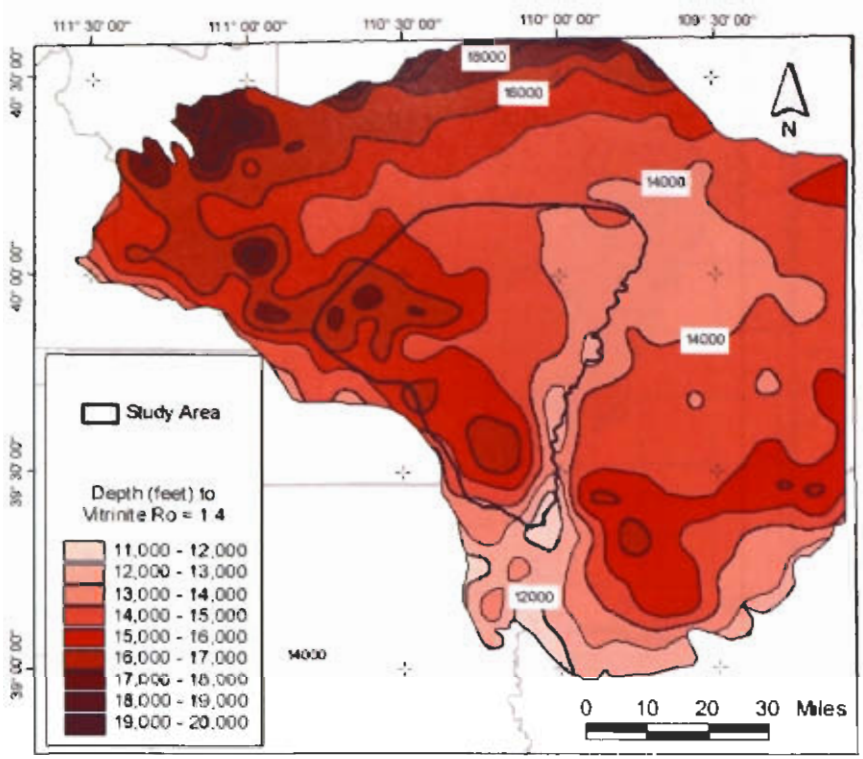

Figure 84. Estimated depth to sediments with a vitrinite reflectance equal to 1.4 (end of the oil window) in the study area and surrounding Uinta Basin, Utah.

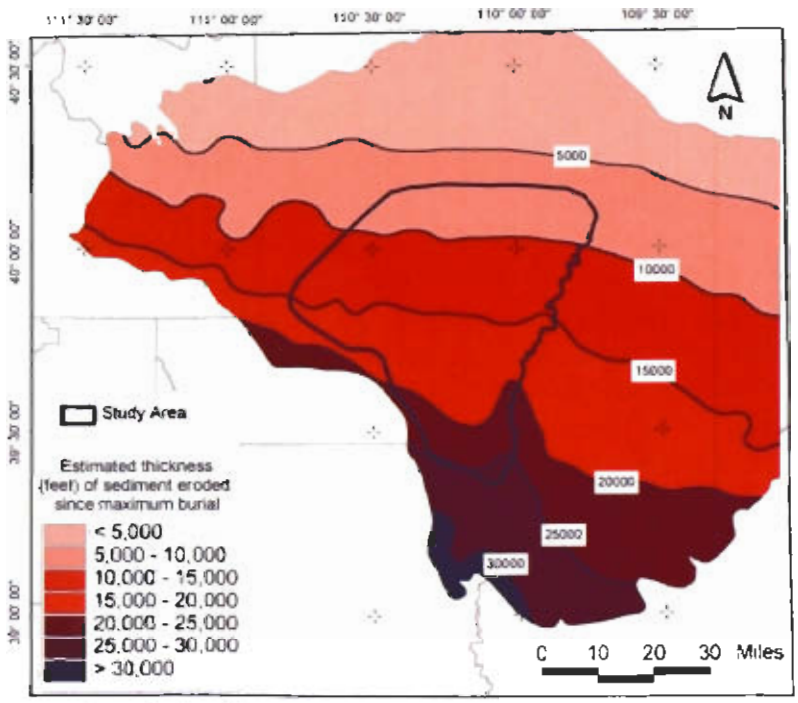

Figure 85. Estimated amount of eroded sediment corresponding to a paleo-surface vitrinite reflectance of 0.25 for the study area and surrounding Uinta Basin, Utah.

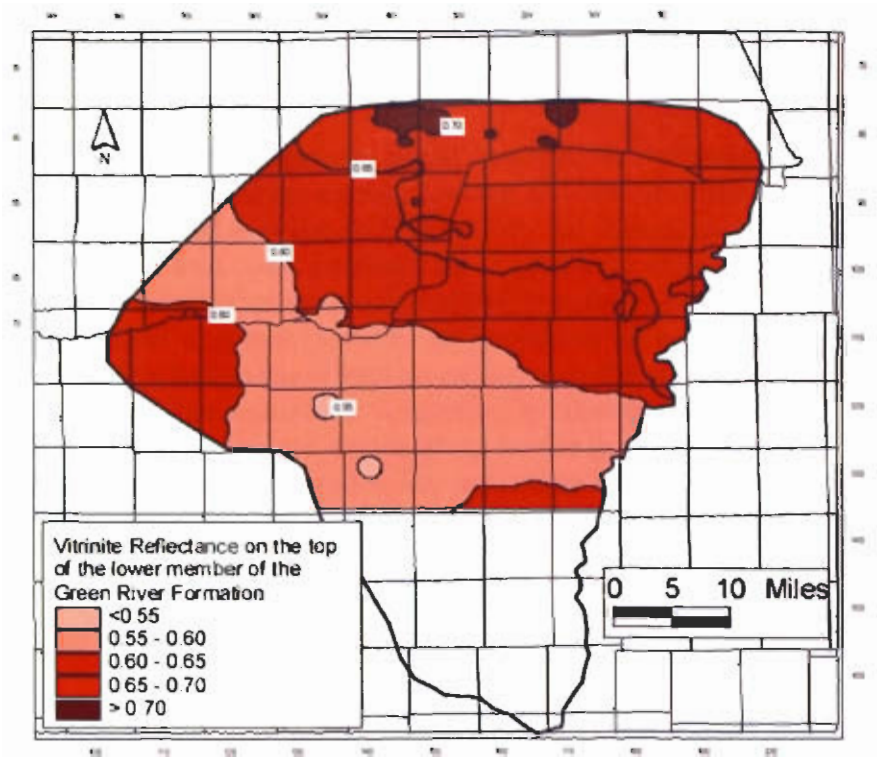

Figure 86. Estimated vitrinite reflectance at the top of the lower member of the Green River Formation in the study area.

FUTURE EXPLOITATION POTENTIAL

Development Potential

The middle and lower member reservoirs in the Green River Formation are currently drilled on 40 acre (16.2 ha) spacing. At the current spacing and rate of drilling, the area proven to be hydrocarbon productive should provide drilling activity for several more years. Drilling activity in the southwest Uinta Basin could continue for at least a decade, and probably much longer, as the proven oil field boundaries are expanded and hopefully, new wildcat discoveries are made. The production life of a typical Green River Formation oil well is several decades.

The work at the Nutter's Ranch study site, an analogue to the oil production in the greater Monument Butte area, indicates that significant volumes of oil could be left behind at a well spacing of 40 acres (16.2 ha). Reducing the well spacing for the greater Monument Butte area or allowing selective infill drilling along the trend of key sandstone beds, could result in a sizable drilling boom.

Exploration Potential

Hydrocarbon Shows

Hydrocarbon shows are very common while drilling the Green River Formation. No systematic attempt was made to study drilling shows because such shows are so common and drilling or mud logs are not available for most of the wells in the study area. Interesting log shows (unusually thick bed(s), abundant or unusually high porosity, for example) were noted while correlating the logs. This is by no means an extensive or all-inclusive study of log shows but a small sample of a few shows that were noted in sparsely drilled portions of the study area is shown on figure 87.

The Twelve Mile Creek 17-1 well (NW1/4SW1/4 section 17, T. 6 S., R. 7 W., SLBL) lies along the western boundary of the study area. The well was drilled at a kelly bushing (KB) elevation of 7,607 feet (2,318.6 m). Well logs show a 22-foot (6.7-m) thick sandstone with 12 feet (3.7 m) having 10 percent or more density-log porosity, in the MGR 5 (upper Douglas Creek reservoir) at a depth of 2,658 feet. The resistivity deep curve indicates 40 ohms with good separation between the shallow, medium, and deep resistivity curves. The spontaneous potential curve shows a strong deflection to the right indicating potential permeability. The MGR 5 was drilled with air and the operator reported oil in the pits while drilling through the interval. There are no reports of the MGR 5 being tested before the well was plugged and abandoned. The drilling show (oil in the pits) may under-represent the oil present in the MGR 5. Because of the shallow depth, the formation temperature may be near the pour-point temperature of the oil. Drilling could have further reduced the temperature in the near-well bore environment preventing the oil from flowing.

The Chokecherry 16-30 well (SE1/4SE1/4 section 30, T. 10 S., R. 15 E., SLBL) has a 52-foot (15.8-m) thick sandstone bed with 44 feet (13.4 m) having 10 percent or more density-log porosity, in the MGR 3 (lower Douglas Creek reservoir) at a depth of 3,835 feet (1,168.9 m). The well was drilled in 1983 from a KB elevation of 7,210 feet (2,197.6 m). There are no reports of the MGR 3 being tested before the well was plugged and abandoned.

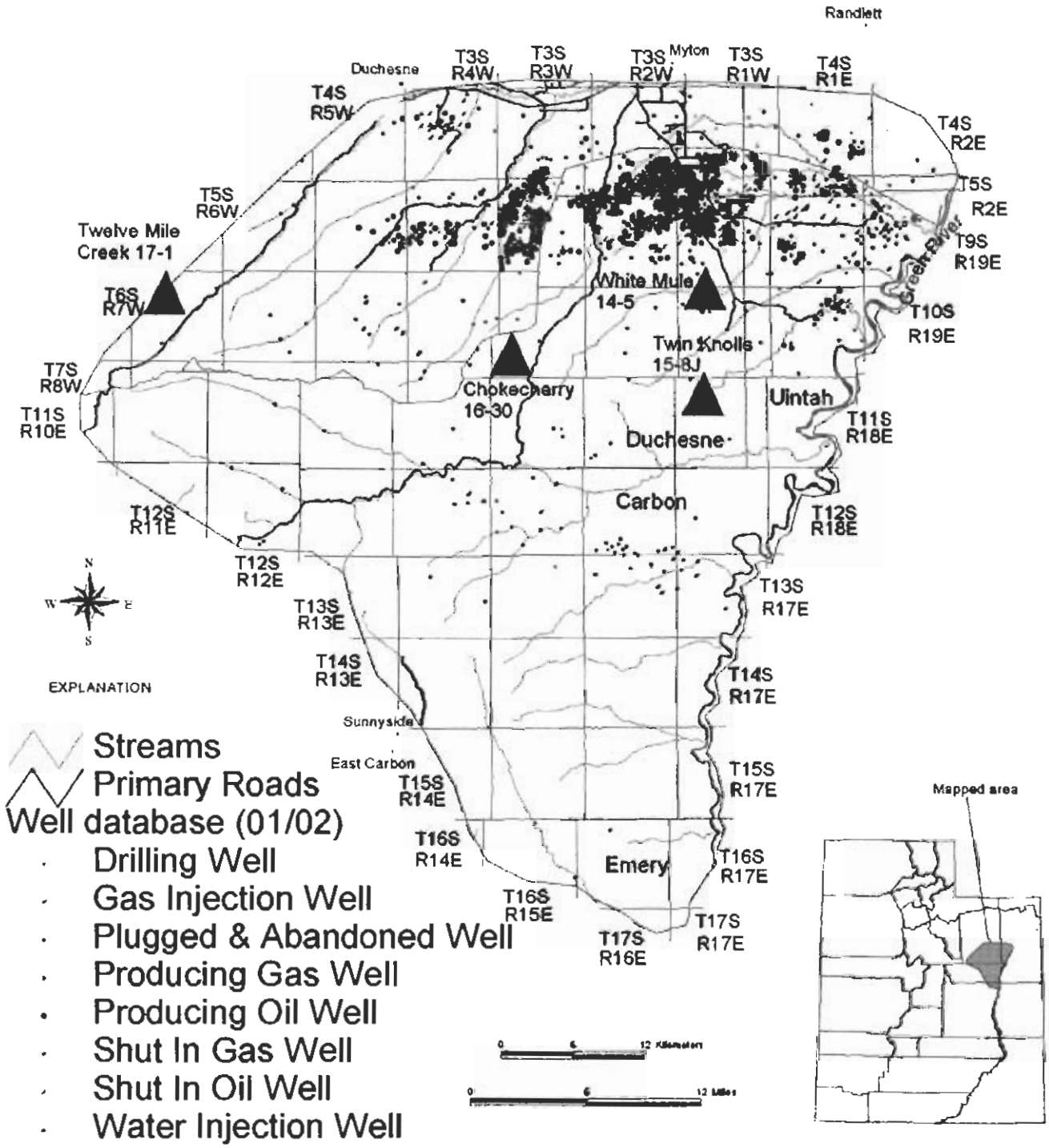

Figure 87. Map showing the location (triangles labeled with the well name and number) of some example wildcat wells with hydrocarbon shows, that are discussed in the report.

The White Mule 14-5 well (SW1/4SW1/4 section 5, T. 10 S., R. 17 E., SLBL) has a 20-foot (6.1-m) thick carbonate marker bed (top of the Castle Peak reservoir) with 10 percent or more density-log porosity at a depth of 4,815 feet (1,467.6 m). The well was drilled in 1983 from a KB elevation of 5,866 feet (1,787.9 m). The carbonate marker bed was perforated along with six other beds in the Castle Peak. The well was completed pumping 4 BO (0.6 m^3) per day but only produced 841 BO (133.7 m^3) before being abandoned. The White Mule 14-5 well was an offset to the Wells Draw 1 well (NW1/4SE1/4 section 8, T. 10 S., R. 17 E., SLBL) drilled in 1961, which encountered a thinner carbonate marker bed at a depth of 4,705 feet (1,434.1 m). An open-hole drill-stem test of the bed recovered 120 feet (36.6 m) of oil and 60 feet (18.3 m) of gas-cut mud in the drill pipe. The well was completed in the deeper Uteland Butte reservoir.

The porosity development in the carbonate marker bed in the White Mule well, could be a lead to a much larger algal-mound reservoir. Osmond (2000) describes a stromatolitic algal-boundstone reservoir (carbonate marker bed) in the West Willow Creek (T. 9 S., R. 19 E., SLBL) and Willow Creek (T. 10 S., R. 20 E., SLBL) fields, both fields are just east of the study area. The mound in the West Willow Creek field covers an area of roughly 1,240 acres (500 ha), reaches a maximum thickness of 100 feet (30.5 m), and has produced 827,912 BO (131,638 m^3) and 4.167 billion cubic feet of gas (118 million m^3) (through April 1999). The mound in the Willow Creek field covers 3,000 acres (1,200 ha), with a maximum thickness of 116 feet (35.4 m). The Willow Creek field produces from the deeper Wasatch Formation because the mound contains water.

The Twin Knolls 15-8J well (SW1/4SE1/4 section 8, T. 11 S., R. 17 E., SLBL) has a 58-foot (17.7-m) thick sandstone bed with 50 feet (15.2 m) having 10 percent or more density-log porosity in the MGR 4 (upper Douglas Creek reservoir) at a depth of 3,104 feet (946.1 m). The well was drilled in 1998 from a KB elevation of 6,515 feet (1,985.8 m). Porous sandstone beds are in the lower Douglas Creek and Castle Peak reservoirs as well. There are no reports of any tests in the Green River Formation before the well was plugged and abandoned.

Exploration Trends

Much of the southwest Uinta Basin has been extensively drilled but there is still room for exploration and discovery of new oil fields. The problem with a study like this with specific boundaries, is that most leads seem to be just developing within the study area and it's necessary to look beyond the boundaries to understand the leads. Never the less, several general exploration trends can be discussed within the limits of the study.

Most of the exploration trends in the middle and lower members of the Green River Formation follow shoreline or shelf-break trends of Lake Uinta. Most of the trends in the Monument Butte area are west to east and appear to shift southwest on the west side of the Monument Butte area into the Indian Canyon and Willow Creek Canyon area which we refer to as the Willow Creek embayment, and southeast on the east side of the Monument Butte area. This Monument Butte bulge crudely defines the Sunnyside delta (Remy, 1992), which dominated middle member depositional patterns in the southwest Uinta Basin. Unfortunately, less sandstone may be encountered as exploration follows the shoreline trends to the west and east side of the delta away from the primary area of sediment input. Long shore drift was from west to east, as a result, the east side of the delta may have good reservoir potential in shallow bar and shoreline deposits.

The Uteland Butte reservoir is a good exploration target with potential in the beach and bar sandstone deposits (figure 88). These sandstone beds typically are thin with low porosity and

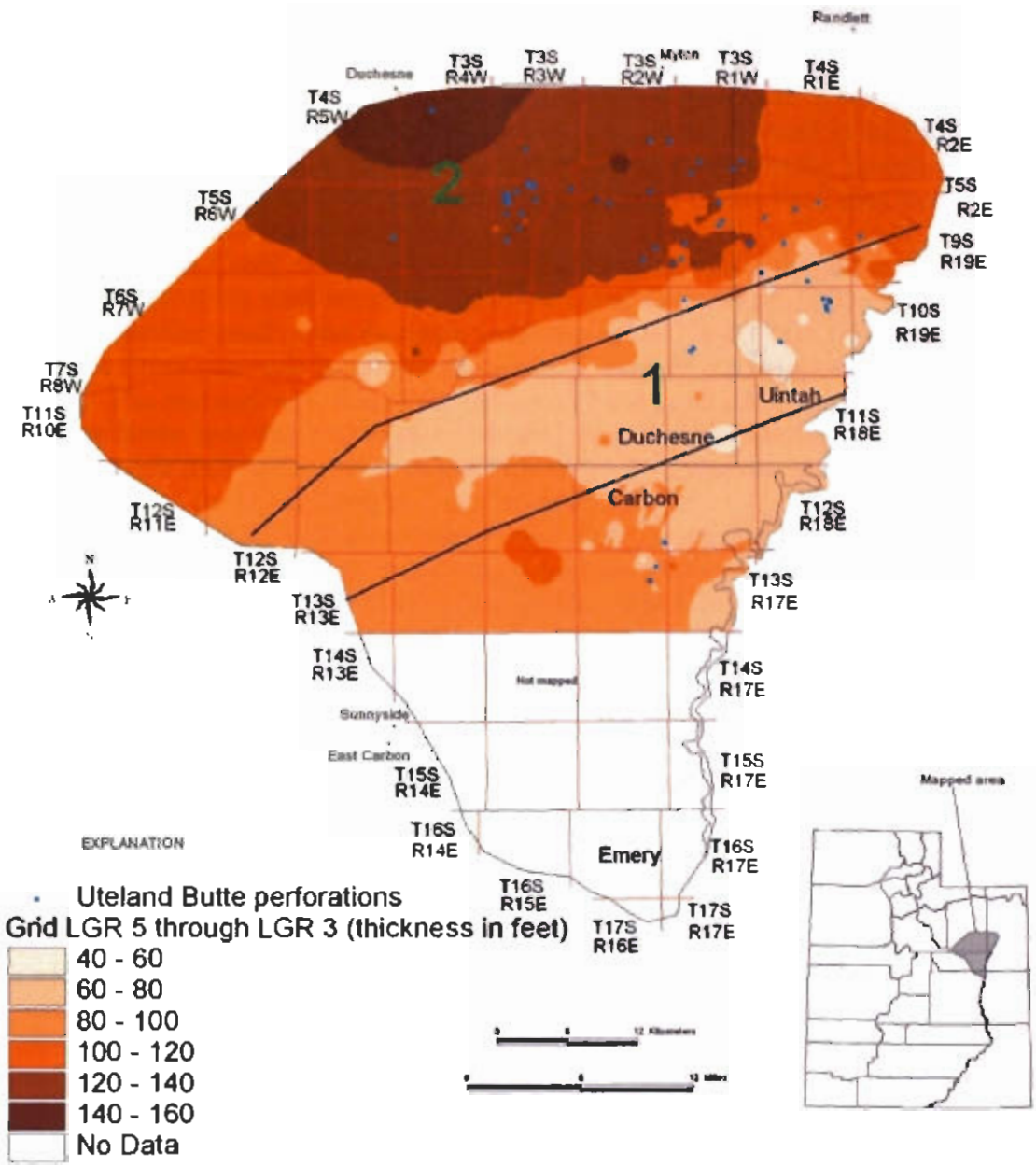

Figure 88. Trend of the Uteland Butte reservoir, lower member of the Green River Formation. Area 1 is the depositional trend of shallow beach and bar sandstone beds. Area 2 consists of distal open-lacustrine low-permeability carbonate beds that typically produce a low volume of oil and is a secondary drilling objective, but the area may also contain some high-permeability crystalline dolomite beds.

permeability but could be laterally extensive. The distal carbonates are a good low-volume secondary objective and have the potential for higher-volume discoveries in thin dolomitized beds. The dolomitized beds identified in core have high porosity but low permeability. Unfortunately, conventional well logs do not measure permeability so a high-porosity high-permeability dolomite can only be distinguished from a high-porosity low-permeability dolomite by testing.

The Castle Peak reservoir is limited in the updip direction by a zone of sediment bypass where well-developed channel sandstone beds pinch out. The shoreline trend in the Monument Butte area is about west to east, but in the western portion of the study area the shoreline turned sharply to the southwest. As a result, the exploration trend for the Castle Peak may trend southwest from the Monument Butte area (figure 89).

The lower Douglas Creek reservoir is a cut-and-fill deposit and is limited in the updip direction by the location of the shelf break during lower Douglas Creek time. The shelf break appears to follow a similar trend as the shoreline trend during the Castle Peak time (figure 90). The upper Douglas Creek reservoir is dominantly stacked, amalgamated channel deposits of the lower delta plain. The east and west side of the delta may have good quality reservoir rock but will probably have fewer beds that will be more isolated than stacked (figure 91). The overall thinning of the reservoir rock and isolation of the beds result in more expensive completions, and create economic limits to the upper Douglas Creek reservoir.

The Garden Gulch reservoir is a secondary target in the southwest Uinta Basin and has not been systematically explored. The Garden Gulch contains a few porous sandstone beds in the northern portion of the study area that have been produced in some wells. The Garden Gulch has not been proven to contain sufficient oil to produce by itself economically. However, because of the shallower drilling depths compared to the other reservoirs, the Garden Gulch could become a primary target in some areas.

Horizontal Drilling Potential

Horizontal drilling has rarely been tried in the middle and lower members of the Green River Formation anywhere in the Uinta Basin. A short lateral was drilled into the Castle Peak sandstone in Brundage Canyon many years ago. Very little is known about this horizontal well and production was not significantly improved. Chevron Oil Company drilled some short laterals into a carbonate bed in the Douglas Creek Member of the Green River Formation, in the Red Wash field to the northeast of the study area. The company did not feel that horizontal drilling increased their production relative to the increased cost, and the program was stopped.

The major deterrent to horizontal drilling in the Uinta Basin has been the number of beds typically perforated in a well. The majority of the wells in the Uinta Basin are marginally economic, therefore operators feel they must perforate and produce as many beds as they can in order to maintain an economical production rate. Horizontal drilling would require selecting a single bed for exploitation while abandoning any oil-productive beds below the horizontal leg.

The best candidate for horizontal drilling is the lower Douglas Creek reservoir. The lower Douglas Creek contains very thick (often > 100 feet [30 m]) sandstone beds that are oil saturated. But oil recovery is often very low because of the internal heterogeneity within the bed. High-porosity units within the lower Douglas Creek beds can be correlated in developed units with wells drilled on 40 acre (16.2 ha) centers. Many of the units in the greater Monument Butte area with thick lower Douglas Creek sandstone produce small quantities from the Castle Peak and Uteland Butte reservoirs below the lower Douglas Creek. The wells in these units may be good candidates for drilling short horizontal laterals from the existing well bores along the

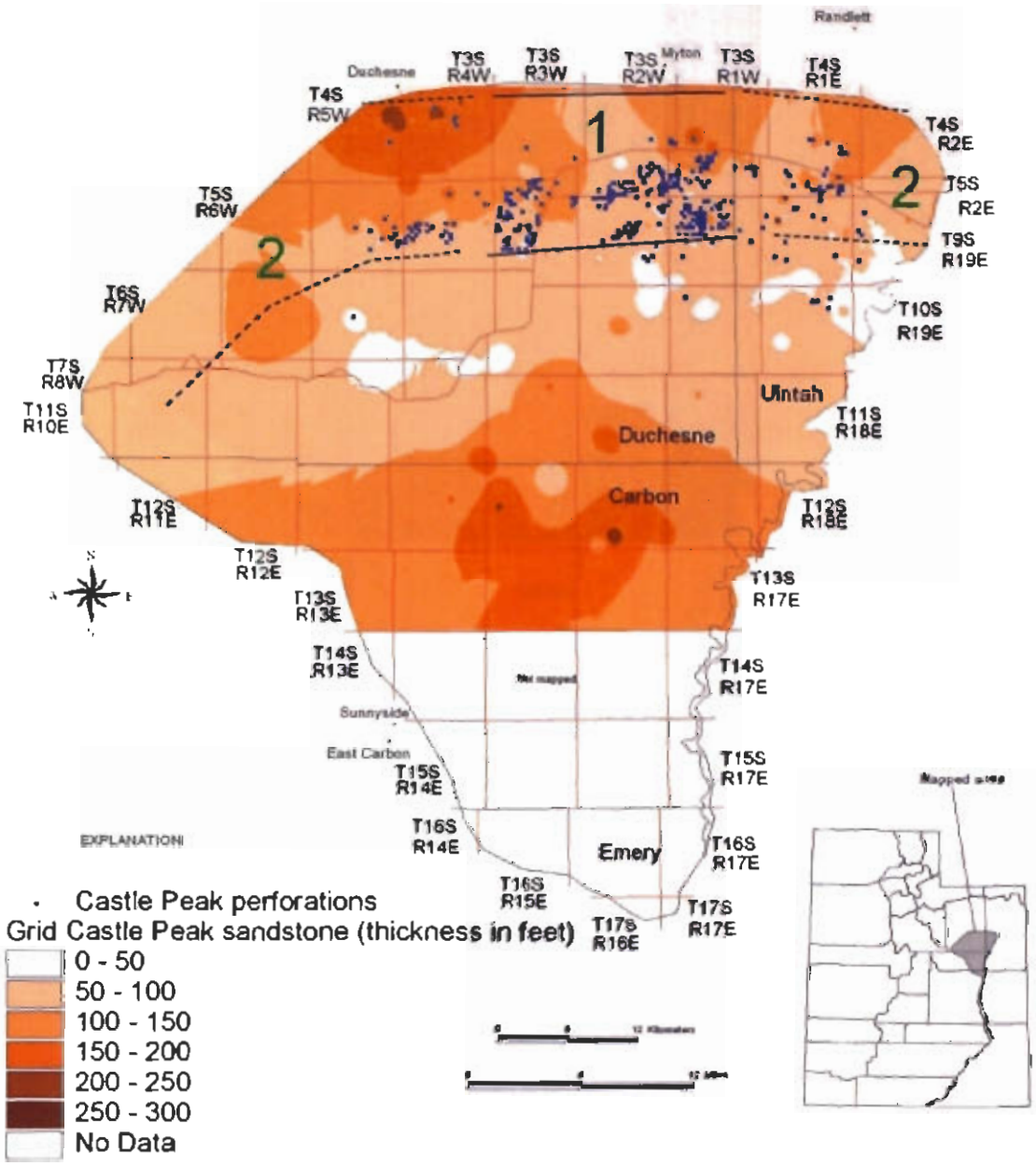

Figure 89. Trend of the Castle Peak reservoir, lower member of the Green River Formation. Area 1 consists of lake-level fall-to-rise cycles resulting in isolated channel and floodplain deposits bounded by carbonate beds. Area 2 may contain similar deposits but is less constrained by well data.

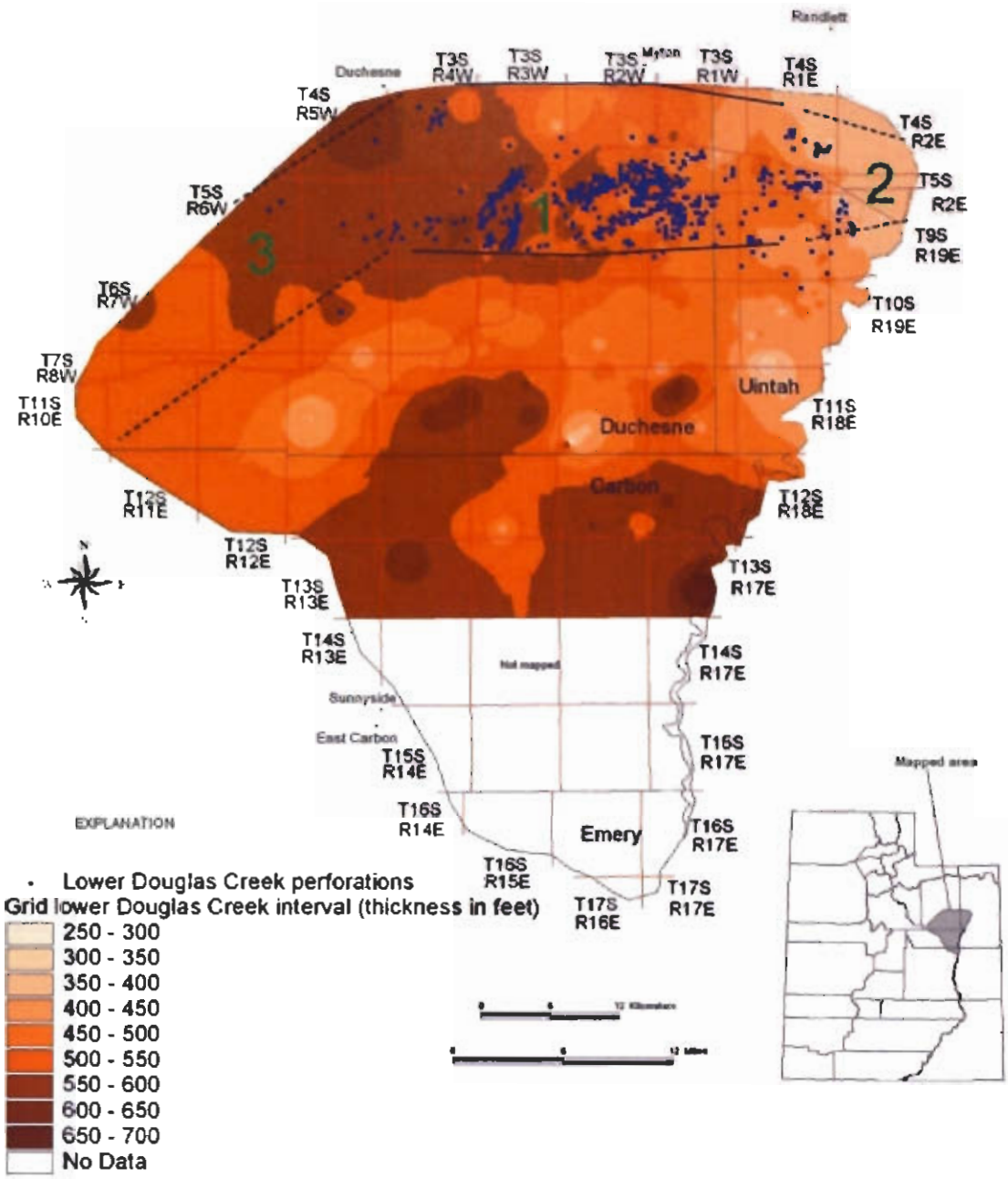

Figure 90. Trend of the lower Douglas Creek reservoir, middle member of the Green River Formation. Area 1 is dominantly thick cut-and-fill, incised valley-fill deposits and some thinner distributary-channel and mouth-bar deposits developed along a generalized shelf break during several lake-level falls. Area 2 consists of distributary-channel and mouth-bar deposits but the eastward extension of the shelf break is uncertain. Area 3 most likely consists of fewer distributary-channel and mouth-bar deposits and is unlikely to contain thick, incised valley-fill deposits.

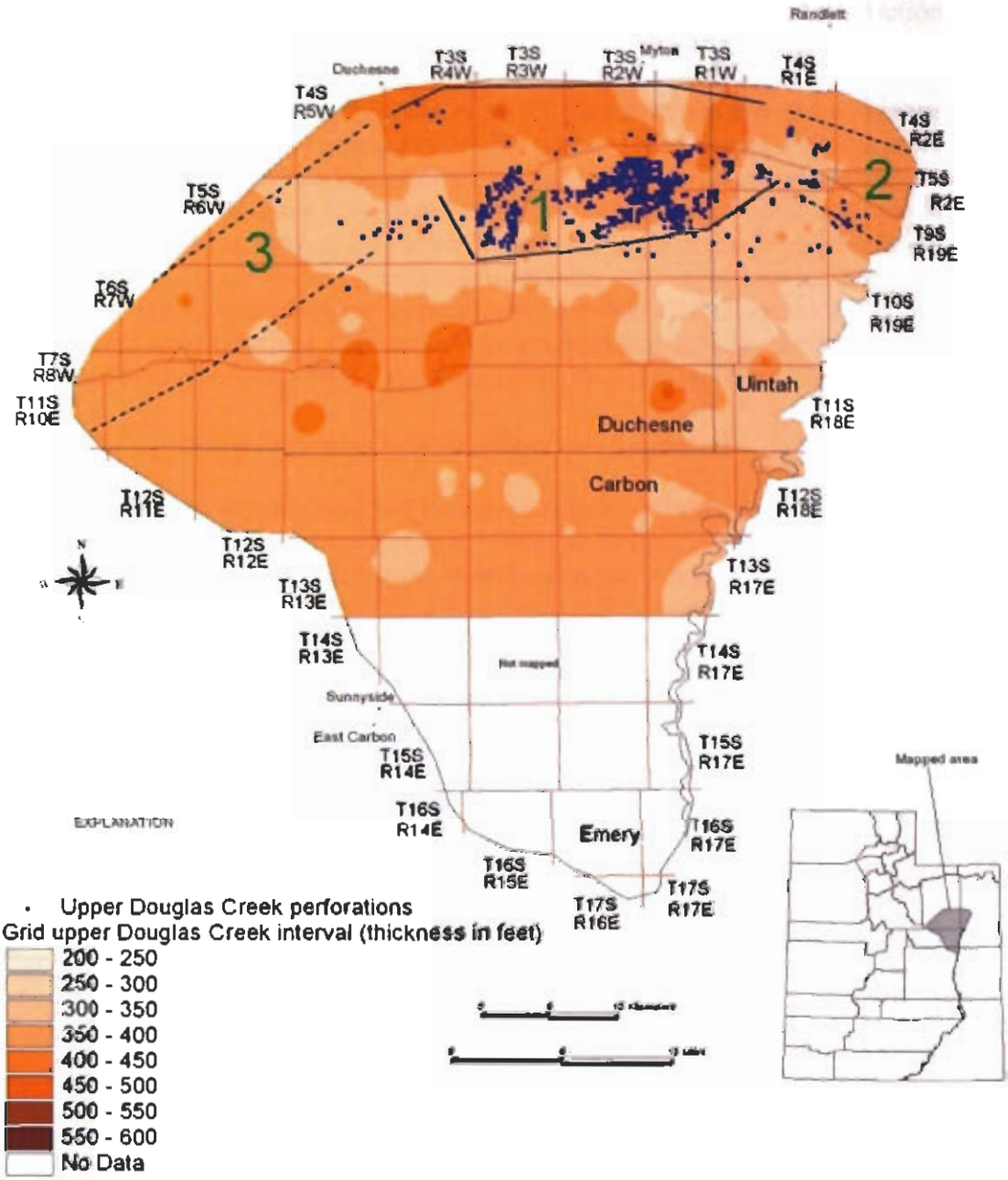

Figure 91. Trend of the upper Douglas Creek reservoir, middle member of the Green River Formation. Area 1 is dominantly amalgamated, stacked, distributary-channel and mouth-bar sandstone beds forming the main body of the lowstand deltas. Area 3 most likely consists of isolated distributary channels and poorly developed distributary mouth bars. Area 2 most likely consists of some distributary-channel and mouth-bar deposits but more wave-dominated shoreline and shallow-bar deposits.

strike of the lower Douglas Creek sandstone bed. Production potential from the deeper Castle Peak and Uteland Butte reservoirs may be insignificant in wells after an initial production period. The increased production from the lower Douglas Creek should more than off set any loss from abandoning the deeper reservoirs.

Horizontal drilling can be a good option in any of the reservoirs where fractures are known to play a dominant role in the production of the wells. This is especially true along the west-to-east trend of the Duchesne fault zone (DFZ). Only one horizontal well has been attempted along the DFZ. A shallow (less than 3,000 feet [900 m]) horizontal well was drilled in fractured shale of the upper member of the Green River Formation in the Duchesne field. Numerous fractures yielding oil were encountered but further drilling penetrated a water-bearing fracture zone. The operator was unable to stop the water production and the well was abandoned. Fractured sandstone and shale have been encountered in the middle and lower members in vertical wells along the DFZ indicating good potential for horizontal drilling.

Secondary and Tertiary Recovery Potential

The greater Monument Butte area has become a major oil producing region in the Uinta Basin since the U. S. Department of Energy Class I (Fluvial-Deltaic Reservoirs) demonstration program showed the economical feasibility of water flooding the middle and lower member reservoirs of the Green River Formation. The Class I study discovered that the reservoirs are near the bubble point and by starting a water flood soon after drilling the wells in a unit, the reservoir pressure is maintained above the bubble point, resulting in greatly increased oil recovery. It is now common practice in the Monument Butte area to develop a section on 40 acre (16.2 ha) spacing, produce all the wells initially for a few months, then convert every other well to a water injection well.

There are numerous tertiary recovery methods that have not been tested in the reservoirs of the Green River Formation. A pilot carbon dioxide (CO_2) flood was attempted in the Red Wash field in the 1980s, injecting CO_2 into four different wells that were producing from the Douglas Creek Member of the Green River Formation. Break through, CO_2 reaching neighboring wells, occurred almost instantly in two of the tests. As a result, the pilot program was abandoned. The greater Monument Butte area is an excellent candidate for tertiary recovery.

The water-flood program has been very successful because it maintains the reservoir pressure above the bubble point but it provides a poor sweep of the reservoir because of the low porosity and permeability. As a result, a large volume of oil is still being left behind that might be produced through tertiary methods. Tertiary methods that should be considered for oil production in the greater Monument Butte area are: (1) water alternating gas (WAG), (2) chemical flood such as a combination of alkalines, surfactant, and polymers (ASP), and (3) microbial.

ACKNOWLEDGMENTS

This report is the result of a study entitled *Reservoir characterization of the lower Green River Formation, southwest Uinta Basin, Utah.* The study was funded in part by the U. S. Department of Energy National Petroleum Technology Office (NPTO) in Tulsa, Oklahoma, under the Fundamental Geoscience for Reservoir Characterization program, contract number DE-AC26-98BC15103. U. S. Department of Energy contract manager is Virginia Weyland, NPTO, Tulsa, Oklahoma.

We appreciate the following company personnel and consultants who served as Technical Advisors to the study: Kevin Weller, Westport Company, Denver (formerly with Inland Resources, Inc.); Ben Crouch, Osage Oil, Hutchinson (formerly with Petroglyph Operating Company, Inc.); Terry Barrett and Jim Turner, formerly with Barrett Resources, Corp, Denver; Phil Moffitt, Questar E&P, Denver; Tom Yeager, Questar Gas Company, Salt Lake City; Logan MacMillan, Dick Castle, Roger Hively, and John Osmond, consultants, Denver; Mary McPherson, consultant, Grand Junction. We appreciate all the companies that have donated core to the Utah Geological Survey.

Many people at the Utah Geological Survey assisted with this study. Thomas Chidsey, Jr., Mark Milligan, and Bryce Tripp, assisted with the field work. Carolyn Olsen and Thomas Dempster prepared and photographed the much of the core. Sharon Wakefield was in charge of all of the GIS work done during the project. Barbara Marin with TerraTek, Salt Lake City, was responsible for all of the SEM work performed during the study. David Keighley, Halifax, completed his research for Shell Oil in Nine Mile Canyon just as our study was beginning. We appreciate Shell Oil allowing David to release the results of his work. David's correlations, sequence stratigraphic interpretation, and personnel advice, were very helpful to our study.

We would also like to thank all of the private ranchers in Nine Mile Canyon for allowing us access to their property. Dennis Willis with the Price office of the U.S. Bureau of Land Management was very helpful in providing us with access to the Desolation Canyon area. The work in Desolation Canyon would not have been possible without our volunteer boatmen; Tom Yeager, Salt Lake City; Jim Yeager, Corinne; Don Neff, Salt Lake City; Darrell and Kyle Buffington, Denver.

REFERENCES

Abbott, W.O., 1957, Tertiary of the Uinta Basin, *in* Seal, O.G., editor, Guidebook to the geology of the Uinta Basin: Intermountain Association of Petroleum Geologists Eighth Annual Field Conference, p. 102-109.

Anders, D.E., Palacas, J.G., and Johnson, R.C., 1992, Thermal maturity of rocks and hydrocarbon deposits, Uinta Basin, Utah, *in* Fouch, T.D., Nuccio, V.F., and Chidsey, T.C., Jr., editors, Hydrocarbon and Mineral Resources of the Uinta Basin, Utah and Colorado: Utah Geological Association Publication 20, p.53-76.

ASTM, 2001, method D 2798-99, Standard test method for microscopical determination of the reflectance of vitrinite in a polished specimen of coal: Annual Book of ASTM standards 2000 section five, volume 05.06. American Society for Testing and Materials, West Conshohocken, PA, p. 208-212.

Borer, J.M., 1998, High-resolution stratigraphy of the lower Green River Formation at Raven Ridge and Red Wash field, NE Uinta Basin - stratigraphic control on petroleum [abs.]: American Association of Petroleum Geologists Annual Convention Abstracts on CD-ROM.

Borer, J.M., and McPherson, M.L., 1996, High-resolution stratigraphy of the Green River Formation, NE Uinta Basin - implications for Red Wash reservoir compartmentalization [abs.]: American Association of Petroleum Geologists Annual Convention with Abstracts p. A18.

Bradley, W.H., 1931, Origin and microfossils of the oil shale of the Green River Formation of Colorado and Utah: U. S. Geological Survey Professional Paper 168, 56 p.

Cashion, W.B., 1967, Geology and fuel resources of the Green River Formation, southeastern Uinta Basin, Utah and Colorado: U. S. Geological Survey Professional Paper 548, 48 p.

Colburn, J.A., Bereskin, S.R., McGinley, D.C., and Schiller, D.M., 1985, Lower Green River Formation in the Pleasant Valley producing area, Duchesne and Uintah Counties, Utah, *in* Picard, M.D., editor, Geology and energy resources, Uinta Basin, Utah: Utah Geological Association Publication 12, p. 177-186.

Crouch, B.W., Hackney, M.L., and Johnson, B.J., 2000, Sequence stratigraphy and reservoir character of lacustrine carbonates in the basal limestone member - lower Green River Formation (Eocene), Duchesne and Antelope Creek fields, Duchesne Co., Utah [abs.]: American Association of Petroleum Geologists Annual Convention Program with Abstracts, p. A34.

Davis, J.C., 1984, Statistics and Data Analysis in Geology: John Wiley and Sons, New York, 550 pp.

Dow, W.G., 1977, Kerogen studies and geological interpretations: Journal of Geochemical Exploration, v. 7, p. 79-99.

Fouch, T.D., 1975, Lithofacies and related hydrocarbon accumulations in Tertiary strata of the western and central Uinta Basin, Utah, *in* Bolyard, D.W., editor, Symposium on deep drilling frontiers in the central Rocky Mountains: Rocky Mountain Association of Geologists, p. 163-173.

Fouch, T.D., Nuccio, V.F., Osmond, J.C., MacMillan, Logan, Cashion, W.B., and Wandrey, C.J., 1992, Oil and gas in uppermost Cretaceous and Tertiary rock, Uinta Basin, Utah, *in* Fouch, T.D., Nuccio, V.F., and Chidsey, T.C., Jr., editors, Hydrocarbon and mineral resources of the Uinta Basin, Utah and Colorado: Utah Geological Association Publication 20, p. 9-47.

Fouch, T.D., Nuccio, V.F., Anders, D.E., Rice D.D., Pitman, J.K., and Mast, R.F., 1994, Green River petroleum system, Uinta Basin, Utah, U.S.A., *in* Magoon, L.B., and Dow, W.G., editors, The petroleum system - from source to trap: American Association of Petroleum Geologist Memoir 60, p. 399-421.

Fouch, T.D., and Pitman, J.K., 1991, Tectonic and climate changes expressed as sedimentary cycles and stratigraphic sequences in the Paleogene Lake Uinta system, central Rocky Mountains, Utah and Colorado [abs.]: American Association of Petroleum Geologists Bulletin, v. 75, no. 3, p. 575.

---1992, Tectonic and climate changes expressed as sedimentary and geochemical cycles - Paleogene lake systems, Utah and Colorado - implications for petroleum source and reservoir rocks, *in* Carter, L.J., editor, U. S. Geological Research on Energy Resources, 1992 McKelvey Forum Program and Abstracts [abs.]: U. S. Geological Survey Circular 1074, p. 29-30.

Franczyk, K.J., Fouch, T.D., Johnson, R.C., Molenaar, C.M., and Cobban, W.A., 1992, Cretaceous and Tertiary paleogeographic reconstructions for the Uinta-Piceance Basin study area, Colorado and Utah: U. S. Geological Survey Bulletin 1787-Q, 37 p.

Hackney, M.L., and Crouch, B.W., 2000, The Castle Peak member of the lower Green River Formation, Antelope Creek field, Duchesne Co., Utah - an example of the effects of a migrating shoreline on the expression of an open-lacustrine carbonate facies [abs.]: American Association of Petroleum Geologists Annual Convention Program with Abstracts, p. A62.

Jacob, A.F., 1969, Delta facies of the Green River Formation (Eocene), Carbon and Duchesne Counties, Utah: Boulder, University of Colorado, Ph.D. dissertation, 97 p.

Johnson, R.C., and Nuccio, V.F., 1993, Surface vitrinite reflectance study of the Uinta and Piceance Basins and adjacent areas, eastern Utah and western Colorado Implications for development of Laramide basins and uplifts: U. S. Geological Survey Bulletin 1787DD, 38 p.

Keighley, David, Collins, Stephen, Flint, Stephen, and Howell, John, 1999, Reservoir-scale distribution of fluvial sandbodies in lacustrine closed basins, and some sequence-stratigraphic implications - Green River Formation, SW Uinta Basin, east-central Utah [abs.]: American Association of Petroleum Geologists Annual Convention Program with Abstracts, p. A71.

Keighley, David, Flint, Stephen, and Howell, John, 2001, High-resolution lacustrine sequence stratigraphy - an example from the Green River Formation, Uinta Basin, east-central Utah [abs.]: American Association of Petroleum Geologists Annual Convention Program with Abstracts, p. A102.

Keighley, David, Flint, Stephen, Howell, John, Anderson, Daniel, Collins, Stephen, Moscariello, Andrea, and Stone, Greg, 2002, Surface and subsurface correlation of the Green River Formation in central Nine Mile Canyon, SW Uinta Basin, Carbon and Duchesne Counties, east-central Utah: Utah Geological Survey Miscellaneous Publication 02-1, CD-ROM.

Little, T.M., 1988, Depositional environments, petrology, and diagenesis of the basal limestone

facies, Green River Formation (Eocene), Uinta Basin, Utah: Salt Lake City, University of Utah, M.S. thesis, 154 p.

Lutz, S.J., Nielson, D.L., and Lomax, J.D., 1994, Lacustrine turbidite deposits in the lower portion of the Green River Formation, Monument Butte field, Uinta Basin, Utah [abs.]: American Association of Petroleum Geologists Annual Meeting Program with Abstracts, v. 3, p. 203.

McDonald, R.E., 1972, Eocene and Paleocene rocks of the southern and central basins, *in* Mallory, W.M., editor, Geologic atlas of the Rocky Mountain region: Rocky Mountain Association of Geologists, p. 243-256.

Morgan, C.D., Chidsey, T.C., Jr., Hanson, J.A., McClure, K.P., Weller, Kevin, Bereskin, S.R., Deo, M.D., and Yeager, Randy, 1999, Reservoir characterization of the lower Green River Formation, southwest Uinta Basin, Utah: Unpublished biannual technical progress report to the U. S. Department of Energy for the period 10/1/98 through 3/31/99, 11 p.

Nuccio, V.F., and Johnson, R.C., 1986, Thermal maturity map of the lower part of the upper Cretaceous Mesaverde Group, Uinta Basin, Utah: Miscellaneous Field Study Map MF-1842.

Osmond, J.C., 1992, Greater Natural Buttes gas field, Uintah County, Utah, *in* Fouch, T.D., Nuccio, V.F., and Chidsey, T.C., Jr., editors, Hydrocarbon and mineral resources of the Uinta Basin, Utah and Colorado: Utah Geological Association Publication 20, p. 143-163.

---2000, West Willow Creek field - first productive lacustrine stromatolite mound in the Eocene Green River Formation, Uinta Basin, Utah: Rocky Mountain Association of Geologists, The Mountain Geologist, v. 37, no. 3, p. 157-170.

Picard, M.D., 1955, Subsurface stratigraphy and lithology of the Green River Formation in Uinta Basin, Utah: American Association of Petroleum Geologists Bulletin, v. 39, no. 1, p. 75-102.

---1957a, Subsurface stratigraphy and lithology of Green River Formation in the Uinta Basin: American Association of Petroleum Geologists Bulletin, v. 39, p. 75-102.

---1957b, Green shale facies, lower Green River Formation, Utah: American Association of Petroleum Geologists Bulletin, v. 41, p. 2373-2376.

Picard, M.D., and High, L.R., 1970. Sedimentology of oil-impregnated, lacustrine and fluvial sandstone, P.R. Spring area, southeast Uinta Basin, Utah: Utah Geological and Mineral Survey Special Studies 33, 32 p.

Pitman, J.K., Fouch, T.D., and Goldaber, M.B., 1982, Depositional setting and diagenetic evolution of some Tertiary unconventional reservoir rocks, Uinta Basin, Utah: American Association of Petroleum Geologists Bulletin, v. 66, no. 10, p. 1581-1596.

Pitman, J.K., Franczyk, K.J., and Anders, D.E., 1988, Diagenesis and burial history of nonmarine upper Cretaceous rocks in the central Uinta Basin, Utah: U. S. Geological Survey Bulletin 1787D, 24 p.

Remy, R.R., 1989, Deltaic and lacustrine facies of the Green River Formation, southern Uinta Basin, Utah, *in* Nummedal, D., and Remy, R.R., editors, Cretaceous shelf sandstones and shelf depositional sequences, Western interior basin, Utah, Colorado, and New Mexico: Washington, D. C., American Geophysical Union, International Geological Congress, 28th Guidebook T-119, p. 1-11.

---1992, Stratigraphy of the Eocene part of the Green River Formation in the south-central part of the Uinta Basin, Utah: U. S. Geological Survey Bulletin 1787-BB, 79 p.

Rice, D.D., Fouch, T.D., and Johnson, R.C., 1992, Influence of source rock type, thermal maturity, and migration on composition and distribution of natural gases, Uinta Basin, Utah, *in* Fouch, T.D., Nuccio, V.F., and Chidsey, T.C., Jr., editors, Hydrocarbon and Mineral Resources of the Uinta Basin, Utah and Colorado: Utah Geological Association Publication 20, p. 95-109.

Ruble, T.E., Lewan, M.D., and Philp, R.P., 2001, New insights on the Green River petroleum system in the Uinta Basin from hydrous pyrolysis experiments: American Association of Petroleum Geologists Bulletin, v. 85, p.1333-1371.

Ryder, R.T., Fouch, T.D., and Elison, J.H., 1976, Early tertiary sedimentation in the western Uinta Basin, Utah: Geological Society of America Bulletin, v. 87, p. 496-512.

Schmoker, J.W., Nuccio, V.F., and Pitman, J.K., 1992, Porosity trends in predominately nonmarine sandstones of the upper Cretaceous Mesaverde Group, Uinta and Piceance Basins, Utah and Colorado, *in* Fouch, T.D., Nuccio, V.F., and Chidsey, T.C., Jr., editors, Hydrocarbon and Mineral Resources of the Uinta Basin, Utah and Colorado: Utah Geological Association Publication 20, p.111-121.

Schumn, S.A., and Ethridge, F.G., 1994, Origin, evolution and morphology of fluvial valleys, *in* Dalrymple, R.W., and Zaitlin, B.A., editors, Incised-valley systems - origin and sedimentary sequences: Society of Sedimentary Geology Special Publication no. 51, p. 11-27.

Szantat, A.W., 1990, Paleohydrology and paleomorphology of Early Eocene Green River channel sandstones, Uinta Basin, Utah: Fort Collins, Colorado State University, M.S. Thesis, 109 p.

Trumbo, D.B., 1993, Brundage Canyon/Sowers Canyon, *in* Hill, B.G., and Bereskin, S.R., editors, Oil and gas fields of Utah: Utah Geological Association Publication 22, unpaginated.

Weiss, M.P., Witkind, I.J., and Cashion, W.B., 1990, Geologic map of the Price 30'X60' Quadrangle, Carbon, Duchesne, Uintah, Utah, and Wasatch Counties, Utah: U. S. Geological Survey Miscellaneous Investigations Series map I-1981, 1 sheet.